

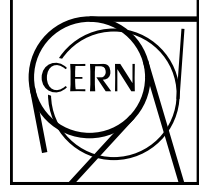
PDF hosted at the Radboud Repository of the Radboud University Nijmegen

The following full text is a preprint version which may differ from the publisher's version.

For additional information about this publication click this link.

<http://hdl.handle.net/2066/103730>

Please be advised that this information was generated on 2017-12-06 and may be subject to change.



CERN-PH-EP-2012-190

Submitted to: JHEP

Search for high-mass resonances decaying to dilepton final states in pp collisions at $\sqrt{s} = 7$ TeV with the ATLAS detector

The ATLAS Collaboration

Abstract

The ATLAS detector at the Large Hadron Collider is used to search for high-mass resonances decaying to an electron-positron pair or a muon-antimuon pair. The search is sensitive to heavy neutral Z' gauge bosons, Randall-Sundrum gravitons, Z^* bosons, techni-mesons, Kaluza-Klein Z/γ bosons, and bosons predicted by Torsion models. Results are presented based on an analysis of pp collisions at a center-of-mass energy of 7 TeV corresponding to an integrated luminosity of 4.9 fb^{-1} in the e^+e^- channel and 5.0 fb^{-1} in the $\mu^+\mu^-$ channel. A Z' boson with Standard Model-like couplings is excluded at 95% confidence level for masses below 2.22 TeV. A Randall-Sundrum graviton with coupling $k/\overline{M}_{\text{Pl}} = 0.1$ is excluded at 95% confidence level for masses below 2.16 TeV. Limits on the other models are also presented, including Technicolor and Minimal Z' Models.

Search for high-mass resonances decaying to dilepton final states in pp collisions at $\sqrt{s} = 7$ TeV with the ATLAS detector

The ATLAS Collaboration

ABSTRACT: The ATLAS detector at the Large Hadron Collider is used to search for high-mass resonances decaying to an electron-positron pair or a muon-antimuon pair. The search is sensitive to heavy neutral Z' gauge bosons, Randall-Sundrum gravitons, Z^* bosons, techni-mesons, Kaluza-Klein Z/γ bosons, and bosons predicted by Torsion models. Results are presented based on an analysis of pp collisions at a center-of-mass energy of 7 TeV corresponding to an integrated luminosity of 4.9 fb^{-1} in the e^+e^- channel and 5.0 fb^{-1} in the $\mu^+\mu^-$ channel. A Z' boson with Standard Model-like couplings is excluded at 95% confidence level for masses below 2.22 TeV. A Randall-Sundrum graviton with coupling $k/\overline{M}_{\text{Pl}} = 0.1$ is excluded at 95% confidence level for masses below 2.16 TeV. Limits on the other models are also presented, including Technicolor and Minimal Z' Models.

Contents

1	Introduction	2
2	ATLAS detector	3
3	Lepton reconstruction	4
4	Event selection	4
5	Simulated samples	6
6	Expected signals and backgrounds	7
7	Systematic uncertainties	9
8	Data-SM expectation comparison	10
9	Limit-setting procedure	13
10	Limits on spin-1 SSM and E_6 Z' bosons	14
11	Limits on spin-1 Z^* bosons	15
12	Limits on spin-2 Randall-Sundrum gravitons	16
13	Limits on Torsion models	18
14	Limits on Technicolor	18
15	Limits on spin-1 Kaluza-Klein S^1/Z_2 bosons	21
16	Limits on Minimal Z' bosons	23
17	Conclusions	24
18	Acknowledgements	25

1 Introduction

Searches for new resonances decaying to a dilepton final state have had a long and successful history. These channels contributed to the discovery of the quarkonium resonances J/ψ and Υ , as well as the discovery of the Z boson. Various models beyond the Standard Model (SM) contain additional bosons which can decay into dileptons, providing a fully reconstructable final state with small, well-understood backgrounds. In this article, data collected by the ATLAS experiment at the LHC are used to search for new resonances decaying into dielectron and dimuon final states.

The Sequential Standard Model (SSM) [1] defines the Z'_{SSM} couplings to SM fermions to be the same as the SM Z boson couplings and is often used in the literature as a benchmark model. A number of models predict additional neutral vector gauge bosons. One class postulates larger symmetry groups in which the SM gauge group is embedded. This is usually motivated by gauge unification or restoration of left-right symmetry, which is violated by the weak interaction. In one scheme, the SM gauge group derives from the E_6 group which, upon symmetry-breaking via the $SU(5)$ subgroup, results in two additional $U(1)$ gauge groups named $U(1)_\chi$ and $U(1)_\psi$ with associated gauge bosons Z'_χ and Z'_ψ that can mix [1, 2]. In the Minimal Z' Models [3], the phenomenology is controlled by only two effective coupling constants in addition to the Z' boson mass. This parameterization encompasses many models, including a left-right symmetric model [4, 5] and the pure (B–L) model [6], where B (L) is the baryon (lepton) number, and B–L is the conserved quantum number.

A second set of models is motivated by various solutions to the hierarchy problem of the SM relating the very different scales of electroweak symmetry breaking and the gravitational Planck scale (M_{Pl}). One class of such models introduces a new doublet of vector bosons (Z^*, W^*) [7] with masses not far from the weak scale [8], which couple to SM fermions only via magnetic-type interactions. Compared to Z' bosons, interactions mediated by Z^* bosons are additionally suppressed in low-energy processes by powers of the small momentum transfer. Thus, the search for the Z^* boson is well-motivated at the LHC.

An alternative solution to the hierarchy problem has been proposed in models that allow the gravitational force to propagate into extra spatial dimensions. Among them, the Randall-Sundrum (RS) model [9] predicts a warped space-time metric in one extra dimension. Due to warping, the apparent strength of gravity in the four-dimensional subspace populated by the SM particles is exponentially suppressed. The RS model predicts excited states of the graviton, G^* , whose couplings to the SM particles are not exponentially suppressed. The graviton is a spin-2 boson that can decay into dilepton final states with a coupling strength of $k/\overline{M}_{\text{Pl}}$, where k is a scale that defines the warp factor of the extra dimension, and $\overline{M}_{\text{Pl}} = M_{\text{Pl}}/\sqrt{8\pi}$.

In Kaluza-Klein TeV^{-1} models [10–12], the extra-dimensional momentum is quantized by the inverse of the size of the extra dimension, creating a tower of massive Kaluza-Klein (KK) states corresponding to each SM particle. The Kaluza-Klein towers corresponding to the photon and the Z boson, γ_{KK} and Z_{KK} , would manifest themselves as nearly degenerate

resonances decaying to dilepton final states. This work is the first direct search for these Kaluza-Klein states. Previous bounds on the Kaluza-Klein boson mass were obtained from indirect measurements [13, 14].

Technicolor models [15–17] provide a dynamical scenario of Standard Model electroweak symmetry breaking (EWSB) by postulating a new strong binding force between techni-fermions. This model predicts additional bound states, techni-mesons, which are resonances with masses of a few hundred GeV that can decay into fermion-antifermion pairs. Two main Technicolor models have a well-developed phenomenology at LHC energies. In Low-scale Technicolor (LSTC) [18, 19], the coupling constant varies slowly (walks) due to the existence of many scales of strong interactions while the phenomenology is dictated by the lowest mass particles. Minimal Walking Technicolor (MWT) [20–22] is a minimal model that is conformal and satisfies electroweak precision measurements.

One of the main limitations of the Standard Model is its inability to incorporate gravity. To address this problem, a consistent quantum theory of all four fundamental forces should be developed to seamlessly unify the SM and General Relativity (GR). However, so far no generally accepted formulation of quantum gravity exists, and therefore it is common to apply a phenomenological approach to the problem by considering extensions of GR and assuming that they might arise from a more fundamental theory, such as String Theory. Among such extensions is gravity with Torsion [23]. In Torsion models, the spin of the elementary particles is the source of an extra field called Torsion, which interacts with SM fermions [24, 25]. This article reports on the first interpretation of a high mass dilepton search in terms of a Torsion resonance.

Previous searches have set direct and indirect constraints on the mass of new heavy resonances [26, 27]. The Tevatron data [28, 29] have excluded a Z'_{SSM} boson with a mass lower than 1.071 TeV [29]. Recent measurements from the LHC experiments [30, 31], based on up to 5 fb^{-1} of data, have excluded a Z'_{SSM} boson with a mass lower than 2.33 TeV [31]. Indirect constraints from LEP [32–35] have excluded Z'_{SSM} bosons with mass less than 1.787 TeV [27]. Constraints on the mass of the RS graviton have been set by the ATLAS [36], CMS [31], CDF [37] and D0 [38] collaborations, excluding RS gravitons with a mass less than 2.14 TeV for $k/\overline{M}_{\text{Pl}} = 0.1$ [31]. A Z^* with mass less than 1.152 TeV has been excluded by ATLAS [39]. A search for the techni-mesons ρ_{T} and ω_{T} in the dilepton final state has been conducted by CDF, resulting in a lower bound on the ρ_{T} and ω_{T} masses of 280 GeV [40]. The constraints from electroweak precision measurements give a lower limit on the $Z_{\text{KK}}/\gamma_{\text{KK}}$ boson masses around 4 TeV [13, 41].

The results reported in this article use the full data sample recorded by ATLAS in 2011, corresponding to a total integrated luminosity of 4.9 (5.0) fb^{-1} in the e^+e^- ($\mu^+\mu^-$) channel.

2 ATLAS detector

The ATLAS detector [42] consists of an inner tracking detector surrounded by a 2 T superconducting solenoid, electromagnetic and hadronic calorimeters, and a muon spectrometer.

Charged particle tracks in the pseudorapidity¹ range $|\eta| < 2.5$ are reconstructed with the inner detector, which consists of silicon pixel, silicon strip, and transition radiation detectors. The superconducting solenoid is surrounded by a hermetic calorimeter that covers $|\eta| < 4.9$. For $|\eta| < 2.5$, the electromagnetic calorimeter is finely segmented and plays an important role in electron identification. Outside the calorimeter, air-core toroids provide the magnetic field for the muon spectrometer. Three stations of precision drift tubes (with cathode strip chambers for the innermost station for $|\eta| > 2.0$) provide an accurate measurement of the muon track curvature in the range $|\eta| < 2.7$. Resistive-plate and thin-gap chambers provide muon triggering capability in the range $|\eta| < 2.4$.

3 Lepton reconstruction

Electron candidates are formed from clusters of cells reconstructed in the electromagnetic calorimeter that are associated with a charged particle track in the inner detector. Measurements of the transverse calorimeter shower shape and the longitudinal leakage into the hadronic compartment [43] are also used to improve electron-hadron identification.

The energy of an electron is obtained from the calorimeter, and its direction from the associated track. At large transverse energy (E_T), the calorimeter energy resolution is dominated by a constant term which is measured in data to be 1.2% in the barrel ($|\eta| < 1.37$) and 1.8% in the endcaps ($1.52 < |\eta| \leq 2.47$) [43]. For dielectron masses above 200 GeV, the mass resolution is below 2% over the entire η range.

Muon tracks are first reconstructed separately in the inner detector (ID) and in the muon spectrometer (MS). The two tracks are then matched and a combined fit is performed to the inner detector and muon spectrometer hits, taking into account the effect of multiple scattering and energy loss in the calorimeters.

The muons used in this work have hits in either three or two (out of three) stations of the muon spectrometer. Muons with hits in three stations, referred to as tight muons, comprise about 95% of the sample, and have transverse momentum (p_T) resolution at 1 TeV ranging from 10% to 25%. Muons with hits in two stations, referred to as loose muons, have slightly worse p_T resolution than the tight muons. Loose muons are accepted only in the barrel region of the muon spectrometer ($|\eta| < 1.05$), excluding small geometrical regions where the detector alignment is known to be less precise.

4 Event selection

The data used for this study are required to have been recorded during periods of stable LHC beams, and when all relevant systems of the detector were operating normally. Collision candidates are selected by requiring a primary vertex with at least three associated charged particle tracks, each with p_T more than 0.4 GeV.

¹ATLAS uses a right-handed coordinate system with the z -axis along the beam pipe. The x -axis points to the centre of the LHC ring, and the y axis points upward. Cylindrical coordinates (r, ϕ) are used in the transverse (x, y) plane, ϕ being the azimuthal angle. The pseudorapidity is defined in terms of the polar angle θ as $\eta = -\ln \tan(\theta/2)$.

In the e^+e^- channel, events were triggered by a diphoton trigger, requiring the presence of two electromagnetic clusters fulfilling a set of requirements [44] on the shape of the energy deposit and with a transverse energy threshold of 20 GeV. The efficiency of the diphoton trigger was measured in data to be 99% for electron pairs forming dilepton masses above 100 GeV. This was done using a tag-and-probe method on electrons from decays of Z bosons, selected using a single-electron trigger and requiring two electrons in the event to pass the event selection described below. Since the trigger signals are saturated for electromagnetic clusters with very high energies, the trigger-level bunch-crossing identification, which uses the pulse shape, is challenging and performed by a dedicated algorithm, implemented in the first-level calorimeter trigger hardware.

Dielectron events are selected by requiring two electron candidates with the *medium* level of identification defined in ref. [43], with transverse energy E_T larger than 25 GeV and $|\eta| \leq 2.47$; the transition region between the barrel and endcap calorimeters is excluded. A hit in the first layer of the pixel detector is required if an active pixel module is traversed, to suppress background from photon conversions. To suppress background from QCD multijet production, the electron with the higher E_T must be isolated, requiring $\Sigma E_T(\Delta R < 0.2)$ less than 7 GeV, where $\Delta R = \sqrt{(\Delta\eta)^2 + (\Delta\phi)^2}$ and $\Sigma E_T(\Delta R < 0.2)$ is the sum of the transverse energies in calorimeter cells around the electron direction in a cone of ΔR smaller than 0.2. The sum excludes the core of the electron energy deposition and is corrected for transverse shower leakage and pile-up from additional pp collisions. The two highest E_T electrons passing the above selection criteria are used to reconstruct the dielectron candidate. The curvature measured by the inner detector for the high-energy electrons relevant to this analysis is not large enough to allow a precise determination of the transverse momentum and charge of the electrons. To avoid losses in efficiency, the two electron candidates are not required to have opposite charge. For the selection criteria described above and dielectron invariant masses (m_{ee}) greater than 130 GeV, the overall event acceptance times efficiency ($\mathcal{A}\epsilon$) for a Z' boson of mass 2 TeV is about 66%.

In the $\mu^+\mu^-$ channel, events were triggered by at least one of two single-muon triggers, one with a p_T threshold of 22 GeV as reconstructed from the combination of ID and MS information, and the second with a p_T threshold of 40 GeV as reconstructed by the MS in the barrel region only. The typical single-muon trigger efficiency was measured in data to be 85% in the barrel (considering the union of both trigger paths) and 86% in the endcaps. The trigger efficiency is lower for muons than it is for electrons because of the smaller geometrical acceptance of the muon trigger detectors.

A dimuon event candidate is constructed from two opposite-charge muons, each with p_T greater than 25 GeV, $|\eta| < 2.4$. In order to reject muons from cosmic radiation, the impact parameter with respect to the primary vertex must be smaller than 0.2 mm in the transverse plane and 1.0 mm along the beam axis, and the primary vertex must be reconstructed within 20 cm from the centre of the detector along the beam direction. To ensure good p_T resolution, each muon is required to have a minimum number of hits in each of the inner detector components as well as in three (two) muon spectrometer stations for tight (loose) muons. Muon candidates are excluded from the analysis if they cross regions of the muon spectrometer in which the bending power of the magnetic field is rapidly changing

with the track position or the detector is less precisely aligned or calibrated. In addition, the difference between the standalone momentum measurements from the inner detector and the muon spectrometer must not exceed five (three) times the sum in quadrature of the standalone resolutions for tight (loose) muons. Finally, to suppress background from QCD multijet production, each muon must be isolated, requiring the sum of the p_T of all other tracks in a cone of size $\Delta R < 0.3$ to be less than 5% of the transverse momentum of the muon.

Dimuon event candidates with two tight muons are considered first (tight dimuon selection). If more than one such pair is found in an event, the one with the highest scalar sum of the leptons' p_T is selected. If no tight muon pair is found, pairs with one tight muon and one loose muon (loose dimuon selection) are considered. Similarly, if more than one loose muon pair is found in an event, the one with the highest $\sum |p_T|$ is selected. For the selection criteria described above, the overall event $\mathcal{A}\epsilon$ for a Z' boson of mass 2 TeV decaying into a dimuon final state is 43%, including 4% from the loose dimuon selection. The lower acceptance compared to the dielectron channel is due to the stringent hit requirements in the muon spectrometer.

For both channels, the dominant and irreducible background is due to the Z/γ^* (Drell-Yan) process, characterized by the same final state as the signal. Small contributions from $t\bar{t}$ and diboson (WW , WZ and ZZ) production are also present in both channels. Semi-leptonic decays of b and c quarks in the e^+e^- and $\mu^+\mu^-$ samples, plus a mixture of photon conversions and hadrons faking electrons in the e^+e^- sample, are backgrounds that are referred to below as QCD background. Events with jets accompanying W bosons (W + jets) may similarly produce dilepton candidates.

The expected signal and backgrounds, with the exception of the ones from QCD and W + jets, are evaluated with simulated samples and rescaled using the most precise available cross-section predictions, as explained in more detail in section 6. The total SM prediction is then normalized to the data in an invariant mass interval around the Z peak (70–110 GeV). In the dielectron channel, the rescaling is done after adding the QCD multijet and W + jets backgrounds evaluated directly from data, as described in section 6.

5 Simulated samples

The Z' , G^* , and LSTC signals, as well as the Z/γ^* process, are generated with PYTHIA 6.421 [45] using MRST2007 LO** [46, 47] parton distribution functions (PDFs). The Minimal Z' and Z_{KK}/γ_{KK} signals are obtained by reweighting the large sample of Z/γ^* events from PYTHIA with the appropriate ratio of differential cross sections [48–50]. Z^* and Torsion signals are generated with CompHEP [51], while MadGraph [52] is used for MWT signals; CTEQ6L1 [53] PDFs are used in both cases.

The diboson processes are generated with HERWIG 6.510 [54] using MRST2007 LO** PDFs. The $t\bar{t}$ background is generated with MC@NLO 4.01 [55] using CTEQ66 [56] PDFs. For $t\bar{t}$ events, JIMMY 4.31 [57] is used to describe multiple parton interactions and HERWIG to describe the remaining underlying event and parton showers. Final-state photon

radiation is handled by PHOTOS [58]. The generated samples are processed through a full ATLAS detector simulation [59] based on GEANT4 [60].

6 Expected signals and backgrounds

The Z/γ^* cross section is calculated at next-to-next-to-leading order (NNLO) in QCD using PHOZPR [61] with MSTW2008 NNLO PDFs [62]. The ratio of this cross section to the leading-order cross section is used to determine a mass-dependent QCD K-factor, which is then applied to the results of the leading-order simulation. The same QCD K-factor is applied to the Z' , Z_{KK}/γ_{KK} , Torsion, and LSTC signals. Its value is 0.91 at 2 TeV and slowly increases up to 1.15 at 250 GeV. A different K-factor is applied to the G^* signal, with values that vary between 1.6 and 1.8 depending on the graviton mass and $k/\overline{M}_{\text{Pl}}$ [63], and with a value of 1.75 above 750 GeV, consistent with ref. [36]. Finally, no QCD K-factor is applied to the leading-order Z^* cross section since the Z^* model uses an effective Lagrangian with a different Lorentz structure.

The Z'_{SSM} , $Z'(E_6)$, Torsion states, and techni-mesons interfere minimally with the Z/γ^* process, and the Z^* and G^* do not interfere at all. The effect of interference on the resonance line-shape is therefore neglected for all these states. On the other hand, the interference of the Z_{KK}/γ_{KK} boson with Z/γ^* is very strong and cannot be neglected [12, 41]. The interference effect is also taken into account in the Minimal Z' Models framework.

Higher-order electroweak corrections (beyond the photon radiation included in the simulation) are calculated using HORACE [64, 65], yielding an electroweak K-factor (K_{EW}) due to virtual heavy gauge boson loops. Its value at 2 TeV is 0.92 in the dielectron channel and 0.93 in the dimuon channel, and slowly increases up to 1.05 at 250 GeV. The electroweak K-factor is applied only to the Z/γ^* background and not to the expected signals, with the exception of Technicolor and Kaluza-Klein states. In the case of Technicolor, K_{EW} is applied because production proceeds via the Z/γ^* process. Since interference is an important feature of the Kaluza-Klein boson model, the electroweak K-factor is applied to the full amplitude (\mathcal{M}) of the process, including the Z_{KK}/γ_{KK} amplitude: $|\mathcal{M}_{Z/\gamma^*} + \mathcal{M}_{Z_{KK}/\gamma_{KK}}|^2 \rightarrow K_{\text{EW}} \times |\mathcal{M}_{Z/\gamma^*} + \mathcal{M}_{Z_{KK}/\gamma_{KK}}|^2$. This approximation is conservative. Although interference is taken into account for Minimal Z' bosons, for consistency with the treatment of the other Z' models the electroweak K-factor is applied only to the pure Z/γ^* part of the amplitude: $|\mathcal{M}_{Z/\gamma^*} + \mathcal{M}_{Z'}|^2 \rightarrow |\mathcal{M}_{Z/\gamma^*} + \mathcal{M}_{Z'}|^2 + (K_{\text{EW}} - 1) \times |\mathcal{M}_{Z/\gamma^*}|^2$.

For the other backgrounds, the diboson cross sections are calculated to next-to-leading order (NLO) using MCFM [66] with an uncertainty of 5%, and the $t\bar{t}$ cross section is predicted at approximate-NNLO, with an uncertainty of +7.0/−9.6% [67, 68].

At very high masses, the statistical significance of the diboson and $t\bar{t}$ simulated samples becomes insufficient. Therefore their invariant mass distribution is fitted to the functional form $y(x) = p_1 \cdot x^{p_2 + p_3 \log x}$ which is then used to extrapolate the $t\bar{t}$ background above 0.8 TeV and the diboson background above 1.5 TeV.

The QCD multijet and W + jets backgrounds in the e^+e^- sample are estimated primarily from data using several techniques.

First, a “reversed electron identification” technique [39] is used, in which only the QCD multijet background is estimated from data, while the $W + \text{jets}$ component comes from the Monte Carlo simulation. Events with both electron candidates failing one of the *medium* identification criteria are used to determine the shape of the QCD multijet background m_{ee} distribution. The chosen criterion, the difference in η between the cluster and the track, does not affect kinematic distributions. The small contamination from non-QCD processes, located mainly beneath the Z peak, is subtracted using MC samples of the other backgrounds (Z/γ^* , $t\bar{t}$, diboson and $W + \text{jets}$). The shape of these backgrounds is obtained by summing their contributions according to the most precise available cross-section predictions. The mass distributions of the QCD and non-QCD backgrounds are fitted for their relative contributions in the $70 \text{ GeV} < m_{ee} < 200 \text{ GeV}$ range. The QCD multijet background shape is fitted in the $110\text{--}800 \text{ GeV}$ range using the functional form $y(x) = p_1 \cdot x^{p_2 + p_3 \log x}$ and is extrapolated beyond 800 GeV . The systematic uncertainty includes the uncertainty from the relative normalization procedure, namely the QCD multijet fraction from the first fit, the uncertainty from the choice of the reversed selection and the uncertainty from the range of the second fit.

A second independent data-driven method is used to obtain an estimate of the QCD multijet and $W + \text{jets}$ backgrounds together. It uses fake rates computed from jet-enriched samples, obtained from jet triggers or from the signal trigger. The fake factors are defined as the probability for a jet to pass the “tight” (T) selection, that is all selection criteria, if it passes the “loose” (L) selection, that is the same reverse identification selection as in the reverse electron identification method. The fake factors depend only slightly on transverse momentum and more importantly on pseudorapidity. Since isolation is applied only to the leading electron, two different fake factors are needed: f_{lead} , applied to the leading electron, and f_{subl} , applied to the subleading electron. The QCD multijet and $\ell + \text{jets}$ backgrounds are estimated by selecting events with candidate pairs having each electron identified either as “tight” or “loose”. The final estimate is then

$$N_{\ell + \text{jets} \ \& \ \text{QCD}} = f_{\text{subl}} N_{\text{TL}} + f_{\text{lead}} N_{\text{LT}} - f_{\text{lead}} f_{\text{subl}} N_{\text{LL}}.$$

The same functional form as before is finally used to fit this estimate between 140 GeV and 850 GeV and extrapolate it above this energy range. The systematic uncertainty includes the uncertainty from the η or p_T dependence of the fake factors and the uncertainty from the range of the fit.

All methods yield consistent results and the final estimate is given by the mean of the central values. The uncertainty, conservatively assigned to be the maximum of the largest of up and down deviations of each method, is 33% at $m_{ee} = 200 \text{ GeV}$ and grows to about 110% at 2 TeV .

In the dimuon channel, the QCD multijet background is estimated in data from a sample of non-isolated dimuon events. The $W + \text{jets}$ background is evaluated using simulated samples. Both backgrounds are found to be negligible in the dimuon channel after the isolation selection is applied.

7 Systematic uncertainties

The systematic uncertainties in this analysis are reduced by the fact that the backgrounds are normalized to the data in the region of the Z peak. This procedure makes the analysis insensitive to the error on the measurement of the integrated luminosity as well as other mass-independent systematic uncertainties. Instead, a constant systematic uncertainty of 5%, due to the uncertainty on the Z/γ^* cross section in the normalization region, is assigned to the signal expectation.

The mass-dependent systematic uncertainties include theoretical effects due to the PDFs, QCD and electroweak corrections, as well as experimental effects, namely efficiency and resolution. These uncertainties are correlated across all bins in the search region. In addition, there is an uncertainty on the QCD and $W + \text{jets}$ backgrounds affecting the dielectron channel. The theoretical uncertainties are applied to the background expectation only. The experimental uncertainties are assumed to be correlated between signal and all types of backgrounds. All systematic uncertainties quoted below refer to narrow resonances with dilepton masses of 2 TeV. All systematic uncertainties estimated to have an impact $\leq 3\%$ on the expected number of events are neglected.

The combined uncertainty on the PDFs, strong coupling α_S , and renormalization/factorization scale variations is 20%, the largest contribution being the uncertainty on the PDFs. The α_S and PDF uncertainties are evaluated using the MSTW2008NNLO eigenvector PDF sets and the PDF sets corresponding to variations of α_S , at the 90% confidence level (CL). The spread of the variations covers the difference between the central values obtained with the CTEQ and MSTW PDF sets. The scale uncertainties are estimated by varying the renormalization (μ_R) and factorization (μ_F) scales independently up and down by a factor of two, but with the constraint $0.5 \leq \mu_F/\mu_R \leq 2$ to avoid large logarithmic corrections. The resulting maximum variations are taken as the uncertainties. In addition, a systematic uncertainty of 4.5% is attributed to electroweak corrections [39] for both channels. This contribution includes the difference in the electroweak scheme definition between PYTHIA and HORACE, and higher order electroweak and $\mathcal{O}(\alpha\alpha_S)$ corrections.

In the dielectron channel, the largest experimental systematic uncertainty is due to the estimate of the QCD multijet and $W + \text{jets}$ backgrounds, which translates into a systematic uncertainty on the total background of 26% at 2 TeV. Other experimental systematic uncertainties in the dielectron channel include uncertainties due to the extrapolation of the $t\bar{t}$ and diboson backgrounds, which are significant only above 2 TeV and uncertainties due to the electron reconstruction and identification efficiency at high E_T , which are estimated to be less than 3% for electron pairs. The uncertainties on the calorimeter energy calibration are estimated to be between 0.5% and 1.5%, depending on transverse energy and pseudorapidity and have a negligible effect on the event yield as do the uncertainties on the corrections applied to the simulation to reproduce the calorimeter resolution at high energy.

In the dimuon channel, the combined uncertainty on the trigger and reconstruction efficiency for muon pairs is estimated to be 6% at 2 TeV. This uncertainty is dominated by a conservative estimate of the impact from large energy loss due to muon bremsstrahlung

Table 1. Summary of systematic uncertainties on the expected numbers of events at $m_{\ell\ell} = 2$ TeV. NA indicates that the uncertainty is not applicable, and “-” denotes a negligible entry.

Source	Dielectrons		Dimuons	
	Signal	Background	Signal	Background
Normalization	5%	NA	5%	NA
PDF/ α_s /scale	NA	20%	NA	20%
Electroweak corrections	NA	4.5%	NA	4.5%
Efficiency	-	-	6%	6%
W + jets and QCD background	NA	26%	NA	-
Total	5%	34%	8%	21%

in the calorimeter, which may interfere with reconstruction in the muon spectrometer. In addition, the uncertainty on the resolution due to residual misalignments in the muon spectrometer propagates to a change in the observed width of the signal line-shape; however, its effect on the final result has a negligible impact for final states which do not interfere strongly with Z/γ^* . Finally, the muon momentum scale is calibrated with a statistical precision of 0.1% using the $Z \rightarrow \ell^+\ell^-$ mass peak. As with the dielectron channel, the momentum calibration uncertainty has negligible impact in the dimuon channel search.

A summary of all systematic uncertainties common to all final states investigated in this search is shown in table 1. Additional systematic uncertainties that apply to strongly interfering states (such as Z_{KK}/γ_{KK}) are discussed later.

8 Data-SM expectation comparison

Figure 1 shows the invariant mass ($m_{\ell\ell}$) distribution for the dielectron (top) and dimuon (bottom) final states after final selection. The bin width of the histograms is constant in $\log m_{\ell\ell}$, chosen such that a possible signal peak spans multiple bins and the templates are smooth. Figure 1 also displays the expected Z'_{SSM} signal for two mass hypotheses. Tables 2 and 3 show the number of data events and the estimated backgrounds in bins of reconstructed dielectron and dimuon invariant mass above 110 GeV. The number of observed events in the normalization region, from 70 to 110 GeV, is 1,236,646 in the dielectron channel and 985,180 in the dimuon channel. The dilepton invariant mass distributions are well described by the Standard Model.

The data are compared to the Monte Carlo simulation in the search region $0.13 \text{ TeV} < m_{\ell\ell} < 3.0 \text{ TeV}$. The agreement is first studied by computing the significance of the difference in each mass bin, with statistical and systematic uncertainties taken into account. The largest positive local significance is about 2σ in the dielectron channel and about 1σ in the dimuon channel, and the largest negative local significance is -2σ in both channels.

The comparison is then performed by means of templates [39, 69]. The templates provide the expected yield of events (\bar{n}) in each $m_{\ell\ell}$ bin. When neglecting interference, \bar{n} is given by $\bar{n} = n_X(\lambda, \boldsymbol{\nu}) + n_{Z/\gamma^*}(\boldsymbol{\nu}) + n_{\text{obg}}(\boldsymbol{\nu})$, where n_X represent the number of events produced by the decay of a new resonance X ($X = Z', Z^*, G^*, \text{TS}, \rho_T/\omega_T, R_1/R_2$, where ρ_T/ω_T and R_1/R_2 are techni-mesons, see below); n_{Z/γ^*} and n_{obg} are the number of Z/γ^*

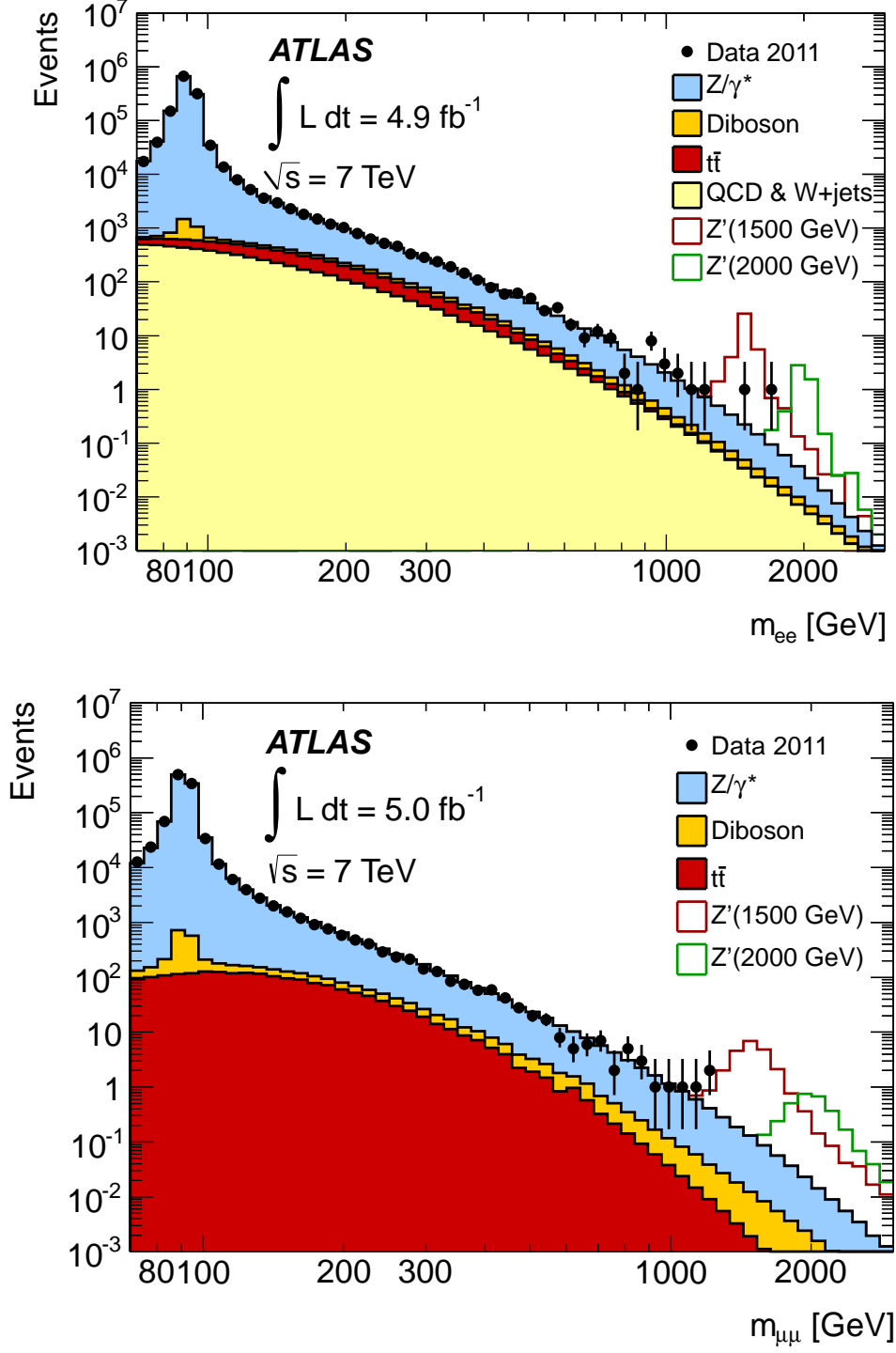


Figure 1. Dielectron (top) and dimuon (bottom) invariant mass ($m_{\ell\ell}$) distributions after final selection, compared with the stacked sum of all expected backgrounds, with two example Z'_{SSM} signals overlaid. The bin width is constant in $\log m_{\ell\ell}$.

Table 2. Expected and observed number of events in the dielectron channel. The errors quoted include both statistical and systematic uncertainties.

$m_{ee}[\text{GeV}]$	110–200	200–400	400–800	800–1200	1200–3000
Z/γ^*	26700 ± 1100	2960 ± 120	265 ± 13	12.1 ± 0.9	1.47 ± 0.18
$t\bar{t}$	1300 ± 120	410 ± 40	26.5 ± 2.8	0.41 ± 0.17	0.034 ± 0.034
Diboson	415 ± 21	146 ± 8	16.2 ± 0.9	0.88 ± 0.05	0.101 ± 0.011
QCD and W + jets	1900 ± 600	510 ± 200	50 ± 31	2.0 ± 1.8	0.26 ± 0.31
Total	30300 ± 1300	4030 ± 240	357 ± 34	15.4 ± 2.0	1.86 ± 0.35
Data	29816	4026	358	17	3

Table 3. Expected and observed number of events in the dimuon channel. The errors quoted include both statistical and systematic uncertainties.

$m_{\mu\mu} [\text{GeV}]$	110–200	200–400	400–800	800–1200	1200–3000
Z/γ^*	21200 ± 1200	2090 ± 230	173 ± 15	7.7 ± 0.8	0.98 ± 0.16
$t\bar{t}$	900 ± 100	270 ± 50	18 ± 11	0.32 ± 0.07	0.019 ± 0.007
Diboson	289 ± 32	97 ± 24	11.8 ± 2.7	0.59 ± 0.26	0.087 ± 0.016
Total	22400 ± 1200	2460 ± 240	203 ± 19	8.7 ± 0.9	1.09 ± 0.16
Data	21945	2294	197	10	2

(Drell-Yan) and other background events, respectively. The symbol λ represents the parameter of interest of the model, and $\boldsymbol{\nu}$ is the set of Gaussian-distributed nuisance parameters incorporating the systematic uncertainties. When including the effects of interference, $\bar{n} = n_{X+Z/\gamma^*}(\lambda, \boldsymbol{\nu}) + n_{\text{obg}}(\boldsymbol{\nu})$, where n_{X+Z/γ^*} is the number of signal plus Z/γ^* events and X can be $Z_{\text{KK}}/\gamma_{\text{KK}}$ or a Minimal Z' boson. Signal templates provide the expected line-shape of the dilepton resonances.

The significance of a signal is summarized by a p -value, the probability of observing a signal-like excess at least as extreme as the one observed in data, assuming the null hypothesis. The outcome of the search is ranked using a log-likelihood ratio (LLR), with the likelihood function defined as the product of the Poisson probabilities over all mass bins in the search region, using a Z'_{SSM} template. Explicitly:

$$\text{LLR} = -2 \ln \frac{\mathcal{L}(\text{data} \mid \hat{n}_{Z'}, \hat{M}_{Z'}, \hat{\boldsymbol{\nu}})}{\mathcal{L}(\text{data} \mid (\hat{n}_{Z'} = 0), \hat{\boldsymbol{\nu}})}$$

where $\hat{n}_{Z'}$, $\hat{M}_{Z'}$, $\hat{\boldsymbol{\nu}}$ and $\hat{\hat{\boldsymbol{\nu}}}$ are respectively the best-fit values for the Z' normalization, Z' mass and nuisance parameters, which maximize the likelihood \mathcal{L} given the data, assuming in the numerator that a Z' signal is present and in the denominator that no signal is present. The LLR is scanned as a function of Z' cross section and $M_{Z'}$ over the full

considered mass range. The observed p -value for the dielectron and dimuon samples is 36% and 68%, respectively. For the combination of both channels, the observed p -value is 40%.

9 Limit-setting procedure

In the absence of a signal, upper limits on the number of events produced by the decay of a new resonance are determined at the 95% Confidence Level (CL).

The limit on the number of signal events is converted into a limit on the ratio of cross section times branching fraction $\sigma B(X \rightarrow \ell^+ \ell^-) / \sigma B(Z \rightarrow \ell^+ \ell^-)$ by dividing by the observed number of Z boson events and the ratio of corresponding acceptances. This ratio of σB is then converted into a limit on $\sigma B(X \rightarrow \ell^+ \ell^-)$ by multiplying it by the theoretical value of $\sigma B(Z \rightarrow \ell^+ \ell^-)$. Because of the strong destructive interference between Kaluza-Klein bosons and Z/γ^* , limits are set on the coupling strength of the resonance to the fermions instead of the cross section times branching ratio. The same is done for the class of Minimal Z' Models, where the coupling strength γ' is one of the two parameters defining the model.

The same Bayesian approach [70] is used in all cases, with a flat prior probability distribution for the signal cross section times branching fraction (σB), when neglecting interference. When including the effects of interference, the prior is flat for the coupling strength to the second or to the fourth power. The most likely number of signal events, and the corresponding confidence intervals, are determined from a likelihood function defined as the product of the Poisson probabilities over all mass bins in the search region, using the appropriate signal templates. The nuisance parameters are integrated out.

Most of the dilepton resonances searched for in this analysis are narrow compared to the detector resolution. The effect of width variations on the resonance line-shape is neglected for the E_6 analysis. On the other hand, the dependence of the width on the coupling strength is taken into account in the MWT, Torsion and G^* analyses by using several templates for a given pole mass in which various values of the couplings are selected. Signal templates include the acceptance times efficiency of the signal, at a given pole mass M_X , over the full search region. The product $\mathcal{A}\epsilon$ is different for each model due to different angular distributions, boosts, and line-shapes.

The expected exclusion limits are determined using simulated pseudo-experiments with only Standard Model processes by evaluating the 95% CL upper limits for each pseudo-experiment for each fixed value of the resonance pole mass M_X . The median of the distribution of limits is chosen to represent the expected limit. The ensemble of limits is also used to find the 68% and 95% envelopes of the expected limits as a function of M_X .

The combination of the dielectron and dimuon channels is performed under the assumption of lepton universality by defining the likelihood function in terms of the total number of signal events produced in both channels. For each source of uncertainty, the correlations across bins, as well as the correlations between signal and background, are taken into account.

Table 4. Mixing angle values for the E_6 models considered.

Model	Z'_ψ	Z'_N	Z'_η	Z'_I	Z'_S	Z'_χ
$\sin \theta_{E_6}$	0	$-1/4$	$\sqrt{3/8}$	$\sqrt{5/8}$	$3\sqrt{6}/8$	1
$\cos \theta_{E_6}$	1	$\sqrt{15}/4$	$\sqrt{5/8}$	$-\sqrt{3/8}$	$-\sqrt{10}/8$	0

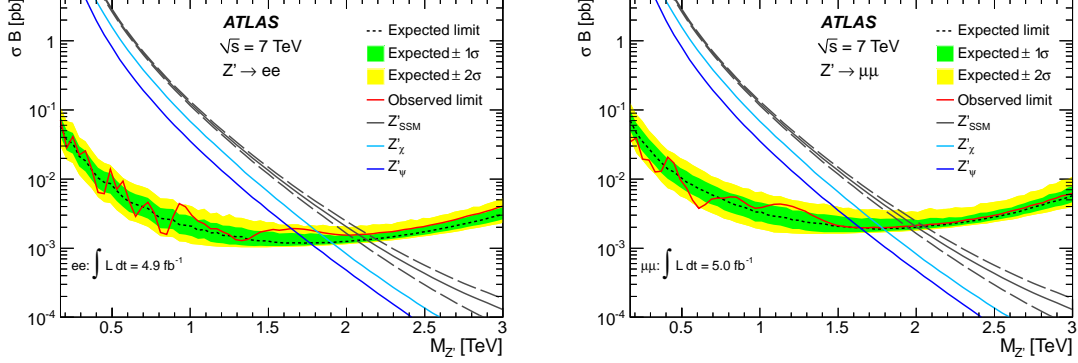


Figure 2. Expected and observed 95% CL limits on σB and expected σB for Z'_{SSM} production and the two E_6 -motivated Z' models with lowest and highest σB for the dielectron (left), and the dimuon (right) selections. The dashed lines around the Z'_{SSM} theory curve represent the theoretical uncertainty, which is similar for the other theory curves.

10 Limits on spin-1 SSM and E_6 Z' bosons

Due to mixing between the $U(1)_\chi$ and $U(1)_\psi$ groups, in the E_6 models the lightest new boson is a linear combination of the Z'_χ and Z'_ψ bosons depending on the mixing angle θ_{E_6} . For six specific values of this mixing angle, the diboson resonance is named Z'_ψ , Z'_N , Z'_η , Z'_I , Z'_S , and Z'_χ . The corresponding mixing angle values are displayed in table 4. Like the SSM, these models prescribe the couplings of the Z' boson to the SM fermions. The expected intrinsic width of the Z' boson in the E_6 models is predicted to be between 0.5% and 1.3% [71, 72] of its mass, while in the SSM the intrinsic width is predicted to be about 3%.

Figure 2 shows the 95% CL observed and expected exclusion limits on $\sigma B(Z' \rightarrow e^+e^-)$ and $\sigma B(Z' \rightarrow \mu^+\mu^-)$ obtained with Z'_{SSM} templates. It also shows the theoretical cross section times branching fraction for the Z'_{SSM} and for the lowest and highest σB of E_6 -motivated Z' models. The combination of the dielectron and dimuon channels is shown in figure 3. The rise of the σB limit at high invariant mass is due mainly to the fast fall of the parton luminosity at high momentum transfer which enhances the low-mass tail, causing a distortion in the resonance peak shape.

The 95% CL σB limit is used to set mass limits for each of the models considered. The limits obtained for the Z'_{SSM} are displayed in table 5. The combined observed (expected) mass limit for the Z'_{SSM} is 2.22 (2.25) TeV. The combined mass limits on E_6 -motivated Z'

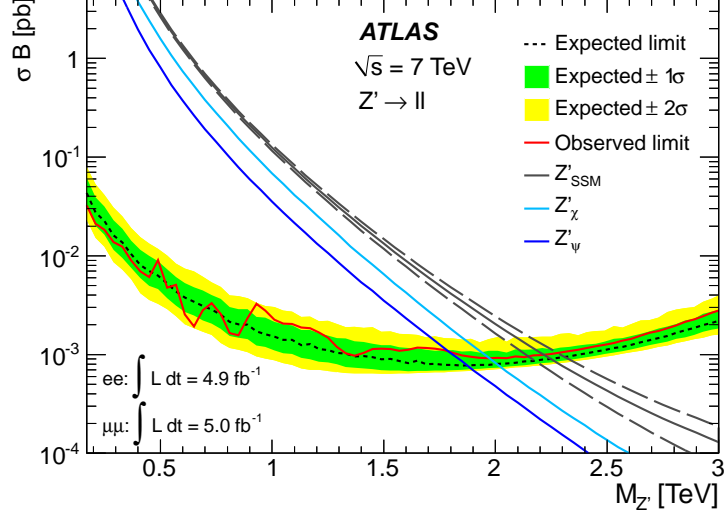


Figure 3. Expected and observed 95% CL limits on σB and expected σB for Z'_{SSM} production and the two E_6 -motivated Z' models with lowest and highest σB for the combination of the dielectron and dimuon channels. The dashed lines around the Z'_{SSM} theory curve represent the theoretical uncertainty, which is similar for the other theory curves.

Table 5. The observed and expected 95% CL lower limits on the mass of the Z'_{SSM} boson for the e^+e^- and $\mu^+\mu^-$ channels separately and for their combination.

	$Z'_{\text{SSM}} \rightarrow e^+e^-$	$Z'_{\text{SSM}} \rightarrow \mu^+\mu^-$	$Z'_{\text{SSM}} \rightarrow \ell^+\ell^-$
Observed limit [TeV]	2.08	1.99	2.22
Expected limit [TeV]	2.13	2.00	2.25

Table 6. The observed and expected 95% CL lower limits on the masses of E_6 -motivated Z' bosons. Both lepton channels are combined.

Model	Z'_ψ	Z'_N	Z'_η	Z'_1	Z'_S	Z'_χ
Observed limit [TeV]	1.79	1.79	1.87	1.86	1.91	1.97
Expected limit [TeV]	1.87	1.87	1.92	1.91	1.95	2.00

are given in table 6.

11 Limits on spin-1 Z^* bosons

A model with quark-lepton universality is adopted [73, 74] to fix the coupling strength of the Z^* boson to fermions. The gauge coupling is chosen to be the same as in the SM SU(2) group, and the scale of the new physics is proportional to the mass of the new heavy

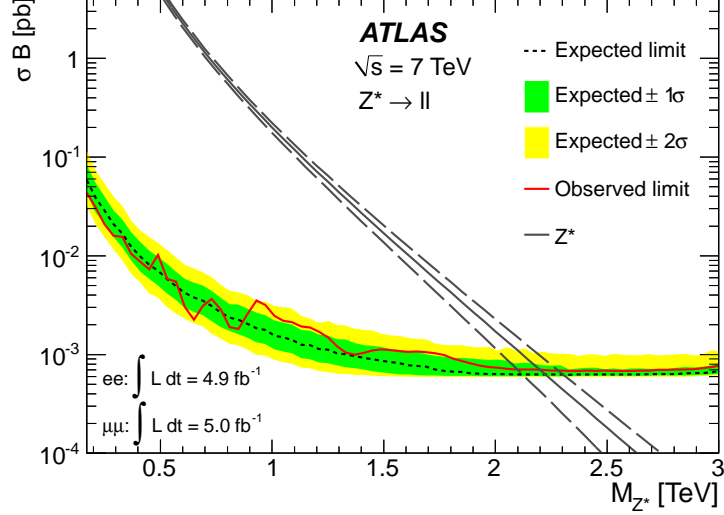


Figure 4. Expected and observed 95% CL limits on σB and expected σB for Z^* boson production for the combination of dielectron and dimuon channels. The dashed lines around the Z^* theory curve represent the theoretical uncertainty.

Table 7. The observed and expected 95% CL lower limits on the mass of the Z^* boson for the e^+e^- and $\mu^+\mu^-$ channels separately and for their combination.

	$Z^* \rightarrow e^+e^-$	$Z^* \rightarrow \mu^+\mu^-$	$Z^* \rightarrow \ell^+\ell^-$
Observed limit [TeV]	2.10	1.97	2.20
Expected limit [TeV]	2.13	1.99	2.22

bosons. The parameters of the model are fixed by requiring that the total and partial decay widths of W^* , the charged partner of Z^* , be the same as those of the W'_{SSM} boson with the same mass. The width of the Z^* is then 3.4% of its mass. As a result of the tensor form of the coupling, the Z^* does not interfere with Z/γ^* , and the angular distribution of its decay to dileptons is different from that of a Z' boson.

Figure 4 shows the 95% CL observed and expected exclusion limits on $\sigma B(Z^* \rightarrow \ell^+\ell^-)$ as well as the cross section times branching fraction expected from theory. The corresponding 95% CL limits on the mass of the Z^* boson are shown in table 7.

12 Limits on spin-2 Randall-Sundrum gravitons

The phenomenology of the RS model used in this work can be described in terms of the mass of the graviton and the ratio $k/\overline{M}_{\text{Pl}}$. The expected intrinsic width of the G^* is proportional to $(k/\overline{M}_{\text{Pl}})^2$, and is 1.4% for $k/\overline{M}_{\text{Pl}} = 0.1$. Limits at the 95% CL on $\sigma B(G^* \rightarrow \ell^+\ell^-)$ are computed assuming two values of $k/\overline{M}_{\text{Pl}}$: 0.1 and 0.2. These limits are then compared to the theoretical cross section times branching fraction assuming eight different values

Table 8. The observed and expected 95% CL lower limits on the mass of the G^* with a coupling of $k/\overline{M}_{\text{Pl}} = 0.1$ for the e^+e^- and $\mu^+\mu^-$ channels separately and for their combination.

	$G^* \rightarrow e^+e^-$	$G^* \rightarrow \mu^+\mu^-$	$G^* \rightarrow \ell^+\ell^-$
Observed limit [TeV]	2.03	1.92	2.16
Expected limit [TeV]	2.04	1.93	2.17

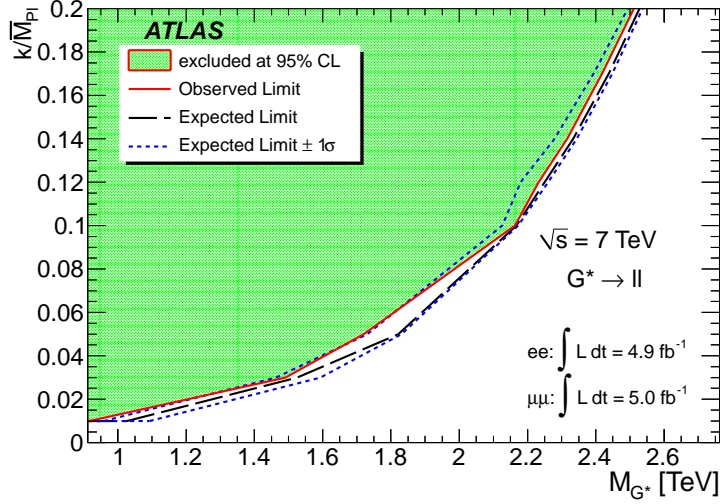


Figure 5. Exclusion regions in the plane of $k/\overline{M}_{\text{Pl}}$ versus graviton mass for the combination of dielectron and dimuon channels. The region above the curve is excluded at 95% CL.

Table 9. The observed and expected 95% CL lower limits on the mass of the G^* with varying coupling $k/\overline{M}_{\text{Pl}}$. Both lepton channels are combined.

$k/\overline{M}_{\text{Pl}}$	0.01	0.03	0.05	0.1	0.12	0.14	0.17	0.2
Observed limit [TeV]	0.92	1.49	1.72	2.16	2.23	2.32	2.42	2.51
Expected limit [TeV]	1.02	1.53	1.81	2.17	2.25	2.33	2.44	2.53

of $k/\overline{M}_{\text{Pl}}$ between 0.01 and 0.2. The σB limits obtained with $k/\overline{M}_{\text{Pl}} = 0.1$ are used for $k/\overline{M}_{\text{Pl}}$ hypotheses below or equal to 0.1, while those with $k/\overline{M}_{\text{Pl}} = 0.2$ are used for $k/\overline{M}_{\text{Pl}}$ hypotheses larger than 0.1 and below or equal to 0.2. Limits at the 95% CL on the graviton mass are derived from this comparison for each $k/\overline{M}_{\text{Pl}}$ hypothesis and are shown in table 8 for $k/\overline{M}_{\text{Pl}} = 0.1$, and in table 9 and figure 5 for the combined dilepton channel for all values of $k/\overline{M}_{\text{Pl}}$.

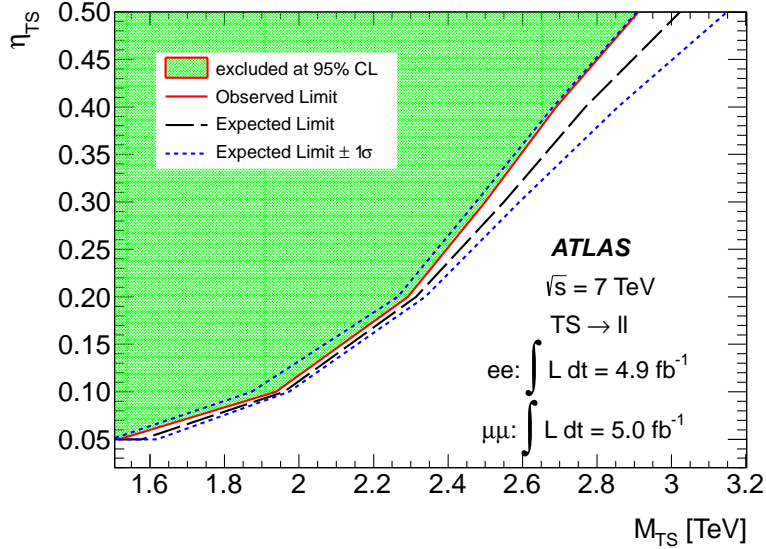


Figure 6. Exclusion regions in the plane of η_{TS} versus Torsion mass for the combination of dielectron and dimuon channels. The region above the curve is excluded at 95% CL.

13 Limits on Torsion models

The Torsion heavy state (TS) can be treated as a fundamental propagating field characterized by its mass, M_{TS} , and the couplings between TS and fermions. These couplings are assumed to be universal at the Planck scale and remain so at the TeV scale for all fermions except the top quark [24]. Therefore the phenomenology of Torsion decays to dilepton states can be described in terms of two parameters: the TS mass and one coupling (η_{TS}). Since η_{TS} can *a priori* take any value between 0 and 1, the intrinsic width could be very large. The interference effects with Z/γ^* are negligible.

Limits are computed on $\sigma B(TS \rightarrow \ell^+ \ell^-)$ for five values of η_{TS} in the range 0.1–0.5. Limits on σB are then translated into limits on M_{TS} in the same way as above for the RS graviton, by comparing them to the theoretical σB as a function of M_{TS} for each value of η_{TS} . Additionally, the σB limits obtained for $\eta_{TS} = 0.1$ are used to set mass limits for $\eta_{TS} = 0.05$, which is conservative because the TS width is smaller for $\eta_{TS} = 0.05$. The resulting exclusion region in the (M_{TS}, η_{TS}) plane is displayed in figure 6 and table 10 for the combined dielectron and dimuon channels. The limits on M_{TS} obtained in each channel for $\eta_{TS} = 0.2$ are shown in table 11.

14 Limits on Technicolor

LSTC model

The Low-scale Technicolor (LSTC) model [18, 19, 75] postulates the existence of vector (ρ_T , ω_T) and axial (a_T) techni-mesons, in addition to light techni-pions (π_T). Due to techni-isospin symmetry, ρ_T and ω_T are nearly degenerate in mass. Therefore this analysis

Table 10. The observed and expected 95% CL lower limits on the mass of Torsion heavy states with varying coupling η_{TS} . Both lepton channels are combined.

η_{TS}	0.05	0.1	0.2	0.3	0.4	0.5
Observed limit [TeV]	1.52	1.94	2.29	2.50	2.69	2.91
Expected limit [TeV]	1.58	1.96	2.31	2.55	2.77	3.02

Table 11. The observed and expected 95% CL lower limits on the mass of Torsion heavy states with a coupling of $\eta_{\text{TS}} = 0.2$ for the e^+e^- and $\mu^+\mu^-$ channels separately and for their combination.

	TS $\rightarrow e^+e^-$	TS $\rightarrow \mu^+\mu^-$	TS $\rightarrow \ell^+\ell^-$
Observed limit [TeV]	2.15	2.07	2.29
Expected limit [TeV]	2.20	2.08	2.31

Table 12. The observed and expected 95% CL lower limits on the mass of the $\rho_{\text{T}}/\omega_{\text{T}}$ in the $M_{\rho_{\text{T}}} - M_{\pi_{\text{T}}} = M_W$ hypothesis for the e^+e^- and $\mu^+\mu^-$ channels separately and for their combination.

	$\rho_{\text{T}}/\omega_{\text{T}} \rightarrow e^+e^-$	$\rho_{\text{T}}/\omega_{\text{T}} \rightarrow \mu^+\mu^-$	$\rho_{\text{T}}/\omega_{\text{T}} \rightarrow \ell^+\ell^-$
Observed limit [TeV]	0.85	0.70	0.85
Expected limit [TeV]	0.85	0.71	0.89

searches for a combination of ρ_{T} and ω_{T} , with ω_{T} being the dominant component since its branching fraction to dileptons is approximately one order of magnitude larger than that of the ρ_{T} . In this work, the LSTC parameters are chosen to be the same as in ref. [75] (in particular, the LSTC parameter $\sin \chi = 1/3$) and the mass of the a_{T} state is assumed to be 10% higher than that of ρ_{T} .

Limits are computed on σB for the decay of the techni-mesons to dilepton final states. When building the signal templates, it is assumed that the mass splitting is $M_{\rho_{\text{T}}} - M_{\pi_{\text{T}}} = M_W$. Negative interference contributions are neglected. The intrinsic widths of the ρ_{T} , ω_{T} and a_{T} resonances are much smaller than the experimental resolution. The resulting limits on the $\rho_{\text{T}}/\omega_{\text{T}}$ mass are displayed in table 12.

The σB limits are then translated into exclusion regions in the $(M_{\rho_{\text{T}}/\omega_{\text{T}}}, M_{\pi_{\text{T}}})$ plane, shown in figure 7. The notation $\rho_{\text{T}}/\omega_{\text{T}}$ indicates the combination of the two resonances. The mass splitting between ρ_{T} and π_{T} determines whether decay modes such as $\rho_{\text{T}} \rightarrow W\pi_{\text{T}}$ or multi- π_{T} are allowed kinematically. Therefore the choice of the value of the mass of π_{T} has an impact on the ratio between the a_{T} and ρ_{T} cross sections. Another foundational assumption of the LSTC model is that the walking TC gauge coupling causes an enhancement of $M_{\pi_{\text{T}}}$ relative to $M_{\rho_{\text{T}}}$ and the other vector meson masses. This tends to close off the $\rho_{\text{T}} \rightarrow \pi_{\text{T}}\pi_{\text{T}}$ decay channel and, even more strongly, closes off the ω_{T} and

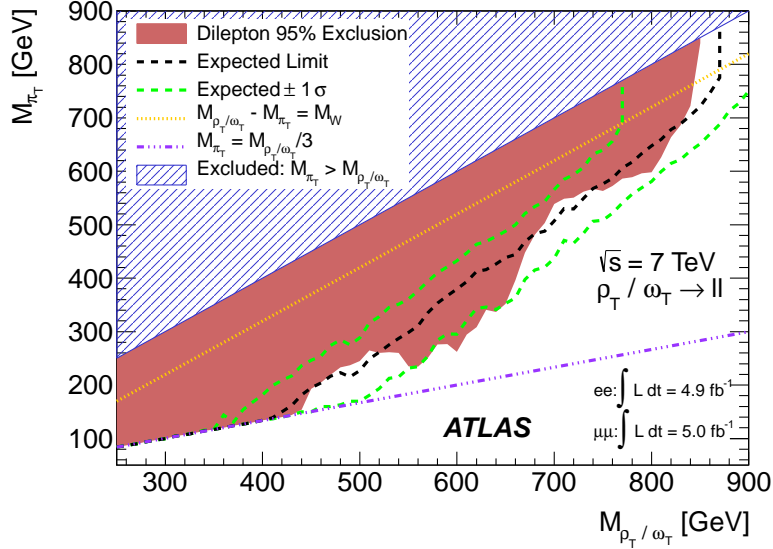


Figure 7. The 95% CL excluded region (in red) in the plane π_T mass as a function of the ρ_T/ω_T mass, assuming $M_{a_T} = 1.1 \times M_{\rho_T/\omega_T}$, for the combination of dielectron and dimuon channels. The dotted line corresponds to $M_{\rho_T/\omega_T} - M_{\pi_T} = M_W$. The black dashed line shows the expected limit, with the green dashed lines showing the $\pm 1\sigma$ bands. The blue hashed region in which $M_{\pi_T} > M_{\rho_T/\omega_T}$ is excluded by theory. This search is insensitive in the region below the purple dashed-dotted line ($M_{\pi_T} < M_{\rho_T/\omega_T}/3$).

$a_T \rightarrow 3\pi_T$ channels [76]. If $M_{\omega_T} > 3M_{\pi_T}$, the $\omega_T \rightarrow \pi_T\pi_T\pi_T$ channel opens up and quickly becomes the dominant decay mode of ω_T . Therefore the dilepton branching fractions become substantially smaller and there is no sensitivity in the $M_{\pi_T} < M_{\rho_T/\omega_T}/3$ region in the dilepton channel.

MWT model

The Minimal Walking Technicolor (MWT) [20–22] model can be characterized by the following parameters:

- bare axial and vector masses: M_A and M_V ;
- \tilde{g} , the strength of the spin-1 resonance interaction;
- M_H , the Higgs boson mass;
- s , the coupling of the Higgs boson to composite spin-1 states;
- S , the S -parameter obtained using the zeroth Weinberg Sum Rule [77, 78].

This model predicts only two resonances, R_1 and R_2 . M_{R_1} is lower than M_{R_2} and generally very close to M_A . In contrast to LSTC, R_1 and R_2 are neither degenerate nor very narrow. In this work, three free parameters have been set to $M_H = 200$ GeV, $s = 0$, and $S = 0.3$, following the recommendation from ref. [79]. The mass of the lightest resonance, M_{R_1} , is then scanned in steps of 100 GeV for various values of \tilde{g} . For each choice of \tilde{g} and M_{R_1} , the values of M_{R_2} , M_A and M_V are uniquely determined.

Table 13. The observed and expected 95% CL lower limits on the M_A parameter with varying coupling \tilde{g} . Both lepton channels are combined.

\tilde{g}	6	5	4	3	2
Observed limit [GeV]	359	485	768	1175	1566
Expected limit [GeV]	352	516	742	1233	1605

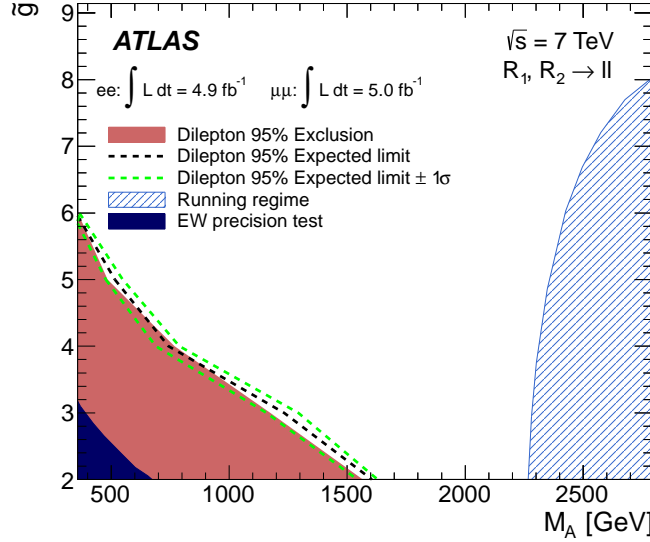


Figure 8. Bounds in the (M_A, \tilde{g}) plane of the MWT parameter space: (i) The electroweak precision measurements exclude the dark area in the bottom left corner. (ii) The requirement to stay in the walking regime excludes the hatched area in the right corner. (iii) The red area (black dashed line) shows the observed (expected) exclusion at 95% CL in the dilepton channel. The green dashed lines show the $\pm 1\sigma$ bands of the expected exclusion limit.

Limits on $\sigma B(R_1/R_2 \rightarrow \ell^+\ell^-)$ are first set as a function of M_{R_1} assuming $\tilde{g} = 2, 3, 4, 5, 6$, where the notation R_1/R_2 indicates that both resonances are taken into account in the spectrum. They are then translated into a 95% CL exclusion area in the (M_A, \tilde{g}) plane, as shown in figure 8 and table 13. The limits from the Tevatron, as well as the theoretical limits, including the requirement to stay in the walking regime, are described in detail in ref. [78]. Note that the edge of the excluded area varies only very weakly as a function of s and M_H , so a Higgs boson mass of ≈ 125 GeV would not change the results significantly. A theoretical re-interpretation of the CMS results from W' boson searches [80], in terms of the parameters M_A and \tilde{g} , is described in ref. [79].

15 Limits on spin-1 Kaluza-Klein S^1/Z_2 bosons

The model proposed in ref. [13] assumes a single extra spatial dimension with size of order 1 TeV^{-1} , compactified onto an S^1/Z_2 orbifold. In the minimal model considered here, all

of the SM fermions are on the same orbifold point. The model is completely specified by a single parameter, the compactification scale, which drives the masses of the KK modes. As for the case of Z'_{SSM} , this type of model can be classified as sequential to the Standard Model since the KK couplings are kept SM-like, although enhanced by a factor of $\sqrt{2}$. However, contrary to any of the Z' models, the interference with Z/γ^* is very strong and is a potentially distinctive feature of this type of model [12, 81].

Because of the strong destructive interference effects mentioned above, it is not possible to put limits on σB as done for the preceding models. Instead, a coupling strength g is introduced that multiplies the fermion couplings, $g_{\lambda_f}^X$, where X stands for the new massive $Z_{\text{KK}}/\gamma_{\text{KK}}$ resonance, and λ_f can be the helicity coupling, $\lambda_f = \text{L, R}$, as done in ref. [12]. The resulting differential cross section, after the $g_{\lambda_f}^X \rightarrow g \times g_{\lambda_f}^X$ transformation, is

$$\frac{d\sigma}{ds} \propto \left| Z/\gamma^* + \frac{g_{\lambda_q}^X g_{\lambda_\ell}^X}{s - m_X^2 + i\Gamma_X m_X} \right|^2 \rightarrow \left| Z/\gamma^* + g^2 \frac{g_{\lambda_q}^X g_{\lambda_\ell}^X}{s - m_X^2 + ig^2 \Gamma_X m_X} \right|^2.$$

Flat priors of g^4 and g^2 are used in the limit-setting procedure, as opposed to σB used earlier. A flat prior in g^4 can be assumed when the pure $Z_{\text{KK}}/\gamma_{\text{KK}}$ cross-section term dominates. If the interference term between $Z_{\text{KK}}/\gamma_{\text{KK}}$ and Z/γ^* dominates, a flat prior in g^2 is better motivated. Two-dimensional templates are produced in order to scan the g parameter in the region 0–2.2 and the $Z_{\text{KK}}/\gamma_{\text{KK}}$ pole masses (M_{KK}) between 130 GeV and 6 TeV.

The strong interference with the Z/γ^* implies a greater sensitivity to shape distortions, especially at the high-end of the mass window, and therefore, two more systematic uncertainties which are found to be negligible in the non-interfering channels have to be taken into account here. First, an uncertainty on the muon momentum resolution, which goes up to 20%–30% above 2.5 TeV. Second, an uncertainty on the extrapolation of the $t\bar{t}$ and diboson backgrounds, due to the fit function choice and the fit range variation; in the dimuon channel, this uncertainty ranges from 2% to 6% in the 2–3 TeV mass range, relative to the full background. These two uncertainties do not affect the dielectron channel due to a better resolution and to the dominance of the QCD and $W + \text{jets}$ background uncertainties over the $t\bar{t}$ and diboson background uncertainties.

The observed and expected limits on g^4 and g^2 are translated into limits on g , which are shown as a function of M_{KK} in figure 9 for the combination of dielectron and dimuon channels. The fast broadening of the expected one and two-sigma bands above 2 TeV is due to the destructive interference becoming the dominant feature of the signal shape.

Lower limits on M_{KK} are derived from the $Z_{\text{KK}}/\gamma_{\text{KK}}$ hypothesis ($g = 1$); they are displayed in table 14. Contrary to the non-interfering case, high-mass candidates in data induce observed limits which are better than expected. The obtained mass limits are higher than the indirect limits from electroweak precision measurements [13, 41].

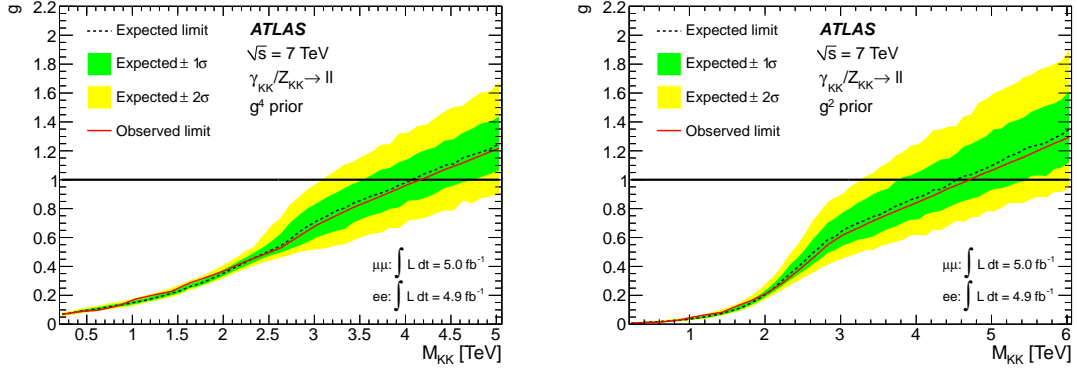


Figure 9. Expected and observed 95% CL limits on g as a function of M_{KK} , for the combination of dielectron and dimuon channels, using a flat prior on g^4 (left) and on g^2 (right).

Table 14. The observed and expected 95% CL lower limits on the mass of the Z_{KK}/γ_{KK} (i.e. $g = 1$) for the e^+e^- and $\mu^+\mu^-$ channels separately and for their combination.

	$Z_{KK}/\gamma_{KK} \rightarrow e^+e^-$	$Z_{KK}/\gamma_{KK} \rightarrow \mu^+\mu^-$	$Z_{KK}/\gamma_{KK} \rightarrow \ell^+\ell^-$
g^4 prior			
Observed Limit [TeV]	3.35	3.55	4.16
Expected Limit [TeV]	3.11	3.38	4.07
g^2 prior			
Observed Limit [TeV]	4.03	3.93	4.71
Expected Limit [TeV]	3.52	3.79	4.53

16 Limits on Minimal Z' bosons

Limits are also set in the framework of Minimal Z' Models [3]. In this framework, the coupling of the new boson Z'_{Min} to fermions is determined by its coupling to the B–L current, g_{BL} , and its coupling to the weak hypercharge Y , g_Y . It is convenient to refer to the ratios $\tilde{g}_{\text{BL}} \equiv g_{\text{BL}}/g_Z$ and $\tilde{g}_Y \equiv g_Y/g_Z$, where g_Z is the coupling of the SM Z boson defined by $g_Z = 2M_Z/v$ ($v = 246$ GeV is the Higgs vacuum expectation value in the SM). γ' and θ are chosen as independent parameters with the following definitions: $\tilde{g}_{\text{BL}} = \gamma' \cos \theta$, $\tilde{g}_Y = \gamma' \sin \theta$. The γ' parameter measures the strength of the Z'_{Min} boson coupling relative to the SM Z boson coupling, while θ determines the mixing between the generators of the B–L and the weak hypercharge Y gauge groups. Specific values of γ' and θ correspond to Z' bosons in various models such as the $Z'_{\text{B-L}}$ boson and Z'_{3R} boson.

Signal templates are built which take into account both the interference and the dependence of the Z'_{Min} boson width on γ' and θ . The coupling to hypothetical right-handed neutrinos and to W boson pairs is neglected. As for the KK model, the two-dimensional signal templates are made by reweighting the simulated Z/γ^* samples with the ratio of differential cross sections $\delta\sigma(Z'_{\text{Min}} + Z/\gamma^*)/\delta\sigma(Z/\gamma^*)$. For a given value of θ and for each of

the tested pole masses, dilepton invariant mass templates are created with varying values of γ' between 0.01 and 2. The templates at these chosen values of γ' are interpolated to all values of γ' by using a smooth interpolating function in each dilepton mass bin. The likelihood fit across all dilepton mass bins finds the most probable value of γ' for each θ and Z'_{Min} boson mass $M_{Z'_{\text{Min}}}$.

Systematic uncertainties are applied as in the case of σB limits. Limits are set on the relative coupling strength γ' as a function of the Z'_{Min} boson mass, as shown in figure 10. The two θ values yielding the minimum and maximum cross sections are used to define a band of limits in the $(\gamma', M_{Z'_{\text{Min}}})$ plane. Table 15 shows the range of the lower limits on the Z'_{Min} boson mass for representative values of γ' . The range of the upper limits on γ' for representative values of the Z'_{Min} boson mass is shown in table 16.

Table 15. Range of the observed and expected 95% CL lower limits on the Z'_{Min} boson mass for $\theta \in [0, \pi]$ and representative values of the relative coupling strength γ' . Both lepton channels are combined.

γ'	0.1	0.2
Observed range [TeV]	0.67-1.43	1.11-2.10
Expected range [TeV]	0.58-1.47	1.17-2.07

Table 16. Range of the observed and expected 95% CL upper limits on the relative coupling strength γ' for $\theta \in [0, \pi]$ and representative values of the Z'_{Min} boson mass. Both lepton channels are combined.

Z'_{Min} mass [TeV]	1	2
Observed limit	0.08-0.16	0.16-1.10
Expected limit	0.07-0.15	0.17-1.01

17 Conclusions

Searches for heavy resonances in the dilepton invariant mass spectrum have been presented. Proton-proton collisions at a center-of-mass energy of 7 TeV with 4.9 fb^{-1} in the e^+e^- channel and 5.0 fb^{-1} in the $\mu^+\mu^-$ channel have been used. The observed invariant mass spectra are consistent with the SM expectations. Limits are set on the cross section times branching fraction σB for spin-1 and spin-2 bosons. The resulting mass limits are 2.22 TeV for the Sequential Standard Model Z' boson, 1.79–1.97 TeV for various E_6 -motivated Z' bosons, and 2.16 (0.92) TeV for a Randall-Sundrum graviton G^* with the coupling parameter $k/\overline{M}_{\text{Pl}}$ equal to 0.1 (0.01). The G^* boson limits are the most stringent to date. Experimental limits have also been set on Technicolor models, on Z^* , and for the first time,

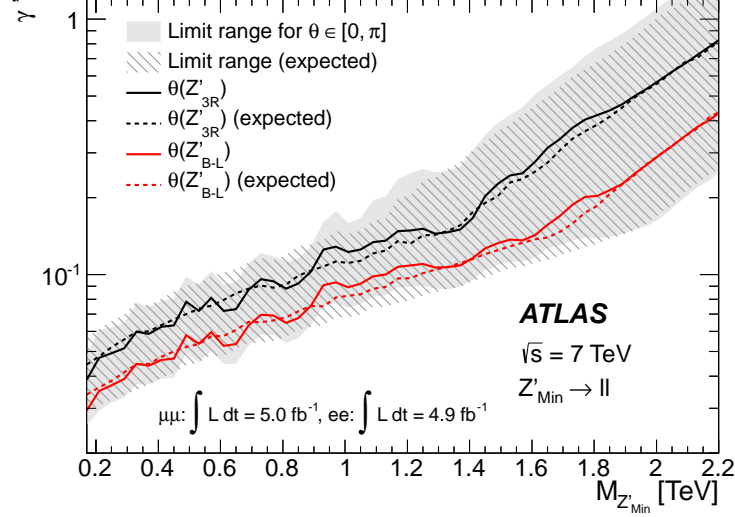


Figure 10. Expected (hatched area and dotted lines) and observed (filled area and solid lines) upper limits on γ' within the Minimal Z' Models parameterization. The limits are shown for different test masses and are obtained by combining the dielectron and dimuon channels. The gray band envelops all limit curves, which depend on the choice of θ . The lower boundary corresponds to $\tan\theta = 1.43$ and the upper boundary to $\tan\theta = -1.19$. The limit curves for two representative values of θ are shown: $\tan\theta = 0$ and $\tan\theta = -2$ which correspond to the Z'_{B-L} model and the Z'_{3R} model at specific values of γ' respectively.

on Kaluza-Klein modes of electroweak bosons, general Minimal Models of Z' bosons, and Torsion models in quantum gravity.

18 Acknowledgements

We thank Kenneth Lane for useful discussions on details of the LSTC model.

We thank CERN for the very successful operation of the LHC, as well as the support staff from our institutions without whom ATLAS could not be operated efficiently.

We acknowledge the support of ANPCyT, Argentina; YerPhI, Armenia; ARC, Australia; BMWF, Austria; ANAS, Azerbaijan; SSTC, Belarus; CNPq and FAPESP, Brazil; NSERC, NRC and CFI, Canada; CERN; CONICYT, Chile; CAS, MOST and NSFC, China; COLCIENCIAS, Colombia; MSMT CR, MPO CR and VSC CR, Czech Republic; DNRF, DNSRC and Lundbeck Foundation, Denmark; EPLANET and ERC, European Union; IN2P3-CNRS, CEA-DSM/IRFU, France; GNAS, Georgia; BMBF, DFG, HGF, MPG and AvH Foundation, Germany; GSRT, Greece; ISF, MINERVA, GIF, DIP and Benoziyo Center, Israel; INFN, Italy; MEXT and JSPS, Japan; CNRST, Morocco; FOM and NWO, Netherlands; RCN, Norway; MNiSW, Poland; GRICES and FCT, Portugal; MERYS (MECTS), Romania; MES of Russia and ROSATOM, Russian Federation; JINR; MSTB, Serbia; MSSR, Slovakia; ARRS and MVZT, Slovenia; DST/NRF, South Africa; MICINN, Spain; SRC and Wallenberg Foundation, Sweden; SER, SNSF and Cantons of

Bern and Geneva, Switzerland; NSC, Taiwan; TAEK, Turkey; STFC, the Royal Society and Leverhulme Trust, United Kingdom; DOE and NSF, United States of America.

The crucial computing support from all WLCG partners is acknowledged gratefully, in particular from CERN and the ATLAS Tier-1 facilities at TRIUMF (Canada), NDGF (Denmark, Norway, Sweden), CC-IN2P3 (France), KIT/GridKA (Germany), INFN-CNAF (Italy), NL-T1 (Netherlands), PIC (Spain), ASGC (Taiwan), RAL (UK) and BNL (USA) and in the Tier-2 facilities worldwide.

References

- [1] P. Langacker, *The Physics of Heavy Z' Gauge Bosons*, *Rev. Mod. Phys.* **81** (2009) 1199–1228.
- [2] D. London and J. L. Rosner, *Extra Gauge Bosons in $E(6)$* , *Phys. Rev.* **D34** (1986) 1530.
- [3] E. Salvioni, G. Villadoro, and F. Zwirner, *Minimal Z' models: present bounds and early LHC reach*, *JHEP* **11** (2009) 068.
- [4] G. Senjanovic and R. N. Mohapatra, *Exact Left-Right Symmetry and Spontaneous Violation of Parity*, *Phys. Rev.* **D12** (1975) 1502.
- [5] R. N. Mohapatra and J. C. Pati, *Left-Right Gauge Symmetry and an Isoconjugate Model of CP Violation*, *Phys. Rev.* **D11** (1975) 566–571.
- [6] L. Basso *et. al.*, *Phenomenology of the minimal B-L extension of the Standard model: Z' and neutrinos*, *Phys. Rev.* **D80** (2009) 055030.
- [7] M. Chizhov, V. Bednyakov, and J. Budagov, *Proposal for chiral-boson search at lhc via their unique new signature*, *Physics of Atomic Nuclei* **71** (2008) 2096–2100.
- [8] M. V. Chizhov and G. Dvali, *Origin and Phenomenology of Weak-Doublet Spin-1 Bosons*, *Phys. Lett.* **B703** (2011) 593–598.
- [9] L. Randall and R. Sundrum, *A large mass hierarchy from a small extra dimension*, *Phys. Rev. Lett.* **83** (1999) 3370–3373.
- [10] I. Antoniadis, *A Possible new dimension at a few TeV*, *Phys. Lett.* **B246** (1990) 377–384.
- [11] I. Antoniadis, K. Benakli, and M. Quiros, *Direct collider signatures of large extra dimensions*, *Phys. Lett.* **B460** (1999) 176–183.
- [12] G. Bella *et. al.*, *A search for heavy Kaluza-Klein electroweak gauge bosons at the LHC*, *JHEP* **09** (2010) 025.
- [13] T. G. Rizzo, *Testing the nature of Kaluza-Klein excitations at future lepton colliders*, *Phys. Rev.* **D61** (2000) 055005.
- [14] K. Nakamura *et. al.*, *Review of particle physics*, *J. Phys.* **G37** (2010) 075021.
- [15] S. Weinberg, *Implications of dynamical symmetry breaking: An addendum*, *Phys. Rev.* **D19** (1979) 1277–1280.
- [16] L. Susskind, *Dynamics of spontaneous symmetry breaking in the weinberg-salam theory*, *Phys. Rev.* **D20** (1979) 2619–2625.
- [17] K. D. Lane, *Technihadron production and decay in low-scale technicolor*, *Phys. Rev.* **D60** (1999) 075007.

- [18] K. D. Lane and S. Mrenna, *The Collider phenomenology of technihadrons in the technicolor straw man model*, *Phys. Rev.* **D67** (2003) 115011.
- [19] E. Eichten and K. D. Lane, *Low-scale technicolor at the Tevatron and LHC*, *Phys. Lett.* **B669** (2008) 235–238.
- [20] F. Sannino and K. Tuominen, *Orientifold theory dynamics and symmetry breaking*, *Phys. Rev.* **D71** (2005) 051901.
- [21] D. D. Dietrich, F. Sannino, and K. Tuominen, *Light composite Higgs from higher representations versus electroweak precision measurements: Predictions for LHC*, *Phys. Rev.* **D72** (2005) 055001.
- [22] R. Foadi *et. al.*, *Minimal Walking Technicolor: Set Up for Collider Physics*, *Phys. Rev.* **D76** (2007) 055005.
- [23] I. L. Shapiro, *Physical aspects of the space-time torsion*, *Phys. Rept.* **357** (2002) 113.
- [24] A. S. Belyaev, I. L. Shapiro, and M. A. B. do Vale, *Torsion phenomenology at the LHC*, *Phys. Rev.* **D75** (2007) 034014.
- [25] F. M. L. de Almeida, Jr., A. A. Nepomuceno, and M. A. B. do Vale, *Torsion Discovery Potential and Its Discrimination at CERN LHC*, *Phys. Rev.* **D79** (2009) 014029.
- [26] C. Hays, A. V. Kotwal, and O. Stelzer-Chilton, *New Techniques in the Search for Z' Bosons and Other Neutral Resonances*, *Modern Physics Letters* **A24** (2009) 2387, and references therein.
- [27] P. Langacker, *Z' Physics at the LHC*, *hep-ph/0911.4294* (2009).
- [28] **D0** Collaboration, V. M. Abazov *et. al.*, *Search for a heavy neutral gauge boson in the dielectron channel with 5.4 fb^{-1} of $p\bar{p}$ collisions at $\sqrt{s} = 1.96 \text{ TeV}$* , *Phys. Lett.* **B695** (2011) 88–94.
- [29] **CDF** Collaboration, T. Aaltonen *et. al.*, *Search for High Mass Resonances Decaying to Muon Pairs in $\sqrt{s} = 1.96 \text{ TeV}$ $p\bar{p}$ Collisions*, *Phys. Rev. Lett.* **106** (2011) 121801.
- [30] **ATLAS** Collaboration, *Search for dilepton resonances in pp collisions at $\sqrt{s} = 7 \text{ TeV}$ with the ATLAS detector*, *Phys. Rev. Lett.* **107** (2011) 272002.
- [31] **CMS** Collaboration, *Search for narrow resonances in dilepton mass spectra in pp collisions at $\sqrt{s} = 7 \text{ TeV}$* , [arXiv:1206.1849](#).
- [32] **OPAL** Collaboration, G. Abbiendi *et. al.*, *Tests of the standard model and constraints on new physics from measurements of fermion pair production at 189 GeV to 209 GeV at LEP*, *Eur. Phys. J.* **C33** (2004) 173–212.
- [33] **DELPHI** Collaboration, J. Abdallah *et. al.*, *Measurement and interpretation of fermion-pair production at LEP energies above the Z resonance*, *Eur. Phys. J.* **C45** (2006) 589–632.
- [34] **L3** Collaboration, P. Achard *et. al.*, *Measurement of hadron and lepton-pair production in e^+e^- collisions at $\sqrt{s} = 192 \text{ GeV}$ to 208 GeV at LEP*, *Eur. Phys. J.* **C47** (2006) 1–19.
- [35] **ALEPH** Collaboration, S. Schael *et. al.*, *Fermion pair production in e^+e^- collisions at 189–209 GeV and constraints on physics beyond the standard model*, *Eur. Phys. J.* **C49** (2007) 411–437.
- [36] **ATLAS** Collaboration, *Search for Extra Dimensions using diphoton events in 7 TeV proton-proton collisions with the ATLAS detector*, *Phys. Lett.* **B710** (2012) 538–556.

- [37] **CDF** Collaboration, T. Aaltonen *et. al.*, *Search for New Dielectron Resonances and Randall-Sundrum Gravitons at the Collider Detector at Fermilab*, *Phys. Rev. Lett.* **107** (2011) 051801.
- [38] **D0** Collaboration, V. M. Abazov *et. al.*, *Search for Randall-Sundrum gravitons in the dielectron and diphoton final states with 5.4 fb^{-1} of data from $p\bar{p}$ collisions at $\sqrt{s} = 1.96 \text{ TeV}$* , *Phys. Rev. Lett.* **104** (2010) 241802.
- [39] **ATLAS** Collaboration, *Search for high mass dilepton resonances in pp collisions at $\sqrt{s} = 7 \text{ TeV}$ with the ATLAS experiment*, *Phys. Lett.* **B700** (2011) 163–180.
- [40] **CDF** Collaboration, A. Abulencia *et. al.*, *Search for new high mass particles decaying to lepton pairs in $p\bar{p}$ collisions at $\sqrt{s} = 1.96 \text{ TeV}$* , *Phys. Rev. Lett.* **95** (2005) 252001.
- [41] G. Azuelos and G. Polesello, *Prospects of the detection of Kaluza-Klein excitations of gauge bosons in the ATLAS detector at the LHC*, *Eur. Phys. J.* **C39** (2004), no. 2 s1–s11.
- [42] **ATLAS** Collaboration, *The ATLAS Experiment at the Large Hadron Collider*, *JINST* **3** (2008) S08003.
- [43] **ATLAS** Collaboration, *Electron performance measurements with the ATLAS detector using the 2010 LHC proton-proton collision data*, *Eur. Phys. J.* **C72** (2012) 1909.
- [44] **ATLAS** Collaboration, *Measurement of the inclusive isolated prompt photon cross section in pp collisions at $\sqrt{s} = 7 \text{ TeV}$ with the ATLAS detector*, *Phys. Rev.* **D83** (2011) 052005.
- [45] T. Sjöstrand, S. Mrenna, and P. Z. Skands, *PYTHIA 6.4 Physics and Manual*, *JHEP* **05** (2006) 026.
- [46] A. Sherstnev and R. S. Thorne, *Parton Distributions for LO Generators*, *Eur. Phys. J.* **C55** (2008) 553.
- [47] A. Sherstnev and R. Thorne, *Different PDF approximations useful for LO Monte Carlo generators*, [arXiv:0807.2132](https://arxiv.org/abs/0807.2132).
- [48] E. Salvioni, G. Villadoro, and F. Zwirner, *Minimal Z-prime models: Present bounds and early LHC reach*, *JHEP* **0911** (2009) 068.
- [49] E. Salvioni, A. Strumia, G. Villadoro, and F. Zwirner, *Non-universal minimal Z' models: present bounds and early LHC reach*, *JHEP* **1003** (2010) 010.
- [50] T. Sjöstrand, S. Mrenna, and P. Z. Skands, *A Brief Introduction to PYTHIA 8.1*, *Comput. Phys. Commun.* **178** (2008) 852–867.
- [51] E. Boos *et. al.*, *CompHEP 4.4: Automatic computations from Lagrangians to events*, *Nucl. Instrum. Meth.* **A534** (2004) 250–259.
- [52] J. Alwall *et. al.*, *MadGraph/MadEvent v4: The New Web Generation*, *JHEP* **09** (2007) 028.
- [53] J. Pumplin *et. al.*, *New generation of parton distributions with uncertainties from global QCD analysis*, *JHEP* **07** (2002) 012.
- [54] G. Corcella *et. al.*, *HERWIG6: an event generator for hadron emission reactions with interfering gluons (including supersymmetric processes)*, *JHEP* **01** (2001) 010.
- [55] S. Frixione and B. R. Webber, *Matching NLO QCD computations and parton shower simulations*, *JHEP* **06** (2002) 029.
- [56] P. M. Nadolsky *et. al.*, *Implications of CTEQ global analysis for collider observables*, *Phys. Rev.* **D78** (2008) 013004.

- [57] J. M. Butterworth, J. R. Forshaw, and M. H. Seymour, *Multiparton interactions in photoproduction at HERA*, *Z. Phys.* **C72** (1996) 637–646.
- [58] P. Golonka and Z. Wąs, *PHOTOS Monte Carlo: a precision tool for QED corrections in Z and W decays*, *Eur. Phys. J.* **C45** (2006) 97–107.
- [59] **ATLAS** Collaboration, *The ATLAS Simulation Infrastructure*, *Eur. Phys. J.* **C70** (2010) 823–874.
- [60] S. Agostinelli *et. al.*, *GEANT4: A simulation toolkit*, *Nucl. Instrum. Meth.* **A506** (2003) 250.
- [61] R. Hamberg, W. L. van Neerven, and T. Matsuura, *A Complete calculation of the order α_s^2 correction to the Drell-Yan K factor*, *Nucl. Phys.* **B359** (1991) 343–405.
- [62] A. Martin *et. al.*, *Parton Distributions for the LHC*, *Eur. Phys. J.* **C63** (2009) 189.
- [63] M. C. Kumar, P. Mathews, V. Ravindran, and A. Tripathi, *Direct photon pair production at the LHC to $\mathcal{O}(\alpha_s)$ in TeV scale gravity models²*, *Nucl. Phys.* **B818** (2009) 28.
- [64] C. M. Carloni Calame *et. al.*, *Precision electroweak calculation of the charged current Drell-Yan process*, *JHEP* **12** (2006) 016.
- [65] C. M. Carloni Calame *et. al.*, *Precision electroweak calculation of the production of a high transverse-momentum lepton pair at hadron colliders*, *JHEP* **10** (2007) 109.
- [66] J. M. Campbell and R. K. Ellis, *An update on vector boson pair production at hadron colliders*, *Phys. Rev.* **D60** (1999) 113006.
- [67] S. Moch and P. Uwer, *Theoretical status and prospects for top-quark pair production at hadron colliders*, *Phys. Rev.* **D78** (2008) 034003.
- [68] U. Langenfeld, S. Moch, and P. Uwer, *New results for $t\bar{t}$ production at hadron colliders*, [arXiv:0907.2527](https://arxiv.org/abs/0907.2527).
- [69] **CDF** Collaboration, T. Aaltonen *et. al.*, *A Search for high-mass resonances decaying to dimuons at CDF*, *Phys. Rev. Lett.* **102** (2009) 091805.
- [70] A. Caldwell, D. Kollar, and K. Kröninger, *BAT - The Bayesian Analysis Toolkit*, *Comput. Phys. Commun.* **180** (2009) 2197.
- [71] M. Dittmar, A.-S. Nicollerat, and A. Djouadi, *Z' studies at the LHC: An update*, *Phys. Lett.* **B583** (2004) 111–120.
- [72] E. Accomando *et. al.*, *Z' physics with early LHC data*, *Phys. Rev.* **D83** (2011) 075012.
- [73] M. V. Chizhov, *A Reference Model for Anomalously Interacting Bosons*, *Phys. Part. Nucl. Lett.* **8** (2011) 512–516.
- [74] M. V. Chizhov, V. A. Bednyakov, and J. A. Budagov, *Anomalously interacting extra neutral bosons*, *Nuovo Cimento* **C33** (2010) 343.
- [75] E. Eichten *et. al.*, *Testing the Technicolor Interpretation of CDF’s Dijet Excess at the LHC*, [arXiv:1201.4396](https://arxiv.org/abs/1201.4396).
- [76] K. D. Lane and E. Eichten, *Two Scale Technicolor*, *Phys. Lett.* **B222** (1989) 274.
- [77] T. Appelquist and F. Sannino, *The Physical spectrum of conformal $SU(N)$ gauge theories*, *Phys.Rev.* **D59** (1999) 067702.
- [78] A. Belyaev *et. al.*, *Technicolor Walks at the LHC*, *Phys. Rev.* **D79** (2009) 035006.

²The authors have kindly provided updates to their calculations, at the LHC energy of 7 TeV.

- [79] J. R. Andersen, T. Hapola, and F. Sannino, *W' and Z' limits for Minimal Walking Technicolor*, *Phys. Rev.* **D85** (2012) 055017.
- [80] **CMS** Collaboration, *Search for a W' boson decaying to a muon and a neutrino in pp collisions at $\sqrt{s} = 7$ TeV*, *Phys. Lett.* **B701** (2011) 160–179.
- [81] T. G. Rizzo, *Indirect Searches for Z' -like Resonances at the LHC*, *JHEP* **08** (2009) 082.

The ATLAS Collaboration

G. Aad⁴⁸, T. Abajyan²¹, B. Abbott¹¹¹, J. Abdallah¹², S. Abdel Khalek¹¹⁵,
A.A. Abdelalim⁴⁹, O. Abdinov¹¹, R. Aben¹⁰⁵, B. Abi¹¹², M. Abolins⁸⁸, O.S. AbouZeid¹⁵⁸,
H. Abramowicz¹⁵³, H. Abreu¹³⁶, B.S. Acharya^{164a,164b}, L. Adamczyk³⁸, D.L. Adams²⁵,
T.N. Addy⁵⁶, J. Adelman¹⁷⁶, S. Adomeit⁹⁸, P. Adragna⁷⁵, T. Adye¹²⁹, S. Aefsky²³,
J.A. Aguilar-Saavedra^{124b,a}, M. Agustoni¹⁷, M. Aharrouche⁸¹, S.P. Ahlen²², F. Ahles⁴⁸,
A. Ahmad¹⁴⁸, M. Ahsan⁴¹, G. Aielli^{133a,133b}, T. Akdogan^{19a}, T.P.A. Åkesson⁷⁹,
G. Akimoto¹⁵⁵, A.V. Akimov⁹⁴, M.S. Alam², M.A. Alam⁷⁶, J. Albert¹⁶⁹, S. Albrand⁵⁵,
M. Aleksa³⁰, I.N. Aleksandrov⁶⁴, F. Alessandria^{89a}, C. Alexa^{26a}, G. Alexander¹⁵³,
G. Alexandre⁴⁹, T. Alexopoulos¹⁰, M. Alhroob^{164a,164c}, M. Aliev¹⁶, G. Alimonti^{89a},
J. Alison¹²⁰, B.M.M. Allbrooke¹⁸, P.P. Allport⁷³, S.E. Allwood-Spiers⁵³, J. Almond⁸²,
A. Aloisio^{102a,102b}, R. Alon¹⁷², A. Alonso⁷⁹, F. Alonso⁷⁰, A.D. Altheimer³⁵,
B. Alvarez Gonzalez⁸⁸, M.G. Alviggi^{102a,102b}, K. Amako⁶⁵, C. Amelung²³,
V.V. Ammosov^{128,*}, A. Amorim^{124a,b}, N. Amram¹⁵³, C. Anastopoulos³⁰, L.S. Ancu¹⁷,
N. Andari¹¹⁵, T. Andeen³⁵, C.F. Anders^{58b}, G. Anders^{58a}, K.J. Anderson³¹,
A. Andreazza^{89a,89b}, V. Andrei^{58a}, X.S. Anduaga⁷⁰, P. Anger⁴⁴, A. Angerami³⁵,
F. Anghinolfi³⁰, A. Anisenkov¹⁰⁷, N. Anjos^{124a}, A. Annovi⁴⁷, A. Antonaki⁹,
M. Antonelli⁴⁷, A. Antonov⁹⁶, J. Antos^{144b}, F. Anulli^{132a}, M. Aoki¹⁰¹, S. Aoun⁸³,
L. Aperio Bella⁵, R. Apolle^{118,c}, G. Arabidze⁸⁸, I. Aracena¹⁴³, Y. Arai⁶⁵, A.T.H. Arce⁴⁵,
S. Arfaoui¹⁴⁸, J-F. Arguin¹⁵, E. Arik^{19a,*}, M. Arik^{19a}, A.J. Armbruster⁸⁷, O. Arnaez⁸¹,
V. Arnal⁸⁰, C. Arnault¹¹⁵, A. Artamonov⁹⁵, G. Artoni^{132a,132b}, D. Arutinov²¹, S. Asai¹⁵⁵,
R. Asfandiyarov¹⁷³, S. Ask²⁸, B. Åsman^{146a,146b}, L. Asquith⁶, K. Assamagan²⁵,
A. Astbury¹⁶⁹, M. Atkinson¹⁶⁵, B. Aubert⁵, E. Auge¹¹⁵, K. Augsten¹²⁷,
M. Auresseau^{145a}, G. Avolio¹⁶³, R. Avramidou¹⁰, D. Axen¹⁶⁸, G. Azuelos^{93,d},
Y. Azuma¹⁵⁵, M.A. Baak³⁰, G. Baccaglioni^{89a}, C. Bacci^{134a,134b}, A.M. Bach¹⁵,
H. Bachacou¹³⁶, K. Bachas³⁰, M. Backes⁴⁹, M. Backhaus²¹, E. Badescu^{26a},
P. Bagnaia^{132a,132b}, S. Bahinipati³, Y. Bai^{33a}, D.C. Bailey¹⁵⁸, T. Bain¹⁵⁸, J.T. Baines¹²⁹,
O.K. Baker¹⁷⁶, M.D. Baker²⁵, S. Baker⁷⁷, E. Banas³⁹, P. Banerjee⁹³, Sw. Banerjee¹⁷³,
D. Banfi³⁰, A. Bangert¹⁵⁰, V. Bansal¹⁶⁹, H.S. Bansil¹⁸, L. Barak¹⁷², S.P. Baranov⁹⁴,
A. Barbaro Galtieri¹⁵, T. Barber⁴⁸, E.L. Barberio⁸⁶, D. Barberis^{50a,50b}, M. Barbero²¹,
D.Y. Bardin⁶⁴, T. Barillari⁹⁹, M. Barisonzi¹⁷⁵, T. Barklow¹⁴³, N. Barlow²⁸,
B.M. Barnett¹²⁹, R.M. Barnett¹⁵, A. Baroncelli^{134a}, G. Barone⁴⁹, A.J. Barr¹¹⁸,
F. Barreiro⁸⁰, J. Barreiro Guimarães da Costa⁵⁷, P. Barrillon¹¹⁵, R. Bartoldus¹⁴³,
A.E. Barton⁷¹, V. Bartsch¹⁴⁹, A. Basye¹⁶⁵, R.L. Bates⁵³, L. Batkova^{144a}, J.R. Batley²⁸,
A. Battaglia¹⁷, M. Battistin³⁰, F. Bauer¹³⁶, H.S. Bawa^{143,e}, S. Beale⁹⁸, T. Beau⁷⁸,
P.H. Beauchemin¹⁶¹, R. Beccherle^{50a}, P. Bechtel²¹, H.P. Beck¹⁷, A.K. Becker¹⁷⁵,
S. Becker⁹⁸, M. Beckingham¹³⁸, K.H. Becks¹⁷⁵, A.J. Beddall^{19c}, A. Beddall^{19c},
S. Bedikian¹⁷⁶, V.A. Bednyakov⁶⁴, C.P. Bee⁸³, L.J. Beemster¹⁰⁵, M. Begel²⁵,
S. Behar Harpaz¹⁵², M. Beimforde⁹⁹, C. Belanger-Champagne⁸⁵, P.J. Bell⁴⁹, W.H. Bell⁴⁹,
G. Bella¹⁵³, L. Bellagamba^{20a}, F. Bellina³⁰, M. Bellomo³⁰, A. Belloni⁵⁷,
O. Beloborodova^{107,f}, K. Belotskiy⁹⁶, O. Beltramello³⁰, O. Benary¹⁵³,
D. Benchekroun^{135a}, K. Bendtz^{146a,146b}, N. Benekos¹⁶⁵, Y. Benhammou¹⁵³,

E. Benhar Noccioli⁴⁹, J.A. Benitez Garcia^{159b}, D.P. Benjamin⁴⁵, M. Benoit¹¹⁵,
 J.R. Bensing²³, K. Benslama¹³⁰, S. Bentvelsen¹⁰⁵, D. Berge³⁰,
 E. Bergeaas Kuutmann⁴², N. Berger⁵, F. Berghaus¹⁶⁹, E. Berglund¹⁰⁵, J. Beringer¹⁵,
 P. Bernat⁷⁷, R. Bernhard⁴⁸, C. Bernius²⁵, T. Berry⁷⁶, C. Bertella⁸³, A. Bertin^{20a,20b},
 F. Bertolucci^{122a,122b}, M.I. Besana^{89a,89b}, G.J. Besjes¹⁰⁴, N. Besson¹³⁶, S. Bethke⁹⁹,
 W. Bhimji⁴⁶, R.M. Bianchi³⁰, M. Bianco^{72a,72b}, O. Biebel⁹⁸, S.P. Bieniek⁷⁷,
 K. Bierwagen⁵⁴, J. Biesiada¹⁵, M. Biglietti^{134a}, H. Bilokon⁴⁷, M. Bindi^{20a,20b}, S. Binet¹¹⁵,
 A. Bingul^{19c}, C. Bini^{132a,132b}, C. Biscarat¹⁷⁸, B. Bittner⁹⁹, K.M. Black²², R.E. Blair⁶,
 J.-B. Blanchard¹³⁶, G. Blanchot³⁰, T. Blazek^{144a}, I. Bloch⁴², C. Blocker²³, J. Blocki³⁹,
 A. Blondel⁴⁹, W. Blum⁸¹, U. Blumenschein⁵⁴, G.J. Bobbink¹⁰⁵, V.B. Bobrovnikov¹⁰⁷,
 S.S. Bocchetta⁷⁹, A. Bocci⁴⁵, C.R. Boddy¹¹⁸, M. Boehler⁴⁸, J. Boek¹⁷⁵, N. Boelaert³⁶,
 J.A. Bogaerts³⁰, A. Bogdanchikov¹⁰⁷, A. Bogouch^{90,*}, C. Bohm^{146a}, J. Bohm¹²⁵,
 V. Boisvert⁷⁶, T. Bold³⁸, V. Boldea^{26a}, N.M. Bolnet¹³⁶, M. Bomben⁷⁸, M. Bona⁷⁵,
 M. Boonekamp¹³⁶, S. Bordini⁷⁸, C. Borer¹⁷, A. Borisov¹²⁸, G. Borissov⁷¹,
 I. Borjanovic^{13a}, M. Borri⁸², S. Borroni⁸⁷, V. Bortolotto^{134a,134b}, K. Bos¹⁰⁵,
 D. Boscherini^{20a}, M. Bosman¹², H. Boterenbrood¹⁰⁵, J. Bouchami⁹³, J. Boudreau¹²³,
 E.V. Bouhova-Thacker⁷¹, D. Boumediene³⁴, C. Bourdarios¹¹⁵, N. Bousson⁸³, A. Boveia³¹,
 J. Boyd³⁰, I.R. Boyko⁶⁴, I. Bozovic-Jelisavcic^{13b}, J. Bracinik¹⁸, P. Branchini^{134a},
 A. Brandt⁸, G. Brandt¹¹⁸, O. Brandt⁵⁴, U. Bratzler¹⁵⁶, B. Brau⁸⁴, J.E. Brau¹¹⁴,
 H.M. Braun^{175,*}, S.F. Brazzale^{164a,164c}, B. Breliev¹⁵⁸, J. Bremer³⁰, K. Brendlinger¹²⁰,
 R. Brenner¹⁶⁶, S. Bressler¹⁷², D. Britton⁵³, F.M. Brochu²⁸, I. Brock²¹, R. Brock⁸⁸,
 F. Broggi^{89a}, C. Bromberg⁸⁸, J. Bronner⁹⁹, G. Brooijmans³⁵, T. Brooks⁷⁶,
 W.K. Brooks^{32b}, G. Brown⁸², H. Brown⁸, P.A. Bruckman de Renstrom³⁹, D. Bruncko^{144b},
 R. Bruneliere⁴⁸, S. Brunet⁶⁰, A. Bruni^{20a}, G. Bruni^{20a}, M. Bruschi^{20a}, T. Buanes¹⁴,
 Q. Buat⁵⁵, F. Bucci⁴⁹, J. Buchanan¹¹⁸, P. Buchholz¹⁴¹, R.M. Buckingham¹¹⁸,
 A.G. Buckley⁴⁶, S.I. Buda^{26a}, I.A. Budagov⁶⁴, B. Budick¹⁰⁸, V. Büscher⁸¹, L. Bugge¹¹⁷,
 O. Bulekov⁹⁶, A.C. Bundock⁷³, M. Bunse⁴³, T. Buran¹¹⁷, H. Burckhart³⁰, S. Burdin⁷³,
 T. Burgess¹⁴, S. Burke¹²⁹, E. Busato³⁴, P. Bussey⁵³, C.P. Buszello¹⁶⁶, B. Butler¹⁴³,
 J.M. Butler²², C.M. Buttar⁵³, J.M. Butterworth⁷⁷, W. Buttinger²⁸, S. Cabrera Urbán¹⁶⁷,
 D. Caforio^{20a,20b}, O. Cakir^{4a}, P. Calafiura¹⁵, G. Calderini⁷⁸, P. Calfayan⁹⁸, R. Calkins¹⁰⁶,
 L.P. Caloba^{24a}, R. Caloi^{132a,132b}, D. Calvet³⁴, S. Calvet³⁴, R. Camacho Toro³⁴,
 P. Camarri^{133a,133b}, D. Cameron¹¹⁷, L.M. Caminada¹⁵, R. Caminal Armadans¹²,
 S. Campana³⁰, M. Campanelli⁷⁷, V. Canale^{102a,102b}, F. Canelli^{31,g}, A. Canepa^{159a},
 J. Cantero⁸⁰, R. Cantrill⁷⁶, L. Capasso^{102a,102b}, M.D.M. Capeans Garrido³⁰, I. Caprini^{26a},
 M. Caprini^{26a}, D. Capriotti⁹⁹, M. Capua^{37a,37b}, R. Caputo⁸¹, R. Cardarelli^{133a},
 T. Carli³⁰, G. Carlino^{102a}, L. Carminati^{89a,89b}, B. Caron⁸⁵, S. Caron¹⁰⁴, E. Carquin^{32b},
 G.D. Carrillo Montoya¹⁷³, A.A. Carter⁷⁵, J.R. Carter²⁸, J. Carvalho^{124a,h}, D. Casadei¹⁰⁸,
 M.P. Casado¹², M. Cascella^{122a,122b}, C. Caso^{50a,50b,*}, A.M. Castaneda Hernandez^{173,i},
 E. Castaneda-Miranda¹⁷³, V. Castillo Gimenez¹⁶⁷, N.F. Castro^{124a}, G. Cataldi^{72a},
 P. Catastini⁵⁷, A. Catinaccio³⁰, J.R. Catmore³⁰, A. Cattai³⁰, G. Cattani^{133a,133b},
 S. Caughron⁸⁸, V. Cavaliere¹⁶⁵, P. Cavalleri⁷⁸, D. Cavalli^{89a}, M. Cavalli-Sforza¹²,
 V. Cavasinni^{122a,122b}, F. Ceradini^{134a,134b}, A.S. Cerqueira^{24b}, A. Cerri³⁰, L. Cerrito⁷⁵,
 F. Cerutti⁴⁷, S.A. Cetin^{19b}, A. Chafaq^{135a}, D. Chakraborty¹⁰⁶, I. Chalupkova¹²⁶,

K. Chan³, P. Chang¹⁶⁵, B. Chapleau⁸⁵, J.D. Chapman²⁸, J.W. Chapman⁸⁷,
 E. Chareyre⁷⁸, D.G. Charlton¹⁸, V. Chavda⁸², C.A. Chavez Barajas³⁰, S. Cheatham⁸⁵,
 S. Chekanov⁶, S.V. Chekulaev^{159a}, G.A. Chelkov⁶⁴, M.A. Chelstowska¹⁰⁴, C. Chen⁶³,
 H. Chen²⁵, S. Chen^{33c}, X. Chen¹⁷³, Y. Chen³⁵, A. Cheplakov⁶⁴,
 R. Cherkaoui El Moursli^{135e}, V. Chernyatin²⁵, E. Cheu⁷, S.L. Cheung¹⁵⁸, L. Chevalier¹³⁶,
 G. Chiefari^{102a,102b}, L. Chikovani^{51a,*}, J.T. Childers³⁰, A. Chilingarov⁷¹, G. Chiodini^{72a},
 A.S. Chisholm¹⁸, R.T. Chislett⁷⁷, A. Chitan^{26a}, M.V. Chizhov⁶⁴, G. Choudalakis³¹,
 S. Chouridou¹³⁷, I.A. Christidi⁷⁷, A. Christov⁴⁸, D. Chromek-Burckhart³⁰, M.L. Chu¹⁵¹,
 J. Chudoba¹²⁵, G. Ciapetti^{132a,132b}, A.K. Ciftci^{4a}, R. Ciftci^{4a}, D. Cinca³⁴, V. Cindro⁷⁴,
 C. Ciocca^{20a,20b}, A. Cicio¹⁵, M. Cirilli⁸⁷, P. Cirkovic^{13b}, M. Citterio^{89a},
 M. Ciubancan^{26a}, A. Clark⁴⁹, P.J. Clark⁴⁶, R.N. Clarke¹⁵, W. Cleland¹²³, J.C. Clemens⁸³,
 B. Clement⁵⁵, C. Clement^{146a,146b}, Y. Coadou⁸³, M. Cobal^{164a,164c}, A. Coccaro¹³⁸,
 J. Cochran⁶³, L. Coffey²³, J.G. Cogan¹⁴³, J. Coggeshall¹⁶⁵, E. Cogneras¹⁷⁸, J. Colas⁵,
 S. Cole¹⁰⁶, A.P. Colijn¹⁰⁵, N.J. Collins¹⁸, C. Collins-Tooth⁵³, J. Collot⁵⁵,
 T. Colombo^{119a,119b}, G. Colon⁸⁴, P. Conde Muiño^{124a}, E. Coniavitis¹¹⁸, M.C. Conidi¹²,
 S.M. Consonni^{89a,89b}, V. Consorti⁴⁸, S. Constantinescu^{26a}, C. Conta^{119a,119b}, G. Conti⁵⁷,
 F. Conventi^{102a,j}, M. Cooke¹⁵, B.D. Cooper⁷⁷, A.M. Cooper-Sarkar¹¹⁸, K. Copic¹⁵,
 T. Cornelissen¹⁷⁵, M. Corradi^{20a}, F. Corriveau^{85,k}, A. Cortes-Gonzalez¹⁶⁵, G. Cortiana⁹⁹,
 G. Costa^{89a}, M.J. Costa¹⁶⁷, D. Costanzo¹³⁹, D. Côté³⁰, L. Courneyea¹⁶⁹, G. Cowan⁷⁶,
 C. Cowden²⁸, B.E. Cox⁸², K. Cranmer¹⁰⁸, F. Crescioli^{122a,122b}, M. Cristinziani²¹,
 G. Crosetti^{37a,37b}, S. Crépé-Renaudin⁵⁵, C.-M. Cuciu^{26a}, C. Cuenca Almenar¹⁷⁶,
 T. Cuhadar Donszelmann¹³⁹, M. Curatolo⁴⁷, C.J. Curtis¹⁸, C. Cuthbert¹⁵⁰,
 P. Cwetanski⁶⁰, H. Czirr¹⁴¹, P. Czodrowski⁴⁴, Z. Czyzula¹⁷⁶, S. D'Auria⁵³,
 M. D'Onofrio⁷³, A. D'Orazio^{132a,132b}, M.J. Da Cunha Sargedas De Sousa^{124a},
 C. Da Via⁸², W. Dabrowski³⁸, A. Dafinca¹¹⁸, T. Dai⁸⁷, C. Dallapiccola⁸⁴, M. Dam³⁶,
 M. Dameri^{50a,50b}, D.S. Damiani¹³⁷, H.O. Danielsson³⁰, V. Dao⁴⁹, G. Darbo^{50a},
 G.L. Darlea^{26b}, J.A. Dassoulas⁴², W. Davey²¹, T. Davidek¹²⁶, N. Davidson⁸⁶,
 R. Davidson⁷¹, E. Davies^{118,c}, M. Davies⁹³, O. Davignon⁷⁸, A.R. Davison⁷⁷,
 Y. Davygora^{58a}, E. Dawe¹⁴², I. Dawson¹³⁹, R.K. Daya-Ishmukhametova²³, K. De⁸,
 R. de Asmundis^{102a}, S. De Castro^{20a,20b}, S. De Cecco⁷⁸, J. de Graat⁹⁸, N. De Groot¹⁰⁴,
 P. de Jong¹⁰⁵, C. De La Taille¹¹⁵, H. De la Torre⁸⁰, F. De Lorenzi⁶³, L. de Mora⁷¹,
 L. De Nooij¹⁰⁵, D. De Pedis^{132a}, A. De Salvo^{132a}, U. De Sanctis^{164a,164c}, A. De Santo¹⁴⁹,
 J.B. De Vivie De Regie¹¹⁵, G. De Zorzi^{132a,132b}, W.J. Dearnaley⁷¹, R. Debbe²⁵,
 C. Debenedetti⁴⁶, B. Dechenaux⁵⁵, D.V. Dedovich⁶⁴, J. Degenhardt¹²⁰,
 C. Del Papa^{164a,164c}, J. Del Peso⁸⁰, T. Del Prete^{122a,122b}, T. Delemontex⁵⁵,
 M. Deliyergiyev⁷⁴, A. Dell'Acqua³⁰, L. Dell'Asta²², M. Della Pietra^{102a,j},
 D. della Volpe^{102a,102b}, M. Delmastro⁵, P.A. Delsart⁵⁵, C. Deluca¹⁰⁵, S. Demers¹⁷⁶,
 M. Demichev⁶⁴, B. Demirkoz^{12,l}, J. Deng¹⁶³, S.P. Denisov¹²⁸, D. Derendarz³⁹,
 J.E. Derkaoui^{135d}, F. Derue⁷⁸, P. Dervan⁷³, K. Desch²¹, E. Devetak¹⁴⁸,
 P.O. Deviveiros¹⁰⁵, A. Dewhurst¹²⁹, B. DeWilde¹⁴⁸, S. Dhaliwal¹⁵⁸, R. Dhullipudi^{25,m},
 A. Di Ciaccio^{133a,133b}, L. Di Ciaccio⁵, A. Di Girolamo³⁰, B. Di Girolamo³⁰,
 S. Di Luise^{134a,134b}, A. Di Mattia¹⁷³, B. Di Micco³⁰, R. Di Nardo⁴⁷,
 A. Di Simone^{133a,133b}, R. Di Sipio^{20a,20b}, M.A. Diaz^{32a}, E.B. Diehl⁸⁷, J. Dietrich⁴²,

T.A. Dietzsch^{58a}, S. Diglio⁸⁶, K. Dindar Yagci⁴⁰, J. Dingfelder²¹, F. Dinut^{26a},
 C. Dionisi^{132a,132b}, P. Dita^{26a}, S. Dita^{26a}, F. Dittus³⁰, F. Djama⁸³, T. Djobava^{51b},
 M.A.B. do Vale^{24c}, A. Do Valle Wemans^{124a,n}, T.K.O. Doan⁵, M. Dobbs⁸⁵,
 R. Dobinson^{30,*}, D. Dobos³⁰, E. Dobson^{30,o}, J. Dodd³⁵, C. Doglioni⁴⁹, T. Doherty⁵³,
 Y. Doi^{65,*}, J. Dolejsi¹²⁶, I. Dolenc⁷⁴, Z. Dolezal¹²⁶, B.A. Dolgoshein^{96,*}, T. Dohmae¹⁵⁵,
 M. Donadelli^{24d}, J. Donini³⁴, J. Dopke³⁰, A. Doria^{102a}, A. Dos Anjos¹⁷³, A. Dotti^{122a,122b},
 M.T. Dova⁷⁰, A.D. Doxiadis¹⁰⁵, A.T. Doyle⁵³, M. Dris¹⁰, J. Dubbert⁹⁹, S. Dube¹⁵,
 E. Duchovni¹⁷², G. Duckeck⁹⁸, D. Duda¹⁷⁵, A. Dudarev³⁰, F. Dudziak⁶³, M. Dührssen³⁰,
 I.P. Duerdoth⁸², L. Dufлот¹¹⁵, M-A. Dufour⁸⁵, L. Duguid⁷⁶, M. Dunford³⁰,
 H. Duran Yildiz^{4a}, R. Duxfield¹³⁹, M. Dwuznik³⁸, F. Dydak³⁰, M. Düren⁵², J. Ebke⁹⁸,
 S. Eckweiler⁸¹, K. Edmonds⁸¹, W. Edson², C.A. Edwards⁷⁶, N.C. Edwards⁵³,
 W. Ehrenfeld⁴², T. Eifert¹⁴³, G. Eigen¹⁴, K. Einsweiler¹⁵, E. Eisenhandler⁷⁵, T. Ekelof¹⁶⁶,
 M. El Kacimi^{135c}, M. Ellert¹⁶⁶, S. Elles⁵, F. Ellinghaus⁸¹, K. Ellis⁷⁵, N. Ellis³⁰,
 J. Elmsheuser⁹⁸, M. Elsing³⁰, D. Emelianov¹²⁹, R. Engelmann¹⁴⁸, A. Engl⁹⁸, B. Epp⁶¹,
 J. Erdmann⁵⁴, A. Ereditato¹⁷, D. Eriksson^{146a}, J. Ernst², M. Ernst²⁵, J. Ernwein¹³⁶,
 D. Errede¹⁶⁵, S. Errede¹⁶⁵, E. Ertel⁸¹, M. Escalier¹¹⁵, H. Esch⁴³, C. Escobar¹²³,
 X. Espinal Curull¹², B. Esposito⁴⁷, F. Etienne⁸³, A.I. Etienvre¹³⁶, E. Etzion¹⁵³,
 D. Evangelakou⁵⁴, H. Evans⁶⁰, L. Fabbri^{20a,20b}, C. Fabre³⁰, R.M. Fakhrutdinov¹²⁸,
 S. Falciano^{132a}, Y. Fang¹⁷³, M. Fanti^{89a,89b}, A. Farbin⁸, A. Farilla^{134a}, J. Farley¹⁴⁸,
 T. Farooque¹⁵⁸, S. Farrell¹⁶³, S.M. Farrington¹⁷⁰, P. Farthouat³⁰, F. Fassi¹⁶⁷,
 P. Fassnacht³⁰, D. Fassouliotis⁹, B. Fatholahzadeh¹⁵⁸, A. Favareto^{89a,89b}, L. Fayard¹¹⁵,
 S. Fazio^{37a,37b}, R. Febbraro³⁴, P. Federic^{144a}, O.L. Fedin¹²¹, W. Fedorko⁸⁸,
 M. Fehling-Kaschek⁴⁸, L. Feligioni⁸³, D. Fellmann⁶, C. Feng^{33d}, E.J. Feng⁶,
 A.B. Fenyuk¹²⁸, J. Ferencei^{144b}, W. Fernando⁶, S. Ferrag⁵³, J. Ferrando⁵³, V. Ferrara⁴²,
 A. Ferrari¹⁶⁶, P. Ferrari¹⁰⁵, R. Ferrari^{119a}, D.E. Ferreira de Lima⁵³, A. Ferrer¹⁶⁷,
 D. Ferrere⁴⁹, C. Ferretti⁸⁷, A. Ferretto Parodi^{50a,50b}, M. Fiascaris³¹, F. Fiedler⁸¹,
 A. Filipčić⁷⁴, F. Filthaut¹⁰⁴, M. Fincke-Keeler¹⁶⁹, M.C.N. Fiolhais^{124a,h}, L. Fiorini¹⁶⁷,
 A. Firan⁴⁰, G. Fischer⁴², M.J. Fisher¹⁰⁹, M. Flechl⁴⁸, I. Fleck¹⁴¹, J. Fleckner⁸¹,
 P. Fleischmann¹⁷⁴, S. Fleischmann¹⁷⁵, T. Flick¹⁷⁵, A. Floderus⁷⁹, L.R. Flores Castillo¹⁷³,
 M.J. Flowerdew⁹⁹, T. Fonseca Martin¹⁷, A. Formica¹³⁶, A. Forti⁸², D. Fortin^{159a},
 D. Fournier¹¹⁵, H. Fox⁷¹, P. Francavilla¹², M. Franchini^{20a,20b}, S. Franchino^{119a,119b},
 D. Francis³⁰, T. Frank¹⁷², S. Franz³⁰, M. Fraternali^{119a,119b}, S. Fratina¹²⁰, S.T. French²⁸,
 C. Friedrich⁴², F. Friedrich⁴⁴, R. Froeschl³⁰, D. Froidevaux³⁰, J.A. Frost²⁸,
 C. Fukunaga¹⁵⁶, E. Fullana Torregrosa³⁰, B.G. Fulsom¹⁴³, J. Fuster¹⁶⁷, C. Gabaldon³⁰,
 O. Gabizon¹⁷², T. Gadfort²⁵, S. Gadomski⁴⁹, G. Gagliardi^{50a,50b}, P. Gagnon⁶⁰,
 C. Galea⁹⁸, E.J. Gallas¹¹⁸, V. Gallo¹⁷, B.J. Gallop¹²⁹, P. Gallus¹²⁵, K.K. Gan¹⁰⁹,
 Y.S. Gao^{143,e}, A. Gaponenko¹⁵, F. Garbersen¹⁷⁶, M. Garcia-Sciveres¹⁵, C. García¹⁶⁷,
 J.E. García Navarro¹⁶⁷, R.W. Gardner³¹, N. Garelli³⁰, H. Garitaonandia¹⁰⁵,
 V. Garonne³⁰, C. Gatti⁴⁷, G. Gaudio^{119a}, B. Gaur¹⁴¹, L. Gauthier¹³⁶, P. Gauzzi^{132a,132b},
 I.L. Gavrilenko⁹⁴, C. Gay¹⁶⁸, G. Gaycken²¹, E.N. Gazis¹⁰, P. Ge^{33d}, Z. Gecse¹⁶⁸,
 C.N.P. Gee¹²⁹, D.A.A. Geerts¹⁰⁵, Ch. Geich-Gimbel²¹, K. Gellerstedt^{146a,146b},
 C. Gemme^{50a}, A. Gemmell⁵³, M.H. Genest⁵⁵, S. Gentile^{132a,132b}, M. George⁵⁴,
 S. George⁷⁶, P. Gerlach¹⁷⁵, A. Gershon¹⁵³, C. Geweniger^{58a}, H. Ghazlane^{135b},

N. Ghodbane³⁴, B. Giacobbe^{20a}, S. Giagu^{132a,132b}, V. Giakoumopoulou⁹,
 V. Giangiobbe¹², F. Gianotti³⁰, B. Gibbard²⁵, A. Gibson¹⁵⁸, S.M. Gibson³⁰,
 D. Gillberg²⁹, A.R. Gillman¹²⁹, D.M. Gingrich^{3,d}, J. Ginzburg¹⁵³, N. Giokaris⁹,
 M.P. Giordani^{164c}, R. Giordano^{102a,102b}, F.M. Giorgi¹⁶, P. Giovannini⁹⁹, P.F. Giraud¹³⁶,
 D. Giugni^{89a}, M. Giunta⁹³, P. Giusti^{20a}, B.K. Gjelsten¹¹⁷, L.K. Gladilin⁹⁷, C. Glasman⁸⁰,
 J. Glatzer⁴⁸, A. Glazov⁴², K.W. Glitza¹⁷⁵, G.L. Glonti⁶⁴, J.R. Goddard⁷⁵, J. Godfrey¹⁴²,
 J. Godlewski³⁰, M. Goebel⁴², T. Göpfert⁴⁴, C. Goeringer⁸¹, C. Gössling⁴³, S. Goldfarb⁸⁷,
 T. Golling¹⁷⁶, A. Gomes^{124a,b}, L.S. Gomez Fajardo⁴², R. Gonçalo⁷⁶,
 J. Goncalves Pinto Firmino Da Costa⁴², L. Gonella²¹, S. González de la Hoz¹⁶⁷,
 G. Gonzalez Parra¹², M.L. Gonzalez Silva²⁷, S. Gonzalez-Sevilla⁴⁹, J.J. Goodson¹⁴⁸,
 L. Goossens³⁰, P.A. Gorbounov⁹⁵, H.A. Gordon²⁵, I. Gorelov¹⁰³, G. Gorfine¹⁷⁵,
 B. Gorini³⁰, E. Gorini^{72a,72b}, A. Gorišek⁷⁴, E. Gornicki³⁹, B. Gosdzik⁴², A.T. Goshaw⁶,
 M. Gosselink¹⁰⁵, M.I. Gostkin⁶⁴, I. Gough Eschrich¹⁶³, M. Gouighri^{135a}, D. Goujdami^{135c},
 M.P. Goulette⁴⁹, A.G. Goussiou¹³⁸, C. Goy⁵, S. Gozpinar²³, I. Grabowska-Bold³⁸,
 P. Grafström^{20a,20b}, K.-J. Grahm⁴², F. Grancagnolo^{72a}, S. Grancagnolo¹⁶, V. Grassi¹⁴⁸,
 V. Gratchev¹²¹, N. Grau³⁵, H.M. Gray³⁰, J.A. Gray¹⁴⁸, E. Graziani^{134a},
 O.G. Grebenyuk¹²¹, T. Greenshaw⁷³, Z.D. Greenwood^{25,m}, K. Gregersen³⁶,
 I.M. Gregor⁴², P. Grenier¹⁴³, J. Griffiths⁸, N. Grigalashvili⁶⁴, A.A. Grillo¹³⁷,
 S. Grinstein¹², Ph. Gris³⁴, Y.V. Grishkevich⁹⁷, J.-F. Grivaz¹¹⁵, E. Gross¹⁷²,
 J. Grosse-Knetter⁵⁴, J. Groth-Jensen¹⁷², K. Grybel¹⁴¹, D. Guest¹⁷⁶, C. Guicheney³⁴,
 S. Guindon⁵⁴, U. Gul⁵³, H. Guler^{85,p}, J. Gunther¹²⁵, B. Guo¹⁵⁸, J. Guo³⁵, P. Gutierrez¹¹¹,
 N. Guttman¹⁵³, O. Gutzwiller¹⁷³, C. Guyot¹³⁶, C. Gwenlan¹¹⁸, C.B. Gwilliam⁷³,
 A. Haas¹⁴³, S. Haas³⁰, C. Haber¹⁵, H.K. Hadavand⁴⁰, D.R. Hadley¹⁸, P. Haefner²¹,
 F. Hahn³⁰, S. Haider³⁰, Z. Hajduk³⁹, H. Hakobyan¹⁷⁷, D. Hall¹¹⁸, J. Haller⁵⁴,
 K. Hamacher¹⁷⁵, P. Hamal¹¹³, M. Hamer⁵⁴, A. Hamilton^{145b,q}, S. Hamilton¹⁶¹, L. Han^{33b},
 K. Hanagaki¹¹⁶, K. Hanawa¹⁶⁰, M. Hance¹⁵, C. Handel⁸¹, P. Hanke^{58a}, J.R. Hansen³⁶,
 J.B. Hansen³⁶, J.D. Hansen³⁶, P.H. Hansen³⁶, P. Hansson¹⁴³, K. Hara¹⁶⁰, G.A. Hare¹³⁷,
 T. Harenberg¹⁷⁵, S. Harkusha⁹⁰, D. Harper⁸⁷, R.D. Harrington⁴⁶, O.M. Harris¹³⁸,
 J. Hartert⁴⁸, F. Hartjes¹⁰⁵, T. Haruyama⁶⁵, A. Harvey⁵⁶, S. Hasegawa¹⁰¹,
 Y. Hasegawa¹⁴⁰, S. Hassani¹³⁶, S. Haug¹⁷, M. Hauschild³⁰, R. Hauser⁸⁸, M. Havranek²¹,
 C.M. Hawkes¹⁸, R.J. Hawkins³⁰, A.D. Hawkins⁷⁹, T. Hayakawa⁶⁶, T. Hayashi¹⁶⁰,
 D. Hayden⁷⁶, C.P. Hays¹¹⁸, H.S. Hayward⁷³, S.J. Haywood¹²⁹, S.J. Head¹⁸, V. Hedberg⁷⁹,
 L. Heelan⁸, S. Heim⁸⁸, B. Heinemann¹⁵, S. Heisterkamp³⁶, L. Helary²², C. Heller⁹⁸,
 M. Heller³⁰, S. Hellman^{146a,146b}, D. Hellmich²¹, C. Helsens¹², R.C.W. Henderson⁷¹,
 M. Henke^{58a}, A. Henrichs⁵⁴, A.M. Henriques Correia³⁰, S. Henrot-Versille¹¹⁵, C. Hensel⁵⁴,
 T. Henß¹⁷⁵, C.M. Hernandez⁸, Y. Hernández Jiménez¹⁶⁷, R. Herrberg¹⁶, G. Herten⁴⁸,
 R. Hertenberger⁹⁸, L. Hervas³⁰, G.G. Hesketh⁷⁷, N.P. Hessey¹⁰⁵, E. Higón-Rodríguez¹⁶⁷,
 J.C. Hill²⁸, K.H. Hiller⁴², S. Hillert²¹, S.J. Hillier¹⁸, I. Hinchliffe¹⁵, E. Hines¹²⁰,
 M. Hirose¹¹⁶, F. Hirsch⁴³, D. Hirschbuehl¹⁷⁵, J. Hobbs¹⁴⁸, N. Hod¹⁵³,
 M.C. Hodgkinson¹³⁹, P. Hodgson¹³⁹, A. Hoecker³⁰, M.R. Hoferkamp¹⁰³, J. Hoffman⁴⁰,
 D. Hoffmann⁸³, M. Hohlfeld⁸¹, M. Holder¹⁴¹, S.O. Holmgren^{146a}, T. Holy¹²⁷,
 J.L. Holzbauer⁸⁸, T.M. Hong¹²⁰, L. Hooft van Huysduynen¹⁰⁸, S. Horner⁴⁸,
 J.-Y. Hostachy⁵⁵, S. Hou¹⁵¹, A. Hoummada^{135a}, J. Howard¹¹⁸, J. Howarth⁸², I. Hristova¹⁶,

J. Hrivnac¹¹⁵, T. Hryn'ova⁵, P.J. Hsu⁸¹, S.-C. Hsu¹⁵, D. Hu³⁵, Z. Hubacek¹²⁷,
 F. Hubaut⁸³, F. Huegging²¹, A. Huettmann⁴², T.B. Huffman¹¹⁸, E.W. Hughes³⁵,
 G. Hughes⁷¹, M. Huhtinen³⁰, M. Hurwitz¹⁵, U. Husemann⁴², N. Huseynov^{64,r},
 J. Huston⁸⁸, J. Huth⁵⁷, G. Iacobucci⁴⁹, G. Iakovidis¹⁰, M. Ibbotson⁸², I. Ibragimov¹⁴¹,
 L. Iconomidou-Fayard¹¹⁵, J. Idarraga¹¹⁵, P. Iengo^{102a}, O. Igonkina¹⁰⁵, Y. Ikegami⁶⁵,
 M. Ikeno⁶⁵, D. Iliadis¹⁵⁴, N. Ilic¹⁵⁸, T. Ince²¹, J. Inigo-Golfin³⁰, P. Ioannou⁹,
 M. Iodice^{134a}, K. Iordanidou⁹, V. Ippolito^{132a,132b}, A. Irles Quiles¹⁶⁷, C. Isaksson¹⁶⁶,
 M. Ishino⁶⁷, M. Ishitsuka¹⁵⁷, R. Ishmukhametov⁴⁰, C. Issever¹¹⁸, S. Istin^{19a},
 A.V. Ivashin¹²⁸, W. Iwanski³⁹, H. Iwasaki⁶⁵, J.M. Izen⁴¹, V. Izzo^{102a}, B. Jackson¹²⁰,
 J.N. Jackson⁷³, P. Jackson¹, M.R. Jaekel³⁰, V. Jain⁶⁰, K. Jakobs⁴⁸, S. Jakobsen³⁶,
 T. Jakoubek¹²⁵, J. Jakubek¹²⁷, D.K. Jana¹¹¹, E. Jansen⁷⁷, H. Jansen³⁰, A. Jantsch⁹⁹,
 M. Janus⁴⁸, G. Jarlskog⁷⁹, L. Jeanty⁵⁷, I. Jen-La Plante³¹, D. Jennens⁸⁶, P. Jenni³⁰,
 A.E. Loevschall-Jensen³⁶, P. Jež³⁶, S. Jézéquel⁵, M.K. Jha^{20a}, H. Ji¹⁷³, W. Ji⁸¹, J. Jia¹⁴⁸,
 Y. Jiang^{33b}, M. Jimenez Belenguer⁴², S. Jin^{33a}, O. Jinnouchi¹⁵⁷, M.D. Joergensen³⁶,
 D. Joffe⁴⁰, M. Johansen^{146a,146b}, K.E. Johansson^{146a}, P. Johansson¹³⁹, S. Johnert⁴²,
 K.A. Johns⁷, K. Jon-And^{146a,146b}, G. Jones¹⁷⁰, R.W.L. Jones⁷¹, T.J. Jones⁷³, C. Joram³⁰,
 P.M. Jorge^{124a}, K.D. Joshi⁸², J. Jovicevic¹⁴⁷, T. Jovin^{13b}, X. Ju¹⁷³, C.A. Jung⁴³,
 R.M. Jungst³⁰, V. Juranek¹²⁵, P. Jussel⁶¹, A. Juste Rozas¹², S. Kabana¹⁷, M. Kaci¹⁶⁷,
 A. Kaczmarek³⁹, P. Kadlecik³⁶, M. Kado¹¹⁵, H. Kagan¹⁰⁹, M. Kagan⁵⁷,
 E. Kajomovitz¹⁵², S. Kalinin¹⁷⁵, L.V. Kalinovskaya⁶⁴, S. Kama⁴⁰, N. Kanaya¹⁵⁵,
 M. Kaneda³⁰, S. Kaneti²⁸, T. Kanno¹⁵⁷, V.A. Kantserov⁹⁶, J. Kanzaki⁶⁵, B. Kaplan¹⁰⁸,
 A. Kapliy³¹, J. Kaplon³⁰, D. Kar⁵³, M. Karagounis²¹, K. Karakostas¹⁰, M. Karnevskiy⁴²,
 V. Kartvelishvili⁷¹, A.N. Karyukhin¹²⁸, L. Kashif¹⁷³, G. Kasieczka^{58b}, R.D. Kass¹⁰⁹,
 A. Kastanas¹⁴, M. Kataoka⁵, Y. Kataoka¹⁵⁵, E. Katsoufis¹⁰, J. Katzy⁴², V. Kaushik⁷,
 K. Kawagoe⁶⁹, T. Kawamoto¹⁵⁵, G. Kawamura⁸¹, M.S. Kayl¹⁰⁵, S. Kazama¹⁵⁵,
 V.A. Kazanin¹⁰⁷, M.Y. Kazarinov⁶⁴, R. Keeler¹⁶⁹, R. Kehoe⁴⁰, M. Keil⁵⁴,
 G.D. Kekelidze⁶⁴, J.S. Keller¹³⁸, M. Kenyon⁵³, O. Kepka¹²⁵, N. Kerschen³⁰,
 B.P. Kerševan⁷⁴, S. Kersten¹⁷⁵, K. Kessoku¹⁵⁵, J. Keung¹⁵⁸, F. Khalil-zada¹¹,
 H. Khandanyan^{146a,146b}, A. Khanov¹¹², D. Kharchenko⁶⁴, A. Khodinov⁹⁶, A. Khomich^{58a},
 T.J. Khoo²⁸, G. Khorauli²¹, A. Khoroshilov¹⁷⁵, V. Khovanskiy⁹⁵, E. Khramov⁶⁴,
 J. Khubua^{51b}, H. Kim^{146a,146b}, S.H. Kim¹⁶⁰, N. Kimura¹⁷¹, O. Kind¹⁶, B.T. King⁷³,
 M. King⁶⁶, R.S.B. King¹¹⁸, J. Kirk¹²⁹, A.E. Kiryunin⁹⁹, T. Kishimoto⁶⁶, D. Kisiielewska³⁸,
 T. Kitamura⁶⁶, T. Kittelmann¹²³, K. Kiuchi¹⁶⁰, E. Kladiva^{144b}, M. Klein⁷³, U. Klein⁷³,
 K. Kleinknecht⁸¹, M. Klemetti⁸⁵, A. Klier¹⁷², P. Klimek^{146a,146b}, A. Klimentov²⁵,
 R. Klingenberg⁴³, J.A. Klinger⁸², E.B. Klinkby³⁶, T. Klioutchnikova³⁰, P.F. Klok¹⁰⁴,
 S. Klous¹⁰⁵, E.-E. Kluge^{58a}, T. Kluge⁷³, P. Kluit¹⁰⁵, S. Kluth⁹⁹, N.S. Knecht¹⁵⁸,
 E. Kneringer⁶¹, E.B.F.G. Knoops⁸³, A. Knue⁵⁴, B.R. Ko⁴⁵, T. Kobayashi¹⁵⁵, M. Kobel⁴⁴,
 M. Kocian¹⁴³, P. Kodys¹²⁶, K. Köneke³⁰, A.C. König¹⁰⁴, S. Koenig⁸¹, L. Köpke⁸¹,
 F. Koetsveld¹⁰⁴, P. Koevesarki²¹, T. Koffas²⁹, E. Koffeman¹⁰⁵, L.A. Kogan¹¹⁸,
 S. Kohlmann¹⁷⁵, F. Kohn⁵⁴, Z. Kohout¹²⁷, T. Kohriki⁶⁵, T. Koi¹⁴³, G.M. Kolachev^{107,*},
 H. Kolanoski¹⁶, V. Kolesnikov⁶⁴, I. Koletsou^{89a}, J. Koll⁸⁸, A.A. Komar⁹⁴, Y. Komori¹⁵⁵,
 T. Kondo⁶⁵, T. Kono^{42,s}, A.I. Kononov⁴⁸, R. Konoplich^{108,t}, N. Konstantinidis⁷⁷,
 S. Koperny³⁸, K. Korcyl³⁹, K. Kordas¹⁵⁴, A. Korn¹¹⁸, A. Korol¹⁰⁷, I. Korolkov¹²,

E.V. Korolkova¹³⁹, V.A. Korotkov¹²⁸, O. Kortner⁹⁹, S. Kortner⁹⁹, V.V. Kostyukhin²¹,
 S. Kotov⁹⁹, V.M. Kotov⁶⁴, A. Kotwal⁴⁵, C. Kourkouvelis⁹, V. Kouskoura¹⁵⁴,
 A. Koutsman^{159a}, R. Kowalewski¹⁶⁹, T.Z. Kowalski³⁸, W. Kozanecki¹³⁶, A.S. Kozhin¹²⁸,
 V. Kral¹²⁷, V.A. Kramarenko⁹⁷, G. Kramberger⁷⁴, M.W. Krasny⁷⁸, A. Krasznahorkay¹⁰⁸,
 J.K. Kraus²¹, S. Kreiss¹⁰⁸, F. Krejci¹²⁷, J. Kretzschmar⁷³, N. Krieger⁵⁴, P. Krieger¹⁵⁸,
 K. Kroeninger⁵⁴, H. Kroha⁹⁹, J. Kroll¹²⁰, J. Kroseberg²¹, J. Krstic^{13a}, U. Kruchonak⁶⁴,
 H. Krüger²¹, T. Kruker¹⁷, N. Krumnack⁶³, Z.V. Krumshteyn⁶⁴, T. Kubota⁸⁶, S. Kuday^{4a},
 S. Kuehn⁴⁸, A. Kugel^{58c}, T. Kuhl⁴², D. Kuhn⁶¹, V. Kukhtin⁶⁴, Y. Kulchitsky⁹⁰,
 S. Kuleshov^{32b}, C. Kummer⁹⁸, M. Kuna⁷⁸, J. Kunkle¹²⁰, A. Kupco¹²⁵, H. Kurashige⁶⁶,
 M. Kurata¹⁶⁰, Y.A. Kurochkin⁹⁰, V. Kus¹²⁵, E.S. Kuwertz¹⁴⁷, M. Kuze¹⁵⁷, J. Kvita¹⁴²,
 R. Kwee¹⁶, A. La Rosa⁴⁹, L. La Rotonda^{37a,37b}, L. Labarga⁸⁰, J. Labbe⁵, S. Lablak^{135a},
 C. Lacasta¹⁶⁷, F. Lacava^{132a,132b}, H. Lacker¹⁶, D. Lacour⁷⁸, V.R. Lacuesta¹⁶⁷,
 E. Ladygin⁶⁴, R. Lafaye⁵, B. Laforge⁷⁸, T. Lagouri¹⁷⁶, S. Lai⁴⁸, E. Laisne⁵⁵,
 M. Lamanna³⁰, L. Lambourne⁷⁷, C.L. Lampen⁷, W. Lampl⁷, E. Lancon¹³⁶,
 U. Landgraf⁴⁸, M.P.J. Landon⁷⁵, J.L. Lane⁸², V.S. Lang^{58a}, C. Lange⁴², A.J. Lankford¹⁶³,
 F. Lanni²⁵, K. Lantzsch¹⁷⁵, S. Laplace⁷⁸, C. Lapoire²¹, J.F. Laporte¹³⁶, T. Lari^{89a},
 A. Larner¹¹⁸, M. Lassnig³⁰, P. Laurelli⁴⁷, V. Lavorini^{37a,37b}, W. Lavrijsen¹⁵, P. Laycock⁷³,
 O. Le Dortz⁷⁸, E. Le Guirriec⁸³, E. Le Menedeu¹², T. LeCompte⁶, F. Ledroit-Guillon⁵⁵,
 H. Lee¹⁰⁵, J.S.H. Lee¹¹⁶, S.C. Lee¹⁵¹, L. Lee¹⁷⁶, M. Lefebvre¹⁶⁹, M. Legendre¹³⁶,
 F. Legger⁹⁸, C. Leggett¹⁵, M. Lehmacher²¹, G. Lehmann Miotto³⁰, X. Lei⁷,
 M.A.L. Leite^{24d}, R. Leitner¹²⁶, D. Lellouch¹⁷², B. Lemmer⁵⁴, V. Lendermann^{58a},
 K.J.C. Leney^{145b}, T. Lenz¹⁰⁵, G. Lenzen¹⁷⁵, B. Lenzi³⁰, K. Leonhardt⁴⁴, S. Leontsinis¹⁰,
 F. Lepold^{58a}, C. Leroy⁹³, J-R. Lessard¹⁶⁹, C.G. Lester²⁸, C.M. Lester¹²⁰, J. Levêque⁵,
 D. Levin⁸⁷, L.J. Levinson¹⁷², A. Lewis¹¹⁸, G.H. Lewis¹⁰⁸, A.M. Leyko²¹, M. Leyton¹⁶,
 B. Li⁸³, H. Li^{173,u}, S. Li^{33b,v}, X. Li⁸⁷, Z. Liang^{118,w}, H. Liao³⁴, B. Liberti^{133a},
 P. Lichard³⁰, M. Lichtnecker⁹⁸, K. Lie¹⁶⁵, W. Liebig¹⁴, C. Limbach²¹, A. Limosani⁸⁶,
 M. Limper⁶², S.C. Lin^{151,x}, F. Linde¹⁰⁵, J.T. Linnemann⁸⁸, E. Lipeles¹²⁰, A. Lipniacka¹⁴,
 T.M. Liss¹⁶⁵, D. Lissauer²⁵, A. Lister⁴⁹, A.M. Litke¹³⁷, C. Liu²⁹, D. Liu¹⁵¹, H. Liu⁸⁷,
 J.B. Liu⁸⁷, L. Liu⁸⁷, M. Liu^{33b}, Y. Liu^{33b}, M. Livan^{119a,119b}, S.S.A. Livermore¹¹⁸,
 A. Lleres⁵⁵, J. Llorente Merino⁸⁰, S.L. Lloyd⁷⁵, E. Lobodzinska⁴², P. Loch⁷,
 W.S. Lockman¹³⁷, T. Loddenkoetter²¹, F.K. Loebinger⁸², A. Loginov¹⁷⁶, C.W. Loh¹⁶⁸,
 T. Lohse¹⁶, K. Lohwasser⁴⁸, M. Lokajicek¹²⁵, V.P. Lombardo⁵, R.E. Long⁷¹, L. Lopes^{124a},
 D. Lopez Mateos⁵⁷, J. Lorenz⁹⁸, N. Lorenzo Martinez¹¹⁵, M. Losada¹⁶², P. Loscutoff¹⁵,
 F. Lo Sterzo^{132a,132b}, M.J. Losty^{159a,*}, X. Lou⁴¹, A. Lounis¹¹⁵, K.F. Loureiro¹⁶², J. Love⁶,
 P.A. Love⁷¹, A.J. Lowe^{143,e}, F. Lu^{33a}, H.J. Lubatti¹³⁸, C. Luci^{132a,132b}, A. Lucotte⁵⁵,
 A. Ludwig⁴⁴, D. Ludwig⁴², I. Ludwig⁴⁸, J. Ludwig⁴⁸, F. Luehring⁶⁰, G. Luijckx¹⁰⁵,
 W. Lukas⁶¹, D. Lumb⁴⁸, L. Luminari^{132a}, E. Lund¹¹⁷, B. Lund-Jensen¹⁴⁷, B. Lundberg⁷⁹,
 J. Lundberg^{146a,146b}, O. Lundberg^{146a,146b}, J. Lundquist³⁶, M. Lungwitz⁸¹, D. Lynn²⁵,
 E. Lytken⁷⁹, H. Ma²⁵, L.L. Ma¹⁷³, G. Maccarrone⁴⁷, A. Macchiolo⁹⁹, B. Maček⁷⁴,
 J. Machado Miguens^{124a}, R. Mackeprang³⁶, R.J. Madaras¹⁵, H.J. Maddocks⁷¹,
 W.F. Mader⁴⁴, R. Maenner^{58c}, T. Maeno²⁵, P. Mättig¹⁷⁵, S. Mättig⁸¹, L. Magnoni¹⁶³,
 E. Magradze⁵⁴, K. Mahboubi⁴⁸, S. Mahmoud⁷³, G. Mahout¹⁸, C. Maiani¹³⁶,
 C. Maidantchik^{24a}, A. Maio^{124a,b}, S. Majewski²⁵, Y. Makida⁶⁵, N. Makovec¹¹⁵, P. Mal¹³⁶,

B. Malaescu³⁰, Pa. Malecki³⁹, P. Malecki³⁹, V.P. Maleev¹²¹, F. Malek⁵⁵, U. Mallik⁶²,
 D. Malon⁶, C. Malone¹⁴³, S. Maltezos¹⁰, V. Malyshev¹⁰⁷, S. Malyukov³⁰,
 R. Mameghani⁹⁸, J. Mamuzic^{13b}, A. Manabe⁶⁵, L. Mandelli^{89a}, I. Mandić⁷⁴,
 R. Mandrysch¹⁶, J. Maneira^{124a}, A. Manfredini⁹⁹, P.S. Mangeard⁸⁸,
 L. Manhaes de Andrade Filho^{24b}, J.A. Manjarres Ramos¹³⁶, A. Mann⁵⁴,
 P.M. Manning¹³⁷, A. Manousakis-Katsikakis⁹, B. Mansoulie¹³⁶, A. Mapelli³⁰,
 L. Mapelli³⁰, L. March⁸⁰, J.F. Marchand²⁹, F. Marchese^{133a,133b}, G. Marchiori⁷⁸,
 M. Marcisovsky¹²⁵, C.P. Marino¹⁶⁹, F. Marroquim^{24a}, Z. Marshall³⁰, F.K. Martens¹⁵⁸,
 L.F. Marti¹⁷, S. Marti-Garcia¹⁶⁷, B. Martin³⁰, B. Martin⁸⁸, J.P. Martin⁹³, T.A. Martin¹⁸,
 V.J. Martin⁴⁶, B. Martin dit Latour⁴⁹, S. Martin-Haugh¹⁴⁹, M. Martinez¹²,
 V. Martinez Outschoorn⁵⁷, A.C. Martyniuk¹⁶⁹, M. Marx⁸², F. Marzano^{132a}, A. Marzin¹¹¹,
 L. Masetti⁸¹, T. Mashimo¹⁵⁵, R. Mashinistov⁹⁴, J. Masik⁸², A.L. Maslennikov¹⁰⁷,
 I. Massa^{20a,20b}, G. Massaro¹⁰⁵, N. Massol⁵, P. Mastrandrea¹⁴⁸, A. Mastroberardino^{37a,37b},
 T. Masubuchi¹⁵⁵, P. Matricon¹¹⁵, H. Matsunaga¹⁵⁵, T. Matsushita⁶⁶, C. Mattravers^{118,c},
 J. Maurer⁸³, S.J. Maxfield⁷³, A. Mayne¹³⁹, R. Mazini¹⁵¹, M. Mazur²¹,
 L. Mazzaferro^{133a,133b}, M. Mazzanti^{89a}, J. Mc Donald⁸⁵, S.P. Mc Kee⁸⁷, A. McCarn¹⁶⁵,
 R.L. McCarthy¹⁴⁸, T.G. McCarthy²⁹, N.A. McCubbin¹²⁹, K.W. McFarlane^{56,*},
 J.A. Mcfayden¹³⁹, G. Mchedlidze^{51b}, T. McLaughlan¹⁸, S.J. McMahon¹²⁹,
 R.A. McPherson^{169,k}, A. Meade⁸⁴, J. Mechnich¹⁰⁵, M. Mechtel¹⁷⁵, M. Medinnis⁴²,
 R. Meera-Lebbai¹¹¹, T. Meguro¹¹⁶, R. Mehdiyev⁹³, S. Mehlhase³⁶, A. Mehta⁷³,
 K. Meier^{58a}, B. Meirose⁷⁹, C. Melachrinou³¹, B.R. Mellado Garcia¹⁷³, F. Meloni^{89a,89b},
 L. Mendoza Navas¹⁶², Z. Meng^{151,u}, A. Mengarelli^{20a,20b}, S. Menke⁹⁹, E. Meoni¹⁶¹,
 K.M. Mercurio⁵⁷, P. Mermod⁴⁹, L. Merola^{102a,102b}, C. Meroni^{89a}, F.S. Merritt³¹,
 H. Merritt¹⁰⁹, A. Messina^{30,y}, J. Metcalfe²⁵, A.S. Mete¹⁶³, C. Meyer⁸¹, C. Meyer³¹,
 J-P. Meyer¹³⁶, J. Meyer¹⁷⁴, J. Meyer⁵⁴, T.C. Meyer³⁰, J. Miao^{33d}, S. Michal³⁰,
 L. Micu^{26a}, R.P. Middleton¹²⁹, S. Migas⁷³, L. Mijović¹³⁶, G. Mikenberg¹⁷²,
 M. Mikestikova¹²⁵, M. Mikuz⁷⁴, D.W. Miller³¹, R.J. Miller⁸⁸, W.J. Mills¹⁶⁸, C. Mills⁵⁷,
 A. Milov¹⁷², D.A. Milstead^{146a,146b}, D. Milstein¹⁷², A.A. Minaenko¹²⁸, M. Miñano
 Moya¹⁶⁷, I.A. Minashvili⁶⁴, A.I. Mincer¹⁰⁸, B. Mindur³⁸, M. Mineev⁶⁴, Y. Ming¹⁷³,
 L.M. Mir¹², G. Mirabelli^{132a}, J. Mitrevski¹³⁷, V.A. Mitsou¹⁶⁷, S. Mitsui⁶⁵,
 P.S. Miyagawa¹³⁹, J.U. Mjörnmark⁷⁹, T. Moa^{146a,146b}, V. Moeller²⁸, K. Mönig⁴²,
 N. Möser²¹, S. Mohapatra¹⁴⁸, W. Mohr⁴⁸, R. Moles-Valls¹⁶⁷, J. Monk⁷⁷, E. Monnier⁸³,
 J. Montejo Berlingen¹², F. Monticelli⁷⁰, S. Monzani^{20a,20b}, R.W. Moore³,
 G.F. Moorhead⁸⁶, C. Mora Herrera⁴⁹, A. Moraes⁵³, N. Morange¹³⁶, J. Morel⁵⁴,
 G. Morello^{37a,37b}, D. Moreno⁸¹, M. Moreno Llácer¹⁶⁷, P. Morettini^{50a}, M. Morgenstern⁴⁴,
 M. Morii⁵⁷, A.K. Morley³⁰, G. Mornacchi³⁰, J.D. Morris⁷⁵, L. Morvaj¹⁰¹, H.G. Moser⁹⁹,
 M. Mosidze^{51b}, J. Moss¹⁰⁹, R. Mount¹⁴³, E. Mountricha^{10,z}, S.V. Mouraviev^{94,*},
 E.J.W. Moyse⁸⁴, F. Mueller^{58a}, J. Mueller¹²³, K. Mueller²¹, T.A. Müller⁹⁸, T. Mueller⁸¹,
 D. Muenstermann³⁰, Y. Munwes¹⁵³, W.J. Murray¹²⁹, I. Mussche¹⁰⁵, E. Musto^{102a,102b},
 A.G. Myagkov¹²⁸, M. Myska¹²⁵, J. Nadal¹², K. Nagai¹⁶⁰, R. Nagai¹⁵⁷, K. Nagano⁶⁵,
 A. Nagarkar¹⁰⁹, Y. Nagasaka⁵⁹, M. Nagel⁹⁹, A.M. Nairz³⁰, Y. Nakahama³⁰,
 K. Nakamura¹⁵⁵, T. Nakamura¹⁵⁵, I. Nakano¹¹⁰, G. Nanava²¹, A. Napier¹⁶¹,
 R. Narayan^{58b}, M. Nash^{77,c}, T. Nattermann²¹, T. Naumann⁴², G. Navarro¹⁶²,

H.A. Neal⁸⁷, P.Yu. Nechaeva⁹⁴, T.J. Neep⁸², A. Negri^{119a,119b}, G. Negri³⁰, M. Negrini^{20a},
 S. Nektarijevic⁴⁹, A. Nelson¹⁶³, T.K. Nelson¹⁴³, S. Nemecek¹²⁵, P. Nemethy¹⁰⁸,
 A.A. Nepomuceno^{24a}, M. Nessi^{30,aa}, M.S. Neubauer¹⁶⁵, M. Neumann¹⁷⁵, A. Neusiedl⁸¹,
 R.M. Neves¹⁰⁸, P. Nevski²⁵, P.R. Newman¹⁸, V. Nguyen Thi Hong¹³⁶, R.B. Nickerson¹¹⁸,
 R. Nicolaidou¹³⁶, B. Nicquevert³⁰, F. Niedercorn¹¹⁵, J. Nielsen¹³⁷, N. Nikiforou³⁵,
 A. Nikiforov¹⁶, V. Nikolaenko¹²⁸, I. Nikolic-Audit⁷⁸, K. Nikolics⁴⁹, K. Nikolopoulos¹⁸,
 H. Nilsen⁴⁸, P. Nilsson⁸, Y. Ninomiya¹⁵⁵, A. Nisati^{132a}, R. Nisius⁹⁹, T. Nobe¹⁵⁷,
 L. Nodulman⁶, M. Nomachi¹¹⁶, I. Nomidis¹⁵⁴, S. Norberg¹¹¹, M. Nordberg³⁰,
 P.R. Norton¹²⁹, J. Novakova¹²⁶, M. Nozaki⁶⁵, L. Nozka¹¹³, I.M. Nugent^{159a},
 A.-E. Nuncio-Quiroz²¹, G. Nunes Hanninger⁸⁶, T. Nunnemann⁹⁸, E. Nurse⁷⁷,
 B.J. O'Brien⁴⁶, D.C. O'Neil¹⁴², V. O'Shea⁵³, L.B. Oakes⁹⁸, F.G. Oakham^{29,d},
 H. Oberlack⁹⁹, J. Ocariz⁷⁸, A. Och⁶⁶, S. Oda⁶⁹, S. Odaka⁶⁵, J. Odier⁸³, H. Ogren⁶⁰,
 A. Oh⁸², S.H. Oh⁴⁵, C.C. Ohm³⁰, T. Ohshima¹⁰¹, H. Okawa²⁵, Y. Okumura³¹,
 T. Okuyama¹⁵⁵, A. Olariu^{26a}, A.G. Olchevski⁶⁴, S.A. Olivares Pino^{32a}, M. Oliveira^{124a,h},
 D. Oliveira Damazio²⁵, E. Oliver Garcia¹⁶⁷, D. Olivito¹²⁰, A. Olszewski³⁹, J. Olszowska³⁹,
 A. Onofre^{124a,ab}, P.U.E. Onyisi³¹, C.J. Oram^{159a}, M.J. Oreglia³¹, Y. Oren¹⁵³,
 D. Orestano^{134a,134b}, N. Orlando^{72a,72b}, I. Orlov¹⁰⁷, C. Oropeza Barrera⁵³, R.S. Orr¹⁵⁸,
 B. Osculati^{50a,50b}, R. Ospanov¹²⁰, C. Osuna¹², G. Otero y Garzon²⁷, J.P. Ottersbach¹⁰⁵,
 M. Ouchrif^{135d}, E.A. Ouellette¹⁶⁹, F. Ould-Saada¹¹⁷, A. Ouraou¹³⁶, Q. Ouyang^{33a},
 A. Ovcharova¹⁵, M. Owen⁸², S. Owen¹³⁹, V.E. Ozcan^{19a}, N. Ozturk⁸, A. Pacheco Pages¹²,
 C. Padilla Aranda¹², S. Pagan Griso¹⁵, E. Paganis¹³⁹, C. Pahl⁹⁹, F. Paige²⁵, P. Pais⁸⁴,
 K. Pajchel¹¹⁷, G. Palacino^{159b}, C.P. Paleari⁷, S. Palestini³⁰, D. Pallin³⁴, A. Palma^{124a},
 J.D. Palmer¹⁸, Y.B. Pan¹⁷³, E. Panagiotopoulou¹⁰, P. Pani¹⁰⁵, N. Panikashvili⁸⁷,
 S. Panitkin²⁵, D. Pantea^{26a}, A. Papadelis^{146a}, Th.D. Papadopoulou¹⁰, A. Paramonov⁶,
 D. Paredes Hernandez³⁴, W. Park^{25,ac}, M.A. Parker²⁸, F. Parodi^{50a,50b}, J.A. Parsons³⁵,
 U. Parzefall⁴⁸, S. Pashapour⁵⁴, E. Pasqualucci^{132a}, S. Passaggio^{50a}, A. Passeri^{134a},
 F. Pastore^{134a,134b,*}, Fr. Pastore⁷⁶, G. Pásztor^{49,ad}, S. Patariaia¹⁷⁵, N. Patel¹⁵⁰,
 J.R. Pater⁸², S. Patricelli^{102a,102b}, T. Pauly³⁰, M. Pecsny^{144a}, S. Pedraza Lopez¹⁶⁷,
 M.I. Pedraza Morales¹⁷³, S.V. Peleganchuk¹⁰⁷, D. Pelikan¹⁶⁶, H. Peng^{33b}, B. Penning³¹,
 A. Penson³⁵, J. Penwell⁶⁰, M. Perantoni^{24a}, K. Perez^{35,ae}, T. Perez Cavalcanti⁴²,
 E. Perez Codina^{159a}, M.T. Pérez García-Estañ¹⁶⁷, V. Perez Reale³⁵, L. Perini^{89a,89b},
 H. Pernegger³⁰, R. Perrino^{72a}, P. Perrodo⁵, V.D. Peshekhonov⁶⁴, K. Peters³⁰,
 B.A. Petersen³⁰, J. Petersen³⁰, T.C. Petersen³⁶, E. Petit⁵, A. Petridis¹⁵⁴, C. Petridou¹⁵⁴,
 E. Petrolo^{132a}, F. Petrucci^{134a,134b}, D. Petschull⁴², M. Petteni¹⁴², R. Pezoa^{32b}, A. Phan⁸⁶,
 P.W. Phillips¹²⁹, G. Piacquadio³⁰, A. Picazio⁴⁹, E. Piccaro⁷⁵, M. Piccinini^{20a,20b},
 S.M. Piec⁴², R. Piegai²⁷, D.T. Pignotti¹⁰⁹, J.E. Pilcher³¹, A.D. Pilkington⁸²,
 J. Pina^{124a,b}, M. Pinamonti^{164a,164c}, A. Pinder¹¹⁸, J.L. Pinfold³, B. Pinto^{124a},
 C. Pizio^{89a,89b}, M. Plamondon¹⁶⁹, M.-A. Pleier²⁵, E. Plotnikova⁶⁴, A. Poblaguev²⁵,
 S. Poddar^{58a}, F. Podlyski³⁴, L. Poggioli¹¹⁵, D. Pohl²¹, M. Pohl⁴⁹, G. Polesello^{119a},
 A. Policicchio^{37a,37b}, A. Polini^{20a}, J. Poll⁷⁵, V. Polychronakos²⁵, D. Pomeroy²³,
 K. Pommès³⁰, L. Pontecorvo^{132a}, B.G. Pope⁸⁸, G.A. Popeneciu^{26a}, D.S. Popovic^{13a},
 A. Poppleton³⁰, X. Portell Bueso³⁰, G.E. Pospelov⁹⁹, S. Pospisil¹²⁷, I.N. Potrap⁹⁹,
 C.J. Potter¹⁴⁹, C.T. Potter¹¹⁴, G. Poulard³⁰, J. Poveda⁶⁰, V. Pozdnyakov⁶⁴, R. Prabhu⁷⁷,

P. Pralavorio⁸³, A. Pranko¹⁵, S. Prasad³⁰, R. Pravahan²⁵, S. Prell⁶³, K. Pretzl¹⁷,
 D. Price⁶⁰, J. Price⁷³, L.E. Price⁶, D. Prieur¹²³, M. Primavera^{72a}, K. Prokofiev¹⁰⁸,
 F. Prokoshin^{32b}, S. Protopopescu²⁵, J. Proudfoot⁶, X. Prudent⁴⁴, M. Przybycien³⁸,
 H. Przysieznik⁵, S. Psoroulas²¹, E. Ptacek¹¹⁴, E. Pueschel⁸⁴, J. Purdham⁸⁷,
 M. Purohit^{25,ac}, P. Puzo¹¹⁵, Y. Pylypchenko⁶², J. Qian⁸⁷, A. Quadt⁵⁴, D.R. Quarrie¹⁵,
 W.B. Quayle¹⁷³, F. Quinonez^{32a}, M. Raas¹⁰⁴, V. Radescu⁴², P. Radloff¹¹⁴, T. Rador^{19a},
 F. Ragusa^{89a,89b}, G. Rahal¹⁷⁸, A.M. Rahimi¹⁰⁹, D. Rahm²⁵, S. Rajagopalan²⁵,
 M. Rammensee⁴⁸, M. Rammes¹⁴¹, A.S. Randle-Conde⁴⁰, K. Randrianarivony²⁹,
 F. Rauscher⁹⁸, T.C. Rave⁴⁸, M. Raymond³⁰, A.L. Read¹¹⁷, D.M. Rebuzzi^{119a,119b},
 A. Redelbach¹⁷⁴, G. Redlinger²⁵, R. Reece¹²⁰, K. Reeves⁴¹, E. Reinherz-Aronis¹⁵³,
 A. Reinsch¹¹⁴, I. Reisinger⁴³, C. Rembser³⁰, Z.L. Ren¹⁵¹, A. Renaud¹¹⁵, M. Rescigno^{132a},
 S. Resconi^{89a}, B. Resende¹³⁶, P. Reznicek⁹⁸, R. Rezvani¹⁵⁸, R. Richter⁹⁹,
 E. Richter-Was^{5,af}, M. Ridel⁷⁸, M. Rijpstra¹⁰⁵, M. Rijssenbeek¹⁴⁸, A. Rimoldi^{119a,119b},
 L. Rinaldi^{20a}, R.R. Rios⁴⁰, I. Riu¹², G. Rivoltella^{89a,89b}, F. Rizatdinova¹¹², E. Rizvi⁷⁵,
 S.H. Robertson^{85,k}, A. Robichaud-Veronneau¹¹⁸, D. Robinson²⁸, J.E.M. Robinson⁸²,
 A. Robson⁵³, J.G. Rocha de Lima¹⁰⁶, C. Roda^{122a,122b}, D. Roda Dos Santos³⁰, A. Roe⁵⁴,
 S. Roe³⁰, O. Røhne¹¹⁷, S. Rolli¹⁶¹, A. Romanouk⁹⁶, M. Romano^{20a,20b}, G. Romeo²⁷,
 E. Romero Adam¹⁶⁷, N. Rompotis¹³⁸, L. Roos⁷⁸, E. Ros¹⁶⁷, S. Rosati^{132a}, K. Rosbach⁴⁹,
 A. Rose¹⁴⁹, M. Rose⁷⁶, G.A. Rosenbaum¹⁵⁸, E.I. Rosenberg⁶³, P.L. Rosendahl¹⁴,
 O. Rosenthal¹⁴¹, L. Rosselet⁴⁹, V. Rossetti¹², E. Rossi^{132a,132b}, L.P. Rossi^{50a},
 M. Rotaru^{26a}, I. Roth¹⁷², J. Rothberg¹³⁸, D. Rousseau¹¹⁵, C.R. Royon¹³⁶, A. Rozanov⁸³,
 Y. Rozen¹⁵², X. Ruan^{33a,ag}, F. Rubbo¹², I. Rubinskiy⁴², N. Ruckstuhl¹⁰⁵, V.I. Rud⁹⁷,
 C. Rudolph⁴⁴, G. Rudolph⁶¹, F. Rühr⁷, A. Ruiz-Martinez⁶³, L. Rumyantsev⁶⁴,
 Z. Rurikova⁴⁸, N.A. Rusakovich⁶⁴, J.P. Rutherford⁷, C. Ruwiedel^{15,*}, P. Ruzicka¹²⁵,
 Y.F. Ryabov¹²¹, M. Rybar¹²⁶, G. Rybkin¹¹⁵, N.C. Ryder¹¹⁸, A.F. Saavedra¹⁵⁰,
 I. Sadeh¹⁵³, H.F.W. Sadrozinski¹³⁷, R. Sadykov⁶⁴, F. Safai Tehrani^{132a}, H. Sakamoto¹⁵⁵,
 G. Salamanna⁷⁵, A. Salamon^{133a}, M. Saleem¹¹¹, D. Salek³⁰, D. Salihagic⁹⁹,
 A. Salnikov¹⁴³, J. Salt¹⁶⁷, B.M. Salvachua Ferrando⁶, D. Salvatore^{37a,37b}, F. Salvatore¹⁴⁹,
 A. Salvucci¹⁰⁴, A. Salzburger³⁰, D. Sampsonidis¹⁵⁴, B.H. Samset¹¹⁷, A. Sanchez^{102a,102b},
 V. Sanchez Martinez¹⁶⁷, H. Sandaker¹⁴, H.G. Sander⁸¹, M.P. Sanders⁹⁸, M. Sandhoff¹⁷⁵,
 T. Sandoval²⁸, C. Sandoval¹⁶², R. Sandstroem⁹⁹, D.P.C. Sankey¹²⁹, A. Sansoni⁴⁷,
 C. Santamarina Rios⁸⁵, C. Santoni³⁴, R. Santonico^{133a,133b}, H. Santos^{124a},
 J.G. Saraiva^{124a}, T. Sarangi¹⁷³, E. Sarkisyan-Grinbaum⁸, F. Sarri^{122a,122b},
 G. Sartisohn¹⁷⁵, O. Sasaki⁶⁵, Y. Sasaki¹⁵⁵, N. Sasao⁶⁷, I. Satsounkevitch⁹⁰, G. Sauvage^{5,*},
 E. Sauvan⁵, J.B. Sauvan¹¹⁵, P. Savard^{158,d}, V. Savinov¹²³, D.O. Savu³⁰, L. Sawyer^{25,m},
 D.H. Saxon⁵³, J. Saxon¹²⁰, C. Sbarra^{20a}, A. Sbrizzi^{20a,20b}, D.A. Scannicchio¹⁶³,
 M. Scarcella¹⁵⁰, J. Schaarschmidt¹¹⁵, P. Schacht⁹⁹, D. Schaefer¹²⁰, U. Schäfer⁸¹,
 S. Schaepe²¹, S. Schaetzel^{58b}, A.C. Schaffer¹¹⁵, D. Schaile⁹⁸, R.D. Schamberger¹⁴⁸,
 A.G. Schamov¹⁰⁷, V. Scharf^{58a}, V.A. Schegelsky¹²¹, D. Scheirich⁸⁷, M. Schernau¹⁶³,
 M.I. Scherzer³⁵, C. Schiavi^{50a,50b}, J. Schieck⁹⁸, M. Schioppa^{37a,37b}, S. Schlenker³⁰,
 E. Schmidt⁴⁸, K. Schmieden²¹, C. Schmitt⁸¹, S. Schmitt^{58b}, M. Schmitz²¹, B. Schneider¹⁷,
 U. Schnoor⁴⁴, A. Schoening^{58b}, A.L.S. Schorlemmer⁵⁴, M. Schott³⁰, D. Schouten^{159a},
 J. Schovancova¹²⁵, M. Schram⁸⁵, C. Schroeder⁸¹, N. Schroer^{58c}, M.J. Schultens²¹,

J. Schultes¹⁷⁵, H.-C. Schultz-Coulon^{58a}, H. Schulz¹⁶, M. Schumacher⁴⁸, B.A. Schumm¹³⁷,
 Ph. Schune¹³⁶, C. Schwanenberger⁸², A. Schwartzman¹⁴³, Ph. Schwegler⁹⁹,
 Ph. Schwemling⁷⁸, R. Schwienhorst⁸⁸, R. Schwierz⁴⁴, J. Schwindling¹³⁶, T. Schwindt²¹,
 M. Schwoerer⁵, G. Sciolla²³, W.G. Scott¹²⁹, J. Searcy¹¹⁴, G. Sedov⁴², E. Sedykh¹²¹,
 S.C. Seidel¹⁰³, A. Seiden¹³⁷, F. Seifert⁴⁴, J.M. Seixas^{24a}, G. Sekhniaidze^{102a},
 S.J. Sekula⁴⁰, K.E. Selbach⁴⁶, D.M. Seliverstov¹²¹, B. Sellden^{146a}, G. Sellers⁷³,
 M. Seman^{144b}, N. Semprini-Cesari^{20a,20b}, C. Serfon⁹⁸, L. Serin¹¹⁵, L. Serkin⁵⁴,
 R. Seuster⁹⁹, H. Severini¹¹¹, A. Sfyrla³⁰, E. Shabalina⁵⁴, M. Shamim¹¹⁴, L.Y. Shan^{33a},
 J.T. Shank²², Q.T. Shao⁸⁶, M. Shapiro¹⁵, P.B. Shatalov⁹⁵, K. Shaw^{164a,164c},
 D. Sherman¹⁷⁶, P. Sherwood⁷⁷, A. Shibata¹⁰⁸, S. Shimizu¹⁰¹, M. Shimojima¹⁰⁰, T. Shin⁵⁶,
 M. Shiyakova⁶⁴, A. Shmeleva⁹⁴, M.J. Shochet³¹, D. Short¹¹⁸, S. Shrestha⁶³, E. Shulga⁹⁶,
 M.A. Shupe⁷, P. Sicho¹²⁵, A. Sidoti^{132a}, F. Siegert⁴⁸, Dj. Sijacki^{13a}, O. Silbert¹⁷²,
 J. Silva^{124a}, Y. Silver¹⁵³, D. Silverstein¹⁴³, S.B. Silverstein^{146a}, V. Simak¹²⁷,
 O. Simard¹³⁶, Lj. Simic^{13a}, S. Simion¹¹⁵, E. Simioni⁸¹, B. Simmons⁷⁷,
 R. Simoniello^{89a,89b}, M. Simonyan³⁶, P. Sinervo¹⁵⁸, N.B. Sinev¹¹⁴, V. Sipica¹⁴¹,
 G. Siragusa¹⁷⁴, A. Sircar²⁵, A.N. Sisakyan^{64,*}, S.Yu. Sivoklov⁹⁷, J. Sjölin^{146a,146b},
 T.B. Sjursen¹⁴, L.A. Skinnari¹⁵, H.P. Skottowe⁵⁷, K. Skovpen¹⁰⁷, P. Skubic¹¹¹,
 M. Slater¹⁸, T. Slavicek¹²⁷, K. Sliwa¹⁶¹, V. Smakhtin¹⁷², B.H. Smart⁴⁶, S.L. Smestad¹¹⁷,
 S.Yu. Smirnov⁹⁶, Y. Smirnov⁹⁶, L.N. Smirnova⁹⁷, O. Smirnova⁷⁹, B.C. Smith⁵⁷,
 D. Smith¹⁴³, K.M. Smith⁵³, M. Smizanska⁷¹, K. Smolek¹²⁷, A.A. Snesarev⁹⁴,
 S.W. Snow⁸², J. Snow¹¹¹, S. Snyder²⁵, R. Sobie^{169,k}, J. Sodomka¹²⁷, A. Soffer¹⁵³,
 C.A. Solans¹⁶⁷, M. Solar¹²⁷, J. Solc¹²⁷, E.Yu. Soldatov⁹⁶, U. Soldevila¹⁶⁷,
 E. Solfaroli Camillocci^{132a,132b}, A.A. Solodkov¹²⁸, O.V. Solovyanov¹²⁸, V. Solovyev¹²¹,
 N. Soni¹, V. Sopko¹²⁷, B. Sopko¹²⁷, M. Sosebee⁸, R. Soualah^{164a,164c}, A. Soukharev¹⁰⁷,
 S. Spagnolo^{72a,72b}, F. Spanò⁷⁶, R. Spighi^{20a}, G. Spigo³⁰, R. Spiwoks³⁰, M. Spousta^{126,ah},
 T. Spreitzer¹⁵⁸, B. Spurlock⁸, R.D. St. Denis⁵³, J. Stahlman¹²⁰, R. Stamen^{58a},
 E. Stanecka³⁹, R.W. Stanek⁶, C. Stanescu^{134a}, M. Stanescu-Bellu⁴², M.M. Stanitzki⁴²,
 S. Stapnes¹¹⁷, E.A. Starchenko¹²⁸, J. Stark⁵⁵, P. Staroba¹²⁵, P. Starovoitov⁴²,
 R. Staszewski³⁹, A. Staude⁹⁸, P. Stavina^{144a,*}, G. Steele⁵³, P. Steinbach⁴⁴, P. Steinberg²⁵,
 I. Stekl¹²⁷, B. Stelzer¹⁴², H.J. Stelzer⁸⁸, O. Stelzer-Chilton^{159a}, H. Stenzel⁵², S. Stern⁹⁹,
 G.A. Stewart³⁰, J.A. Stillings²¹, M.C. Stockton⁸⁵, K. Stoerig⁴⁸, G. Stoicea^{26a},
 S. Stonjek⁹⁹, P. Strachota¹²⁶, A.R. Stradling⁸, A. Straessner⁴⁴, J. Strandberg¹⁴⁷,
 S. Strandberg^{146a,146b}, A. Strandlie¹¹⁷, M. Strang¹⁰⁹, E. Strauss¹⁴³, M. Strauss¹¹¹,
 P. Strizenec^{144b}, R. Ströhmer¹⁷⁴, D.M. Strom¹¹⁴, J.A. Strong^{76,*}, R. Stroynowski⁴⁰,
 J. Strube¹²⁹, B. Stugu¹⁴, I. Stumer^{25,*}, J. Stupak¹⁴⁸, P. Sturm¹⁷⁵, N.A. Styles⁴²,
 D.A. Soh^{151,w}, D. Su¹⁴³, H.S. Subramania³, A. Succurro¹², Y. Sugaya¹¹⁶, C. Suhr¹⁰⁶,
 M. Suk¹²⁶, V.V. Sulin⁹⁴, S. Sultansoy^{4d}, T. Sumida⁶⁷, X. Sun⁵⁵, J.E. Sundermann⁴⁸,
 K. Suruliz¹³⁹, G. Susinno^{37a,37b}, M.R. Sutton¹⁴⁹, Y. Suzuki⁶⁵, Y. Suzuki⁶⁶, M. Svatos¹²⁵,
 S. Swedish¹⁶⁸, I. Sykora^{144a}, T. Sykora¹²⁶, J. Sánchez¹⁶⁷, D. Ta¹⁰⁵, K. Tackmann⁴²,
 A. Taffard¹⁶³, R. Tafrout^{159a}, N. Taiblum¹⁵³, Y. Takahashi¹⁰¹, H. Takai²⁵,
 R. Takashima⁶⁸, H. Takeda⁶⁶, T. Takeshita¹⁴⁰, Y. Takubo⁶⁵, M. Talby⁸³,
 A. Talyshchev^{107,f}, M.C. Tamsett²⁵, J. Tanaka¹⁵⁵, R. Tanaka¹¹⁵, S. Tanaka¹³¹, S. Tanaka⁶⁵,
 A.J. Tanasijczuk¹⁴², K. Tani⁶⁶, N. Tannoury⁸³, S. Tapprogge⁸¹, D. Tardif¹⁵⁸, S. Tarem¹⁵²,

F. Tarrade²⁹, G.F. Tartarelli^{89a}, P. Tas¹²⁶, M. Tasevsky¹²⁵, E. Tassi^{37a,37b},
 M. Tatarkhanov¹⁵, Y. Tayalati^{135d}, C. Taylor⁷⁷, F.E. Taylor⁹², G.N. Taylor⁸⁶,
 W. Taylor^{159b}, M. Teinturier¹¹⁵, F.A. Teischinger³⁰, M. Teixeira Dias Castanheira⁷⁵,
 P. Teixeira-Dias⁷⁶, K.K. Temming⁴⁸, H. Ten Kate³⁰, P.K. Teng¹⁵¹, S. Terada⁶⁵,
 K. Terashi¹⁵⁵, J. Terron⁸⁰, M. Testa⁴⁷, R.J. Teuscher^{158,k}, J. Therhaag²¹,
 T. Theveneaux-Pelzer⁷⁸, S. Thoma⁴⁸, J.P. Thomas¹⁸, E.N. Thompson³⁵,
 P.D. Thompson¹⁸, P.D. Thompson¹⁵⁸, A.S. Thompson⁵³, L.A. Thomsen³⁶,
 E. Thomson¹²⁰, M. Thomson²⁸, W.M. Thong⁸⁶, R.P. Thun⁸⁷, F. Tian³⁵, M.J. Tibbetts¹⁵,
 T. Tic¹²⁵, V.O. Tikhomirov⁹⁴, Y.A. Tikhonov^{107,f}, S. Timoshenko⁹⁶, P. Tipton¹⁷⁶,
 S. Tisserant⁸³, T. Todorov⁵, S. Todorova-Nova¹⁶¹, B. Toggerson¹⁶³, J. Tojo⁶⁹,
 S. Tokár^{144a}, K. Tokushuku⁶⁵, K. Tollefson⁸⁸, M. Tomoto¹⁰¹, L. Tompkins³¹, K. Toms¹⁰³,
 A. Tonoyan¹⁴, C. Topfel¹⁷, N.D. Topilin⁶⁴, I. Torchiani³⁰, E. Torrence¹¹⁴, H. Torres⁷⁸,
 E. Torró Pastor¹⁶⁷, J. Toth^{83,ad}, F. Touchard⁸³, D.R. Tovey¹³⁹, T. Trefzger¹⁷⁴,
 L. Tremblet³⁰, A. Tricoli³⁰, I.M. Trigger^{159a}, S. Trincaz-Duvoid⁷⁸, M.F. Tripiana⁷⁰,
 N. Triplett²⁵, W. Trischuk¹⁵⁸, B. Trocmé⁵⁵, C. Troncon^{89a}, M. Trottier-McDonald¹⁴²,
 M. Trzebinski³⁹, A. Trzupek³⁹, C. Tsarouchas³⁰, J.C-L. Tseng¹¹⁸, M. Tsiakiris¹⁰⁵,
 P.V. Tsiareshka⁹⁰, D. Tsionou^{5,ai}, G. Tsipolitis¹⁰, S. Tsiskaridze¹², V. Tsiskaridze⁴⁸,
 E.G. Tskhadadze^{51a}, I.I. Tsukerman⁹⁵, V. Tsulaia¹⁵, J.-W. Tsung²¹, S. Tsuno⁶⁵,
 D. Tsybychev¹⁴⁸, A. Tua¹³⁹, A. Tudorache^{26a}, V. Tudorache^{26a}, J.M. Tuggle³¹,
 M. Turala³⁹, D. Turecek¹²⁷, I. Turk Cakir^{4e}, E. Turlay¹⁰⁵, R. Turra^{89a,89b}, P.M. Tuts³⁵,
 A. Tykhonov⁷⁴, M. Tylmad^{146a,146b}, M. Tyndel¹²⁹, G. Tzanakos⁹, K. Uchida²¹,
 I. Ueda¹⁵⁵, R. Ueno²⁹, M. Ugland¹⁴, M. Uhlenbrock²¹, M. Uhrmacher⁵⁴, F. Ukegawa¹⁶⁰,
 G. Unal³⁰, A. Undrus²⁵, G. Unel¹⁶³, Y. Unno⁶⁵, D. Urbaniec³⁵, P. Urquijo²¹, G. Usai⁸,
 M. Uslenghi^{119a,119b}, L. Vacavant⁸³, V. Vacek¹²⁷, B. Vachon⁸⁵, S. Vahsen¹⁵, J. Valenta¹²⁵,
 S. Valentineti^{20a,20b}, A. Valero¹⁶⁷, S. Valkar¹²⁶, E. Valladolid Gallego¹⁶⁷,
 S. Vallecorsa¹⁵², J.A. Valls Ferrer¹⁶⁷, P.C. Van Der Deijl¹⁰⁵, R. van der Geer¹⁰⁵,
 H. van der Graaf¹⁰⁵, R. Van Der Leeuw¹⁰⁵, E. van der Poel¹⁰⁵, D. van der Ster³⁰,
 N. van Eldik³⁰, P. van Gemmeren⁶, I. van Vulpen¹⁰⁵, M. Vanadia⁹⁹, W. Vandelli³⁰,
 A. Vaniachine⁶, P. Vankov⁴², F. Vannucci⁷⁸, R. Vari^{132a}, T. Varol⁸⁴, D. Varouchas¹⁵,
 A. Vartapetian⁸, K.E. Varvell¹⁵⁰, V.I. Vassilikopoulos⁵⁶, F. Vazeille³⁴,
 T. Vazquez Schroeder⁵⁴, G. Vegni^{89a,89b}, J.J. Veillet¹¹⁵, F. Veloso^{124a}, R. Veness³⁰,
 S. Veneziano^{132a}, A. Ventura^{72a,72b}, D. Ventura⁸⁴, M. Venturi⁴⁸, N. Venturi¹⁵⁸,
 V. Vercesi^{119a}, M. Verducci¹³⁸, W. Verkerke¹⁰⁵, J.C. Vermeulen¹⁰⁵, A. Vest⁴⁴,
 M.C. Vetterli^{142,d}, I. Vichou¹⁶⁵, T. Vickey^{145b,aj}, O.E. Vickey Boeriu^{145b},
 G.H.A. Viehhauser¹¹⁸, S. Viel¹⁶⁸, M. Villa^{20a,20b}, M. Villaplana Perez¹⁶⁷, E. Vilucchi⁴⁷,
 M.G. Vincker²⁹, E. Vinek³⁰, V.B. Vinogradov⁶⁴, M. Virchaux^{136,*}, J. Virzi¹⁵,
 O. Vitells¹⁷², M. Viti⁴², I. Vivarelli⁴⁸, F. Vives Vaque³, S. Vlachos¹⁰, D. Vladoiu⁹⁸,
 M. Vlasak¹²⁷, A. Vogel²¹, P. Vokac¹²⁷, G. Volpi⁴⁷, M. Volpi⁸⁶, G. Volpini^{89a},
 H. von der Schmitt⁹⁹, H. von Radziewski⁴⁸, E. von Toerne²¹, V. Vorobel¹²⁶,
 V. Vorwerk¹², M. Vos¹⁶⁷, R. Voss³⁰, T.T. Voss¹⁷⁵, J.H. Vossebeld⁷³, N. Vranjes¹³⁶,
 M. Vranjes Milosavljevic¹⁰⁵, V. Vrba¹²⁵, M. Vreeswijk¹⁰⁵, T. Vu Anh⁴⁸, R. Vuillermet³⁰,
 I. Vukotic³¹, W. Wagner¹⁷⁵, P. Wagner¹²⁰, H. Wahlen¹⁷⁵, S. Wahrmund⁴⁴,
 J. Wakabayashi¹⁰¹, S. Walch⁸⁷, J. Walder⁷¹, R. Walker⁹⁸, W. Walkowiak¹⁴¹, R. Wall¹⁷⁶,

P. Waller⁷³, B. Walsh¹⁷⁶, C. Wang⁴⁵, H. Wang¹⁷³, H. Wang^{33b,ak}, J. Wang¹⁵¹, J. Wang⁵⁵, R. Wang¹⁰³, S.M. Wang¹⁵¹, T. Wang²¹, A. Warburton⁸⁵, C.P. Ward²⁸, M. Warsinsky⁴⁸, A. Washbrook⁴⁶, C. Wasicki⁴², I. Watanabe⁶⁶, P.M. Watkins¹⁸, A.T. Watson¹⁸, I.J. Watson¹⁵⁰, M.F. Watson¹⁸, G. Watts¹³⁸, S. Watts⁸², A.T. Waugh¹⁵⁰, B.M. Waugh⁷⁷, M.S. Weber¹⁷, P. Weber⁵⁴, A.R. Weidberg¹¹⁸, P. Weigell⁹⁹, J. Weingarten⁵⁴, C. Weiser⁴⁸, P.S. Wells³⁰, T. Wenaus²⁵, D. Wendland¹⁶, Z. Weng^{151,w}, T. Wengler³⁰, S. Wenig³⁰, N. Wermes²¹, M. Werner⁴⁸, P. Werner³⁰, M. Werth¹⁶³, M. Wessels^{58a}, J. Wetter¹⁶¹, C. Weydert⁵⁵, K. Whalen²⁹, S.J. Wheeler-Ellis¹⁶³, A. White⁸, M.J. White⁸⁶, S. White^{122a,122b}, S.R. Whitehead¹¹⁸, D. Whiteson¹⁶³, D. Whittington⁶⁰, F. Wicek¹¹⁵, D. Wicke¹⁷⁵, F.J. Wickens¹²⁹, W. Wiedenmann¹⁷³, M. Wieler¹²⁹, P. Wienemann²¹, C. Wiglesworth⁷⁵, L.A.M. Wiik-Fuchs⁴⁸, P.A. Wijeratne⁷⁷, A. Wildauer⁹⁹, M.A. Wildt^{42,s}, I. Wilhelm¹²⁶, H.G. Wilkens³⁰, J.Z. Will⁹⁸, E. Williams³⁵, H.H. Williams¹²⁰, W. Willis³⁵, S. Willocq⁸⁴, J.A. Wilson¹⁸, M.G. Wilson¹⁴³, A. Wilson⁸⁷, I. Wingerter-Seez⁵, S. Winkelmann⁴⁸, F. Winklmeier³⁰, M. Wittgen¹⁴³, S.J. Wollstadt⁸¹, M.W. Wolter³⁹, H. Wolters^{124a,h}, W.C. Wong⁴¹, G. Wooden⁸⁷, B.K. Wosiek³⁹, J. Wotschack³⁰, M.J. Woudstra⁸², K.W. Wozniak³⁹, K. Wraight⁵³, M. Wright⁵³, B. Wrona⁷³, S.L. Wu¹⁷³, X. Wu⁴⁹, Y. Wu^{33b,al}, E. Wulf³⁵, B.M. Wynne⁴⁶, S. Xella³⁶, M. Xiao¹³⁶, S. Xie⁴⁸, C. Xu^{33b,z}, D. Xu¹³⁹, B. Yabsley¹⁵⁰, S. Yacoob^{145a,am}, M. Yamada⁶⁵, H. Yamaguchi¹⁵⁵, A. Yamamoto⁶⁵, K. Yamamoto⁶³, S. Yamamoto¹⁵⁵, T. Yamamura¹⁵⁵, T. Yamanaka¹⁵⁵, J. Yamaoka⁴⁵, T. Yamazaki¹⁵⁵, Y. Yamazaki⁶⁶, Z. Yan²², H. Yang⁸⁷, U.K. Yang⁸², Y. Yang⁶⁰, Z. Yang^{146a,146b}, S. Yanush⁹¹, L. Yao^{33a}, Y. Yao¹⁵, Y. Yasu⁶⁵, G.V. Ybeles Smit¹³⁰, J. Ye⁴⁰, S. Ye²⁵, M. Yilmaz^{4c}, R. Yoosoofmiya¹²³, K. Yorita¹⁷¹, R. Yoshida⁶, C. Young¹⁴³, C.J. Young¹¹⁸, S. Youssef²², D. Yu²⁵, J. Yu⁸, J. Yu¹¹², L. Yuan⁶⁶, A. Yurkewicz¹⁰⁶, M. Byszewski³⁰, B. Zabinski³⁹, R. Zaidan⁶², A.M. Zaitsev¹²⁸, Z. Zajacova³⁰, S. Zambito²³, L. Zanello^{132a,132b}, D. Zanzi⁹⁹, A. Zaytsev²⁵, C. Zeitnitz¹⁷⁵, M. Zeman¹²⁵, A. Zemla³⁹, C. Zendler²¹, O. Zenin¹²⁸, T. Ženiš^{144a}, Z. Zinonos^{122a,122b}, S. Zenz¹⁵, D. Zerwas¹¹⁵, G. Zevi della Porta⁵⁷, Z. Zhan^{33d}, D. Zhang^{33b,ak}, H. Zhang⁸⁸, J. Zhang⁶, X. Zhang^{33d}, Z. Zhang¹¹⁵, L. Zhao¹⁰⁸, T. Zhao¹³⁸, Z. Zhao^{33b}, A. Zhemchugov⁶⁴, J. Zhong¹¹⁸, B. Zhou⁸⁷, N. Zhou¹⁶³, Y. Zhou¹⁵¹, C.G. Zhu^{33d}, H. Zhu⁴², J. Zhu⁸⁷, Y. Zhu^{33b}, X. Zhuang⁹⁸, V. Zhuravlov⁹⁹, D. Zieminska⁶⁰, N.I. Zimin⁶⁴, R. Zimmermann²¹, S. Zimmermann²¹, S. Zimmermann⁴⁸, M. Ziolkowski¹⁴¹, R. Zitoun⁵, L. Živković³⁵, V.V. Zmouchko^{128,*}, G. Zobernig¹⁷³, A. Zoccoli^{20a,20b}, M. zur Nedden¹⁶, V. Zutshi¹⁰⁶, L. Zwalinski³⁰.

¹ School of Chemistry and Physics, University of Adelaide, North Terrace Campus, 5000, SA, Australia

² Physics Department, SUNY Albany, Albany NY, United States of America

³ Department of Physics, University of Alberta, Edmonton AB, Canada

⁴ ^(a)Department of Physics, Ankara University, Ankara; ^(b)Department of Physics, Dumlupinar University, Kutahya; ^(c)Department of Physics, Gazi University, Ankara;

^(d)Division of Physics, TOBB University of Economics and Technology, Ankara;

^(e)Turkish Atomic Energy Authority, Ankara, Turkey

⁵ LAPP, CNRS/IN2P3 and Université de Savoie, Annecy-le-Vieux, France

- ⁶ High Energy Physics Division, Argonne National Laboratory, Argonne IL, United States of America
- ⁷ Department of Physics, University of Arizona, Tucson AZ, United States of America
- ⁸ Department of Physics, The University of Texas at Arlington, Arlington TX, United States of America
- ⁹ Physics Department, University of Athens, Athens, Greece
- ¹⁰ Physics Department, National Technical University of Athens, Zografou, Greece
- ¹¹ Institute of Physics, Azerbaijan Academy of Sciences, Baku, Azerbaijan
- ¹² Institut de Física d'Altes Energies and Departament de Física de la Universitat Autònoma de Barcelona and ICREA, Barcelona, Spain
- ¹³ ^(a)Institute of Physics, University of Belgrade, Belgrade; ^(b)Vinca Institute of Nuclear Sciences, University of Belgrade, Belgrade, Serbia
- ¹⁴ Department for Physics and Technology, University of Bergen, Bergen, Norway
- ¹⁵ Physics Division, Lawrence Berkeley National Laboratory and University of California, Berkeley CA, United States of America
- ¹⁶ Department of Physics, Humboldt University, Berlin, Germany
- ¹⁷ Albert Einstein Center for Fundamental Physics and Laboratory for High Energy Physics, University of Bern, Bern, Switzerland
- ¹⁸ School of Physics and Astronomy, University of Birmingham, Birmingham, United Kingdom
- ¹⁹ ^(a)Department of Physics, Bogazici University, Istanbul; ^(b)Division of Physics, Dogus University, Istanbul; ^(c)Department of Physics Engineering, Gaziantep University, Gaziantep; ^(d)Department of Physics, Istanbul Technical University, Istanbul, Turkey
- ²⁰ ^(a)INFN Sezione di Bologna; ^(b)Dipartimento di Fisica, Università di Bologna, Bologna, Italy
- ²¹ Physikalisches Institut, University of Bonn, Bonn, Germany
- ²² Department of Physics, Boston University, Boston MA, United States of America
- ²³ Department of Physics, Brandeis University, Waltham MA, United States of America
- ²⁴ ^(a)Universidade Federal do Rio De Janeiro COPPE/EE/IF, Rio de Janeiro; ^(b)Federal University of Juiz de Fora (UFJF), Juiz de Fora; ^(c)Federal University of Sao Joao del Rei (UFSJ), Sao Joao del Rei; ^(d)Instituto de Fisica, Universidade de Sao Paulo, Sao Paulo, Brazil
- ²⁵ Physics Department, Brookhaven National Laboratory, Upton NY, United States of America
- ²⁶ ^(a)National Institute of Physics and Nuclear Engineering, Bucharest; ^(b)University Politehnica Bucharest, Bucharest; ^(c)West University in Timisoara, Timisoara, Romania
- ²⁷ Departamento de Física, Universidad de Buenos Aires, Buenos Aires, Argentina
- ²⁸ Cavendish Laboratory, University of Cambridge, Cambridge, United Kingdom
- ²⁹ Department of Physics, Carleton University, Ottawa ON, Canada
- ³⁰ CERN, Geneva, Switzerland
- ³¹ Enrico Fermi Institute, University of Chicago, Chicago IL, United States of America
- ³² ^(a)Departamento de Física, Pontificia Universidad Católica de Chile, Santiago; ^(b)Departamento de Física, Universidad Técnica Federico Santa María, Valparaíso, Chile

- ³³ ^(a)Institute of High Energy Physics, Chinese Academy of Sciences, Beijing;
^(b)Department of Modern Physics, University of Science and Technology of China, Anhui;
^(c)Department of Physics, Nanjing University, Jiangsu; ^(d)School of Physics, Shandong University, Shandong, China
- ³⁴ Laboratoire de Physique Corpusculaire, Clermont Université and Université Blaise Pascal and CNRS/IN2P3, Aubiere Cedex, France
- ³⁵ Nevis Laboratory, Columbia University, Irvington NY, United States of America
- ³⁶ Niels Bohr Institute, University of Copenhagen, Copenhagen, Denmark
- ³⁷ ^(a)INFN Gruppo Collegato di Cosenza; ^(b)Dipartimento di Fisica, Università della Calabria, Arcavata di Rende, Italy
- ³⁸ AGH University of Science and Technology, Faculty of Physics and Applied Computer Science, Krakow, Poland
- ³⁹ The Henryk Niewodniczanski Institute of Nuclear Physics, Polish Academy of Sciences, Krakow, Poland
- ⁴⁰ Physics Department, Southern Methodist University, Dallas TX, United States of America
- ⁴¹ Physics Department, University of Texas at Dallas, Richardson TX, United States of America
- ⁴² DESY, Hamburg and Zeuthen, Germany
- ⁴³ Institut für Experimentelle Physik IV, Technische Universität Dortmund, Dortmund, Germany
- ⁴⁴ Institut für Kern-und Teilchenphysik, Technical University Dresden, Dresden, Germany
- ⁴⁵ Department of Physics, Duke University, Durham NC, United States of America
- ⁴⁶ SUPA - School of Physics and Astronomy, University of Edinburgh, Edinburgh, United Kingdom
- ⁴⁷ INFN Laboratori Nazionali di Frascati, Frascati, Italy
- ⁴⁸ Fakultät für Mathematik und Physik, Albert-Ludwigs-Universität, Freiburg, Germany
- ⁴⁹ Section de Physique, Université de Genève, Geneva, Switzerland
- ⁵⁰ ^(a)INFN Sezione di Genova; ^(b)Dipartimento di Fisica, Università di Genova, Genova, Italy
- ⁵¹ ^(a)E. Andronikashvili Institute of Physics, Tbilisi State University, Tbilisi; ^(b)High Energy Physics Institute, Tbilisi State University, Tbilisi, Georgia
- ⁵² II Physikalisches Institut, Justus-Liebig-Universität Giessen, Giessen, Germany
- ⁵³ SUPA - School of Physics and Astronomy, University of Glasgow, Glasgow, United Kingdom
- ⁵⁴ II Physikalisches Institut, Georg-August-Universität, Göttingen, Germany
- ⁵⁵ Laboratoire de Physique Subatomique et de Cosmologie, Université Joseph Fourier and CNRS/IN2P3 and Institut National Polytechnique de Grenoble, Grenoble, France
- ⁵⁶ Department of Physics, Hampton University, Hampton VA, United States of America
- ⁵⁷ Laboratory for Particle Physics and Cosmology, Harvard University, Cambridge MA, United States of America
- ⁵⁸ ^(a)Kirchhoff-Institut für Physik, Ruprecht-Karls-Universität Heidelberg, Heidelberg;
^(b)Physikalisches Institut, Ruprecht-Karls-Universität Heidelberg, Heidelberg; ^(c)ZITI

- Institut für technische Informatik, Ruprecht-Karls-Universität Heidelberg, Mannheim, Germany
- ⁵⁹ Faculty of Applied Information Science, Hiroshima Institute of Technology, Hiroshima, Japan
- ⁶⁰ Department of Physics, Indiana University, Bloomington IN, United States of America
- ⁶¹ Institut für Astro-und Teilchenphysik, Leopold-Franzens-Universität, Innsbruck, Austria
- ⁶² University of Iowa, Iowa City IA, United States of America
- ⁶³ Department of Physics and Astronomy, Iowa State University, Ames IA, United States of America
- ⁶⁴ Joint Institute for Nuclear Research, JINR Dubna, Dubna, Russia
- ⁶⁵ KEK, High Energy Accelerator Research Organization, Tsukuba, Japan
- ⁶⁶ Graduate School of Science, Kobe University, Kobe, Japan
- ⁶⁷ Faculty of Science, Kyoto University, Kyoto, Japan
- ⁶⁸ Kyoto University of Education, Kyoto, Japan
- ⁶⁹ Department of Physics, Kyushu University, Fukuoka, Japan
- ⁷⁰ Instituto de Física La Plata, Universidad Nacional de La Plata and CONICET, La Plata, Argentina
- ⁷¹ Physics Department, Lancaster University, Lancaster, United Kingdom
- ⁷² ^(a)INFN Sezione di Lecce; ^(b)Dipartimento di Matematica e Fisica, Università del Salento, Lecce, Italy
- ⁷³ Oliver Lodge Laboratory, University of Liverpool, Liverpool, United Kingdom
- ⁷⁴ Department of Physics, Jožef Stefan Institute and University of Ljubljana, Ljubljana, Slovenia
- ⁷⁵ School of Physics and Astronomy, Queen Mary University of London, London, United Kingdom
- ⁷⁶ Department of Physics, Royal Holloway University of London, Surrey, United Kingdom
- ⁷⁷ Department of Physics and Astronomy, University College London, London, United Kingdom
- ⁷⁸ Laboratoire de Physique Nucléaire et de Hautes Energies, UPMC and Université Paris-Diderot and CNRS/IN2P3, Paris, France
- ⁷⁹ Fysiska institutionen, Lunds universitet, Lund, Sweden
- ⁸⁰ Departamento de Física Teórica C-15, Universidad Autónoma de Madrid, Madrid, Spain
- ⁸¹ Institut für Physik, Universität Mainz, Mainz, Germany
- ⁸² School of Physics and Astronomy, University of Manchester, Manchester, United Kingdom
- ⁸³ CPPM, Aix-Marseille Université and CNRS/IN2P3, Marseille, France
- ⁸⁴ Department of Physics, University of Massachusetts, Amherst MA, United States of America
- ⁸⁵ Department of Physics, McGill University, Montreal QC, Canada
- ⁸⁶ School of Physics, University of Melbourne, Victoria, Australia
- ⁸⁷ Department of Physics, The University of Michigan, Ann Arbor MI, United States of

America

⁸⁸ Department of Physics and Astronomy, Michigan State University, East Lansing MI, United States of America

⁸⁹ ^(a)INFN Sezione di Milano; ^(b)Dipartimento di Fisica, Università di Milano, Milano, Italy

⁹⁰ B.I. Stepanov Institute of Physics, National Academy of Sciences of Belarus, Minsk, Republic of Belarus

⁹¹ National Scientific and Educational Centre for Particle and High Energy Physics, Minsk, Republic of Belarus

⁹² Department of Physics, Massachusetts Institute of Technology, Cambridge MA, United States of America

⁹³ Group of Particle Physics, University of Montreal, Montreal QC, Canada

⁹⁴ P.N. Lebedev Institute of Physics, Academy of Sciences, Moscow, Russia

⁹⁵ Institute for Theoretical and Experimental Physics (ITEP), Moscow, Russia

⁹⁶ Moscow Engineering and Physics Institute (MEPhI), Moscow, Russia

⁹⁷ Skobeltsyn Institute of Nuclear Physics, Lomonosov Moscow State University, Moscow, Russia

⁹⁸ Fakultät für Physik, Ludwig-Maximilians-Universität München, München, Germany

⁹⁹ Max-Planck-Institut für Physik (Werner-Heisenberg-Institut), München, Germany

¹⁰⁰ Nagasaki Institute of Applied Science, Nagasaki, Japan

¹⁰¹ Graduate School of Science and Kobayashi-Maskawa Institute, Nagoya University, Nagoya, Japan

¹⁰² ^(a)INFN Sezione di Napoli; ^(b)Dipartimento di Scienze Fisiche, Università di Napoli, Napoli, Italy

¹⁰³ Department of Physics and Astronomy, University of New Mexico, Albuquerque NM, United States of America

¹⁰⁴ Institute for Mathematics, Astrophysics and Particle Physics, Radboud University Nijmegen/Nikhef, Nijmegen, Netherlands

¹⁰⁵ Nikhef National Institute for Subatomic Physics and University of Amsterdam, Amsterdam, Netherlands

¹⁰⁶ Department of Physics, Northern Illinois University, DeKalb IL, United States of America

¹⁰⁷ Budker Institute of Nuclear Physics, SB RAS, Novosibirsk, Russia

¹⁰⁸ Department of Physics, New York University, New York NY, United States of America

¹⁰⁹ Ohio State University, Columbus OH, United States of America

¹¹⁰ Faculty of Science, Okayama University, Okayama, Japan

¹¹¹ Homer L. Dodge Department of Physics and Astronomy, University of Oklahoma, Norman OK, United States of America

¹¹² Department of Physics, Oklahoma State University, Stillwater OK, United States of America

¹¹³ Palacký University, RCPTM, Olomouc, Czech Republic

¹¹⁴ Center for High Energy Physics, University of Oregon, Eugene OR, United States of America

- ¹¹⁵ LAL, Université Paris-Sud and CNRS/IN2P3, Orsay, France
- ¹¹⁶ Graduate School of Science, Osaka University, Osaka, Japan
- ¹¹⁷ Department of Physics, University of Oslo, Oslo, Norway
- ¹¹⁸ Department of Physics, Oxford University, Oxford, United Kingdom
- ¹¹⁹ ^(a)INFN Sezione di Pavia; ^(b)Dipartimento di Fisica, Università di Pavia, Pavia, Italy
- ¹²⁰ Department of Physics, University of Pennsylvania, Philadelphia PA, United States of America
- ¹²¹ Petersburg Nuclear Physics Institute, Gatchina, Russia
- ¹²² ^(a)INFN Sezione di Pisa; ^(b)Dipartimento di Fisica E. Fermi, Università di Pisa, Pisa, Italy
- ¹²³ Department of Physics and Astronomy, University of Pittsburgh, Pittsburgh PA, United States of America
- ¹²⁴ ^(a)Laboratorio de Instrumentacao e Fisica Experimental de Particulas - LIP, Lisboa, Portugal; ^(b)Departamento de Fisica Teorica y del Cosmos and CAFPE, Universidad de Granada, Granada, Spain
- ¹²⁵ Institute of Physics, Academy of Sciences of the Czech Republic, Praha, Czech Republic
- ¹²⁶ Faculty of Mathematics and Physics, Charles University in Prague, Praha, Czech Republic
- ¹²⁷ Czech Technical University in Prague, Praha, Czech Republic
- ¹²⁸ State Research Center Institute for High Energy Physics, Protvino, Russia
- ¹²⁹ Particle Physics Department, Rutherford Appleton Laboratory, Didcot, United Kingdom
- ¹³⁰ Physics Department, University of Regina, Regina SK, Canada
- ¹³¹ Ritsumeikan University, Kusatsu, Shiga, Japan
- ¹³² ^(a)INFN Sezione di Roma I; ^(b)Dipartimento di Fisica, Università La Sapienza, Roma, Italy
- ¹³³ ^(a)INFN Sezione di Roma Tor Vergata; ^(b)Dipartimento di Fisica, Università di Roma Tor Vergata, Roma, Italy
- ¹³⁴ ^(a)INFN Sezione di Roma Tre; ^(b)Dipartimento di Fisica, Università Roma Tre, Roma, Italy
- ¹³⁵ ^(a)Faculté des Sciences Ain Chock, Réseau Universitaire de Physique des Hautes Energies - Université Hassan II, Casablanca; ^(b)Centre National de l'Energie des Sciences Techniques Nucleaires, Rabat; ^(c)Faculté des Sciences Semlalia, Université Cadi Ayyad, LPHEA-Marrakech; ^(d)Faculté des Sciences, Université Mohamed Premier and LPTPM, Oujda; ^(e)Faculté des sciences, Université Mohammed V-Agdal, Rabat, Morocco
- ¹³⁶ DSM/IRFU (Institut de Recherches sur les Lois Fondamentales de l'Univers), CEA Saclay (Commissariat a l'Energie Atomique), Gif-sur-Yvette, France
- ¹³⁷ Santa Cruz Institute for Particle Physics, University of California Santa Cruz, Santa Cruz CA, United States of America
- ¹³⁸ Department of Physics, University of Washington, Seattle WA, United States of America
- ¹³⁹ Department of Physics and Astronomy, University of Sheffield, Sheffield, United

Kingdom

¹⁴⁰ Department of Physics, Shinshu University, Nagano, Japan

¹⁴¹ Fachbereich Physik, Universität Siegen, Siegen, Germany

¹⁴² Department of Physics, Simon Fraser University, Burnaby BC, Canada

¹⁴³ SLAC National Accelerator Laboratory, Stanford CA, United States of America

¹⁴⁴ ^(a)Faculty of Mathematics, Physics & Informatics, Comenius University, Bratislava;

^(b)Department of Subnuclear Physics, Institute of Experimental Physics of the Slovak Academy of Sciences, Kosice, Slovak Republic

¹⁴⁵ ^(a)Department of Physics, University of Johannesburg, Johannesburg; ^(b)School of Physics, University of the Witwatersrand, Johannesburg, South Africa

¹⁴⁶ ^(a)Department of Physics, Stockholm University; ^(b)The Oskar Klein Centre, Stockholm, Sweden

¹⁴⁷ Physics Department, Royal Institute of Technology, Stockholm, Sweden

¹⁴⁸ Departments of Physics & Astronomy and Chemistry, Stony Brook University, Stony Brook NY, United States of America

¹⁴⁹ Department of Physics and Astronomy, University of Sussex, Brighton, United Kingdom

¹⁵⁰ School of Physics, University of Sydney, Sydney, Australia

¹⁵¹ Institute of Physics, Academia Sinica, Taipei, Taiwan

¹⁵² Department of Physics, Technion: Israel Institute of Technology, Haifa, Israel

¹⁵³ Raymond and Beverly Sackler School of Physics and Astronomy, Tel Aviv University, Tel Aviv, Israel

¹⁵⁴ Department of Physics, Aristotle University of Thessaloniki, Thessaloniki, Greece

¹⁵⁵ International Center for Elementary Particle Physics and Department of Physics, The University of Tokyo, Tokyo, Japan

¹⁵⁶ Graduate School of Science and Technology, Tokyo Metropolitan University, Tokyo, Japan

¹⁵⁷ Department of Physics, Tokyo Institute of Technology, Tokyo, Japan

¹⁵⁸ Department of Physics, University of Toronto, Toronto ON, Canada

¹⁵⁹ ^(a)TRIUMF, Vancouver BC; ^(b)Department of Physics and Astronomy, York University, Toronto ON, Canada

¹⁶⁰ Institute of Pure and Applied Sciences, University of Tsukuba, 1-1-1 Tennodai, Tsukuba, Ibaraki 305-8571, Japan

¹⁶¹ Science and Technology Center, Tufts University, Medford MA, United States of America

¹⁶² Centro de Investigaciones, Universidad Antonio Narino, Bogota, Colombia

¹⁶³ Department of Physics and Astronomy, University of California Irvine, Irvine CA, United States of America

¹⁶⁴ ^(a)INFN Gruppo Collegato di Udine; ^(b)ICTP, Trieste; ^(c)Dipartimento di Chimica, Fisica e Ambiente, Università di Udine, Udine, Italy

¹⁶⁵ Department of Physics, University of Illinois, Urbana IL, United States of America

¹⁶⁶ Department of Physics and Astronomy, University of Uppsala, Uppsala, Sweden

¹⁶⁷ Instituto de Física Corpuscular (IFIC) and Departamento de Física Atómica,

Molecular y Nuclear and Departamento de Ingeniería Electrónica and Instituto de Microelectrónica de Barcelona (IMB-CNM), University of Valencia and CSIC, Valencia, Spain

¹⁶⁸ Department of Physics, University of British Columbia, Vancouver BC, Canada

¹⁶⁹ Department of Physics and Astronomy, University of Victoria, Victoria BC, Canada

¹⁷⁰ Department of Physics, University of Warwick, Coventry, United Kingdom

¹⁷¹ Waseda University, Tokyo, Japan

¹⁷² Department of Particle Physics, The Weizmann Institute of Science, Rehovot, Israel

¹⁷³ Department of Physics, University of Wisconsin, Madison WI, United States of America

¹⁷⁴ Fakultät für Physik und Astronomie, Julius-Maximilians-Universität, Würzburg, Germany

¹⁷⁵ Fachbereich C Physik, Bergische Universität Wuppertal, Wuppertal, Germany

¹⁷⁶ Department of Physics, Yale University, New Haven CT, United States of America

¹⁷⁷ Yerevan Physics Institute, Yerevan, Armenia

¹⁷⁸ Domaine scientifique de la Doua, Centre de Calcul CNRS/IN2P3, Villeurbanne Cedex, France

^a Also at Laboratorio de Instrumentacao e Fisica Experimental de Particulas - LIP, Lisboa, Portugal

^b Also at Faculdade de Ciencias and CFNUL, Universidade de Lisboa, Lisboa, Portugal

^c Also at Particle Physics Department, Rutherford Appleton Laboratory, Didcot, United Kingdom

^d Also at TRIUMF, Vancouver BC, Canada

^e Also at Department of Physics, California State University, Fresno CA, United States of America

^f Also at Novosibirsk State University, Novosibirsk, Russia

^g Also at Fermilab, Batavia IL, United States of America

^h Also at Department of Physics, University of Coimbra, Coimbra, Portugal

ⁱ Also at Department of Physics, UASLP, San Luis Potosi, Mexico

^j Also at Università di Napoli Parthenope, Napoli, Italy

^k Also at Institute of Particle Physics (IPP), Canada

^l Also at Department of Physics, Middle East Technical University, Ankara, Turkey

^m Also at Louisiana Tech University, Ruston LA, United States of America

ⁿ Also at Dep Fisica and CEFITEC of Faculdade de Ciencias e Tecnologia, Universidade Nova de Lisboa, Caparica, Portugal

^o Also at Department of Physics and Astronomy, University College London, London, United Kingdom

^p Also at Group of Particle Physics, University of Montreal, Montreal QC, Canada

^q Also at Department of Physics, University of Cape Town, Cape Town, South Africa

^r Also at Institute of Physics, Azerbaijan Academy of Sciences, Baku, Azerbaijan

^s Also at Institut für Experimentalphysik, Universität Hamburg, Hamburg, Germany

^t Also at Manhattan College, New York NY, United States of America

^u Also at School of Physics, Shandong University, Shandong, China

- ^v Also at CPPM, Aix-Marseille Université and CNRS/IN2P3, Marseille, France
- ^w Also at School of Physics and Engineering, Sun Yat-sen University, Guanzhou, China
- ^x Also at Academia Sinica Grid Computing, Institute of Physics, Academia Sinica, Taipei, Taiwan
- ^y Also at Dipartimento di Fisica, Università La Sapienza, Roma, Italy
- ^z Also at DSM/IRFU (Institut de Recherches sur les Lois Fondamentales de l'Univers), CEA Saclay (Commissariat à l'Energie Atomique), Gif-sur-Yvette, France
- ^{aa} Also at Section de Physique, Université de Genève, Geneva, Switzerland
- ^{ab} Also at Departamento de Fisica, Universidade de Minho, Braga, Portugal
- ^{ac} Also at Department of Physics and Astronomy, University of South Carolina, Columbia SC, United States of America
- ^{ad} Also at Institute for Particle and Nuclear Physics, Wigner Research Centre for Physics, Budapest, Hungary
- ^{ae} Also at California Institute of Technology, Pasadena CA, United States of America
- ^{af} Also at Institute of Physics, Jagiellonian University, Krakow, Poland
- ^{ag} Also at LAL, Université Paris-Sud and CNRS/IN2P3, Orsay, France
- ^{ah} Also at Nevis Laboratory, Columbia University, Irvington NY, United States of America
- ^{ai} Also at Department of Physics and Astronomy, University of Sheffield, Sheffield, United Kingdom
- ^{aj} Also at Department of Physics, Oxford University, Oxford, United Kingdom
- ^{ak} Also at Institute of Physics, Academia Sinica, Taipei, Taiwan
- ^{al} Also at Department of Physics, The University of Michigan, Ann Arbor MI, United States of America
- ^{am} Also at Discipline of Physics, University of KwaZulu-Natal, Durban, South Africa
- * Deceased